THEORETICAL STUDIES ON STRUCTURE AND REACTIVITY OF MOLECULES AND CLUSTERS

A THESIS
SUBMITTED FOR THE DEGREE OF
DOCTOR OF PHILOSOPHY

BY

G.NARAHARI SASTRY

SCHOOL OF CHEMISTRY
UNIVERSITY OF HYDERABAD
HYDERABAD - 500134, INDIA

JANUARY 1994

THEORETICAL STUDIES ON STRUCTURE AND REACTIVITY OF MOLECULES AND CLUSTERS

A THESIS
SUBMITTED FOR THE DEGREE OF
DOCTOR OF PHILOSOPHY

BY

G.NARAHARI SASTRY

SCHOOL OF CHEMISTRY
UNIVERSITY OF HYDERABAD
HYDERABAD - 500134, INDIA

JANUARY 1994

to my beloved

AMMA

NANNA

& MADHAVI

CONTENTS

STATEMENT . . . i

CERTIFICATE . . . ii

ACKNOWLEDGEMENTS . . . iii

ABBREVIATIONS . . . v

SYNOPSIS . . . vi

CHAPTER 1 : Introduction

1.1 Introduction . . . 2

1.2 References . . . 12

CHAPTER 2 : Disubstituted cyclobutadienes: relative stabilities and reactivity with quinones

2.0 General Introduction . . . 16

2.1 Relative stabilities of disubstituted cyclobutadienes. An ab initio molecular orbital study

2.1.1 Abstract . . . 17

2.1.2 Introduction . . . 18

2.1.3 Method of calculation . . . 19

2.1.4 Results and discussion . . . 20

2.1.5 Conclusions . . . 36

2.2 Vicinal disubstituted cyclobutadienes: oligomerization and reactivity with quinones

2.2.1 Abstract . . . 37

2.2.2 Introduction . . . 38

2.2.3 Results and discussion . . . 40

2.2.4 Conclusions . . . 49

2.3. References . . . 50

2.4 Appendix . . . 54

CHAPTER 3 : Dyotropic rearrangements of Cp_2ZrL_n complexes and the electronic structure and reactivity of $Cp_2Zr=E$ (E = S, O, NH and PH) complexes.

3.0 General introduction . . . 62

3.1 Dyotropic rearragements of Cp_2ZrL_n complexes

3.1.1 Abstract . . . 63

3.1.2 Introduction . . . 64

3.1.3 Results and Discussion . . . 68

3.1.4 Conclusions . . . 86

3.2 Electronic structure and reactivity of $Cp_2Zr=E$ (E = S, O, NH and PH) complexes.

3.2.1 Abstract . . . 87

3.2.2 Introduction . . . 88

3.2.3 Results and discussion . . . 90

3.2.4 Conclusions . . . 97

3.3. References . . . 98

3.4 Appendix . . . 102

CHAPTER 4 : Possibility of bond stretch isomerism in $[Cp(CO)_2M]_2(\mu\text{-}E)$ complexes (M = Mn, Re, Cr and W; E = S, Se and Te); a molecular orbital study.

4.1 Abstract . . . 104

4.2 Introduction . . . 105

4.3 Results and discussion . . . 108

4.4 Conclusions . . . 123

4.5 References . . . 126

4.6 Appendix

CHAPTER 5 : Molecular mehchanics and MNDO calculations on C_{60} and C_{70} and their substructures

5.0 General introduction . . . 129

5.1 Molecular mechanics and MNDO calculations on sumanene and related substructures of C_{60}.

5.1.1 Abstract . . . 130

5.1.2 Introduction . . . 131

5.1.3 Results and discussion . . . 135

5.1.4 Conclusions . . . 144

5.2 Molecular mechanics and MNDO calculations on pinakene and related substructures of C_{70}.

5.2.1 Abstract . . . 145

5.2.2 Introduction . . . 146

5.2.3 Results and discussion . . . 149

5.2.4 Conclusions . . . 164

5.3. References . . . 165

Vitae

STATEMENT

I hereby declare that the matter embodied in this thesis is the result of investigations carried out by me in the School of Chemistry, University of Hyderabad, Hyderabad, India under the supervision of Professor Eluvathingal D. Jemmis.

In keeping with the general practice of reporting scientific observations due acknowledgements have been made wherever the work described is based on the findings of other investigators.

Hyderabad,
January, 1994.

G. Narahari Sastry.

CERTIFICATE

Certified that the work contained in this thesis entitled: **"THEORETICAL STUDIES ON STRUCTURE AND REACTIVITY OF MOLECULES AND CLUSTERS"** has been carried out by Mr. G. Narahari Sastry, under my supervision and the same has not been submitted elsewhere for any degree.

E.D. Jemmis
(Thesis Supervisor)

DEAN
School of Chemistry

ACKNOWLEDGEMENTS

With pleasure I express my deep sense of gratitude to my supervisor Professor E.D. Jemmis who has introduced me to this subject and taught me the art of doing research. His valuable guidance and councelling helped me to study several problems theoretically and also bring out this thesis.

I also record my gratitude to Professor Goverdhan Mehta, for actively involving me in collaborative projects. I thank him for several scientific discussions I had with him. Special thanks are due to Dr. M. Durga Prasad for some helpful discussions.

It is extremely fortunate to have collegues like Dr. P.N.V. Pavan Kumar, Dr. Bharatam V. Prasad, Dr. A. Chandrasekhar Reddy, Mr.G. Subramanian, Mr. G. Naga Srinivas, Mr. B. Kiran, Ms. G. Madhavi, Mr.K.T. Giju and Mr. T.V. Vedavyasa and Ms. G. Sreelatha. They greatly helped me in polishing my perception towards chemistry and also helped in the preparation of the thesis. I thank them all.

I thank the University of Hyderabad computer centre as well as the Super Computing Facility, Australian National University, Canberra, for computational facilities. I thank my teachers at Osmania University, where I obtained my masters degrees in Chemistry.

The Dean, Professor P.S. Zacharias, and the former deans, Professor R. Jagannathan and Professor K.D. Sen are thanked for their help. I also thank all the members of the faculty of the

School of Chemistry for the opportunities they provided for learning.

All the research scholars of the School of Chemisty, and the inmates of RS hostel made my stay in the campus memorable. I especially thank Bhaskar Raju, Rajender Reddy, Satish Goud, Peddireddi, Venkat, Rama Reddy, Harikrishna Reddy, Sekhar Reddy, Ramkishan Rao, Bhanu Prasad, Dharma Rao, Bhaskar Kanth, Ramakrishna and others for many happy moments we shared together.

The love and affection provided by my parents, whose primary concern is the education of their children, transcends my ability to do things. My deepest gratitude goes to them. I thank my elder brother (Sekhar annaiah) and Vadina for shaping my career in a proper way. I am indebted to my parents-in-law, who have been of immense help to me at several critical moments in the last two years. Without their undaunting support and love the thesis could not be completed in time. I thank bavagaru (Mr. Kameswara Rao), Durga, Ramana, Pavan, Sekhar and Sarada for their affection and for providing constant encouragement over the years. My little son, Kaushik, always has a complaint that he is not getting his share of time to play with me - I accept it.

Financial Assistance from Council of Scientific and Industrial Research, New Delhi is greatly acknowledged.

Finally, I express my heartfelt appreciation to my wife, Madhavi, for her caring, encouragement and help in the preparation of this thesis.

ABBREVIATIONS

AM1	Austin Model 1
Cp	Cyclopentadienyl
Cp^*	Pentamethylcyclobutadienyl
eV	electron Volt
E	Main group element
EH	Extended Huckel
HF	Hartree-Fock
HOMO	Highest Occupied Molecular Orbital
L	Ligand
LUMO	Lowest Unoccupied Molecular Orbital
M	Transition Metal Fragment
Me	Methyl
MM2	Molecular Mechanics 2
MNDO	Modified Neglect of Diatomic Overlap
MO	Molecular Orbital
MP	Moller Plesset
Ph	Phenyl
SCF	Self Consistent Field
VE	Valence electrons
VEC	valence electron count
ZDO	Zero Differential Overlap

SYNOPSIS

This thesis discusses structure, stability and reactivity of some organic and organometallic complexes. A variety of theoretical methods based on ab intio and semiempirical molecular orbital theory and on empirical force fields are used here. The thesis is divided into five chapters The first chapter gives a general introduction. The second chapter deals with the effect of disubstitution on relative stabilities of cyclobutadienes. Cyclobutadienes are often generated in situ from their $Fe(CO)_3$ complexes. Reactivities of 1,2-dicarbomethoxycyclobutadienes with several substrates are studied using molecular orbital theory. In chapter 3, a series of reactions involving biscyclopentadienyl complexes are studied. The reactivity of $Cp_2Zr{=}X$ where X = O, S, NH and PH is also analyzed here.

Addition of another metal presents many new problems as exemplified by MEM complexes (M = $Cp(CO)_2M$, E = S, Se and Te) which are studied in chapter IV. Some of these could turn out to be the first examples of bond stretch isomerism. Chapter 5 discusses the strain energy analysis of various key fragments along stepwise synthetic procedures towards C_{60} and C_{70}. We also discuss the bond localization in C_{60} and C_{70} by taking the fragments as models. Brief contents of each chapter follow.

Chapter 1 : **Introduction**

The role of theory in developing chemistry as a whole is highlighted in this chapter. The various projects studied in the

thesis are presented using this point of view. A brief description to the various theoretical methods used is also given here.

Chapter 2: **Disubstituted cyclobutadienes: relative stabilities and reactivity.**

a. Relative Stabilities of disubstituted cyclobutadienes. An ab initio molecular orbital study.

Cyclobutadiene has been a target of many theoretical and experimental studies. Cyclobutadiene has a rectangular geometry in the ground state. Though there are several studies on the parent cyclobutadiene, the effect of substitution on cyclobutadiene is not studied in detail. Among the substituted cyclobutadienes the disubstituted ones are often encountered in experimental literature and are of interest regarding their relative stabilities. There are three possible isomers (I, II and III).

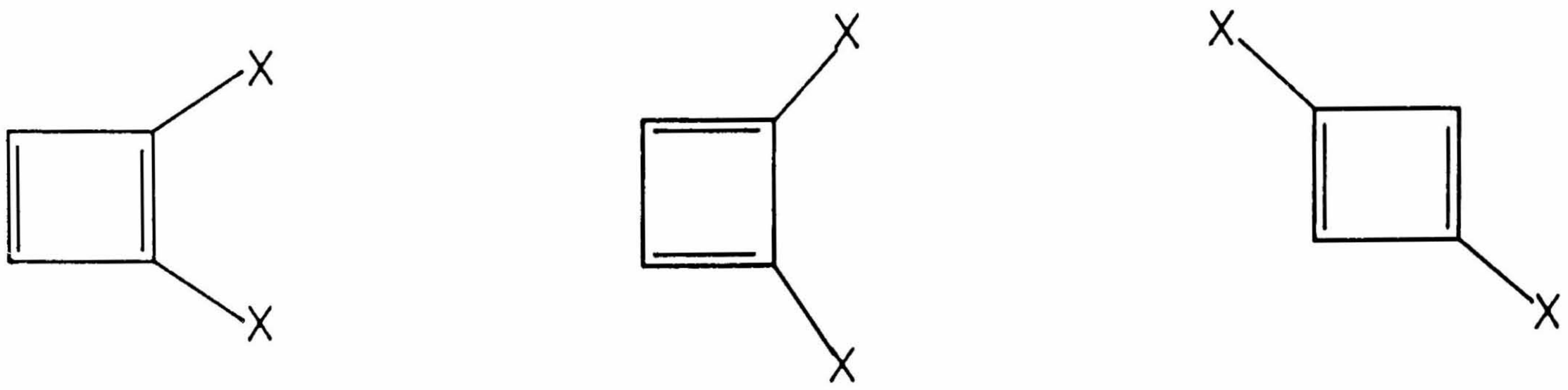

I II III

	a	b	c	d	e	f
X	CH_3	OH	CN	$CH{=}CH_2$	CH_2^+	CH_2^-

The effect of substitution on the three forms of disubstituted cyclobutadienes is studied by ab initio electronic structure calculations at the HF/6-31G* and MP2/6-31G* levels. The existence of two distinct isomeric forms for the vicinal disubstituted cyclobutadienes, I and II, is clearly established. The relative stabilities observed between X = CN, CH_3 and OH are opposite to those obtained for X = $CH{=}CH_2$. The latter substituent is similar to phenyl in terms of extending conjugation. Thus the reversal of relative stabilities observed experimentally between X = CN and Ph is confirmed by the present study. The repulsion between the two double bonds in cyclobutadienes, the stabilization from extraconjugation, the ability of ethylene to add on substituents and electrostatic interactions are among the factors that control the relative stabilities. Methyl and hydroxy substituted cyclobutadienes have several conformations. The relative energies of various conformational isomers by ab initio calculations are explained by qualitative models.

b. Reactivity: oligomerization and reactivity with quinones

Parent cyclobutadiene and many of its derivatives are very reactive and dimerize quickly. However further oligomerizations are not observed. If we understand why the oligomerization of cyclobutadiene does not proceed beyond the dimer stage, it should be possible to design substituted systems that may undergo further [4+2] cycloaddition and thus promote a cycloaddition cascade leading to higher ladderanes. To this end, we examined the frontier orbital control of the oligomerization process. The

molecular orbitals were obtained using the semiempirical AM1 method. This study predicted 1,2-dicarboxylic acid derivatives to be good candidates for oligomerizations. This is realized experimentally in a collaborative study. (Angew. Chem. Int. Ed. Engl. 1992, **31**, 1488-1490.)

Frontier Molecular Orbital Theory is used to explain the observed regioselectivities in the [4+2] cycloadditions between 1,2-dicarbomethoxycyclobutadienes and quinones (benzoquinone and naphthoquinone). The calculations are performed at AM1 level. (J. Chem. Soc. Perkin Trans. 2, **1994**, 0000)

Chapter 3: **Dyotropic rearrangements of Cp_2ZrL_n complexes and the electronic Structure and Reactivity of $Cp_2Zr{=}E$ (E = S, O, NH and PH) Complexes.**

a. Dyotropic Rearrangements of Cp_2ZrL_n complexes

The bent metallocene fragment, Cp_2Zr provides frontier orbitals exclusively in a plane perpendicular to the plane formed by the centroid of the Cp (cyclopentadiene) rings and the metal. There are a number of ways in which this mononuclear fragment can bind ligands. An interesting reaction which leads to C-C bond formation by dyotropic rearrangement is studied here. Eq. 1 is considered as a dyotropic rearrangement with X and SMe as migrating groups around Cp_2Zr-$CHSiMe_3$ bond.

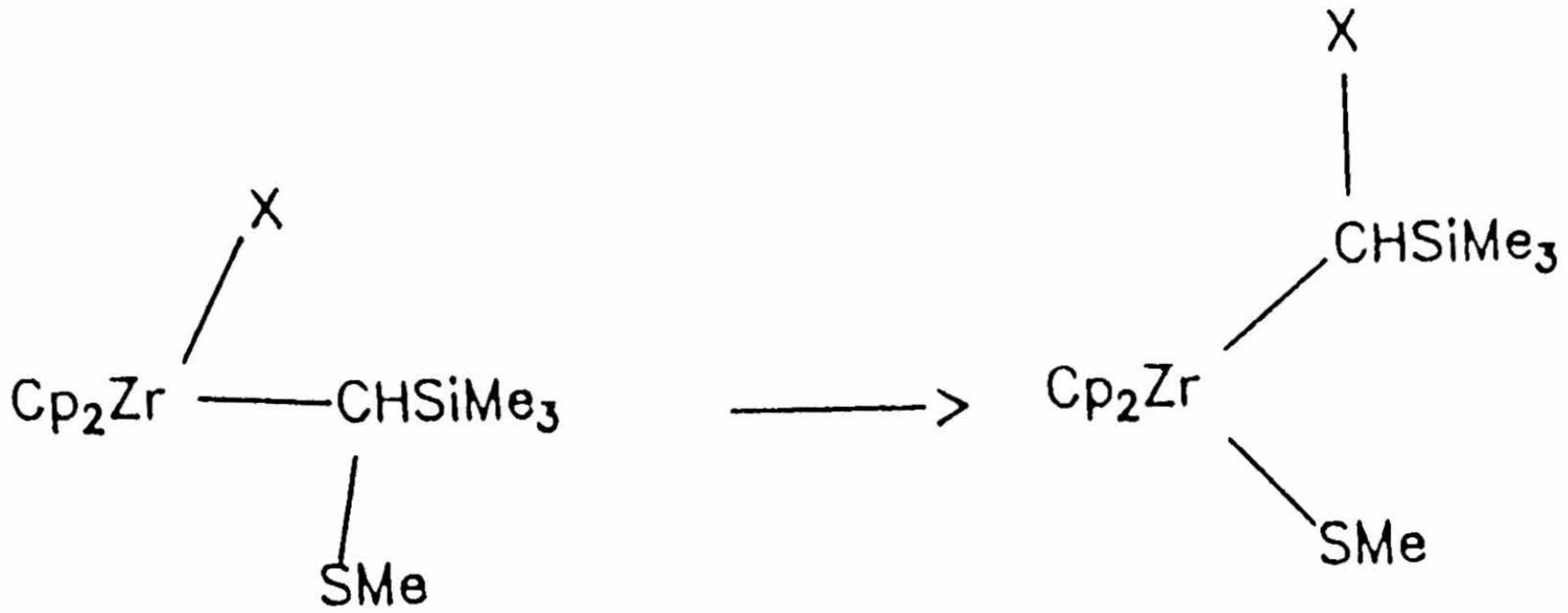

Eq. 1

	a	b	c	d
X	Ph	Me	CH_2Ph	Cl

The reaction takes place only when X = Ph but not when X = Me, Cl or CH_2Ph. The higher reactivity for the compound with X = Ph in comparison to that with X = Me, Cl or CH_2Ph is related to the energy match of molecular orbitals of the migrating fragment with those of the remaining fragment along an assumed reaction coordinate. Electronic structure calculations are done by the Fragment Molecular Orbital approach within the extended Huckel approximation. The reasons for the reactivity of Ph (and not the remaining groups) in eq. 1 are probed. Similar dyotropic rearrangements involving Cp_2Zr ligand complexes are also studied. The difficulties involved in assigning the migratory aptitudes of groups independent of the reactions are explained by comparing the interaction diagram with the two groups. (J. Organomet. Chem. 1990, **388**, 289-299).

b. Electronic structure and reactivity of $Cp_2Zr = E$ (E = O, S, NH and PH) complexes

Extended Huckel calculations are carried out on $Cp_2Zr=E$ (E = O, S, NH and PH) to understand their reactivity. These complexes are generated *in situ* and are trapped by ligands such as acetylenes and nitriles where there are two π orbitals perpendicular to each other. In contrast, these $Cp_2Zr=E$ complexes are not trapped by the ligands such as ethylenes or carbonyls where only one double bond is present. Fragment Molecular Orbital approach is used within the extended Huckel formalism to explain the reactivity of these class of compounds. The HOMO of $Cp_2Zr=E$ is an M-E π^* orbital. This is responsible for the higher reactivity of acetylenes and nitriles over ethylenes and carbonyls.

Chapter 4: Possibility of bond stretch isomerism in $[Cp(CO)_2M]_2(\mu$-E) complexes (M = Mn, Re, Cr and W; E = S, Se and Te); a molecular orbital study.

With two transition metal fragments (M) around a central main group element three basically different arrangements are possible: linear (4), bent (5) and triangular (6). All the complexes with 36 VEC are linear and those with 40 VEC are bent. The complexes with 38 VEC are present in both bent and triangular forms. Existence of two different structures which are connected by the variation of one interatomic distance as in 5 and 6 for the same number of electrons constitute bond stretch isomerism which is analyzed in this chapter.

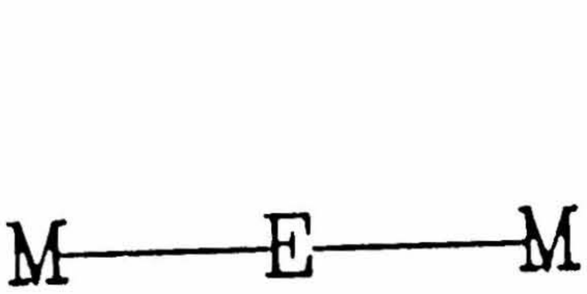

1

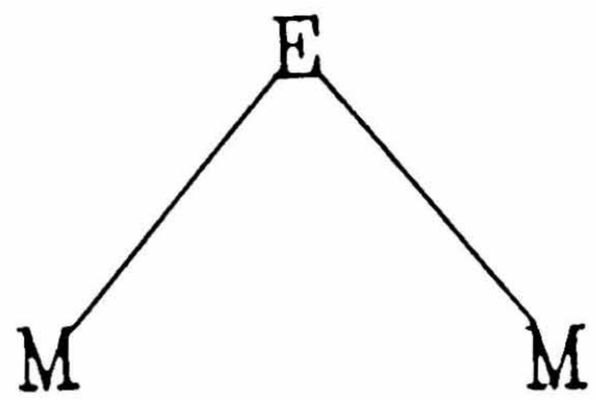

2

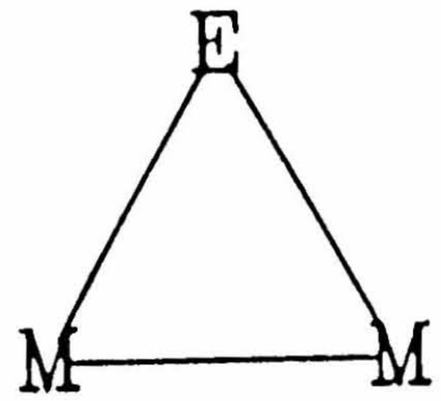

3

Molecular orbital study of $[Cp(CO)_2M]_2(\mu\text{-}E)$ (M = Mn, Re, W and Cr; E = S, Se and Te) indicates that a suitable M and E combination provides a double minima on the potential energy surface for M-M stretching. Mn (or Cr) complex with tellurido bridge has two minima, bent and triangular. The two minima are energetically comparable and are separated by a high barrier. Ab initio calculations on fixed geometries using the LANL1MB basis set supported the relative energies obtained as sum of one electron energies from extended Huckel calculations. Experimentally, the structure with bent geometry is known. Attempts to prepare the triangular structure should be rewarding. Similar bond stretch isomerism involving bent and triangular structures is unlikely in the remaining M and E combinations. (J. Organomet. Chem., **1994**, 0000)

Chapter 5: **Molecular mechanics and MNDO calculations on C_{60} and C_{70} and their substructures**

The discovery of fullerenes have generated a great deal of interest and activity at the interfaces of chemistry, physics and material science. In this chapter, we consider some possible synthetic avenues to C_{60} and C_{70}, along different symmetry

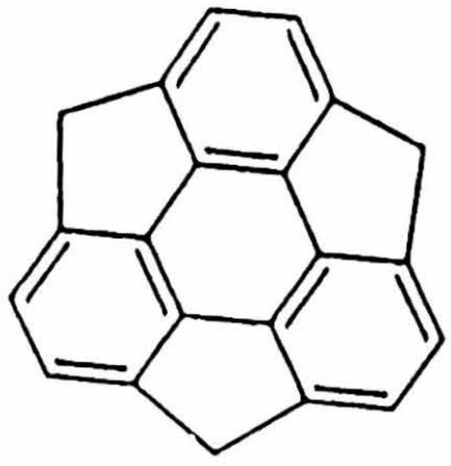

7, $C_{21}H_{12}$

8, $C_{20}H_{10}$

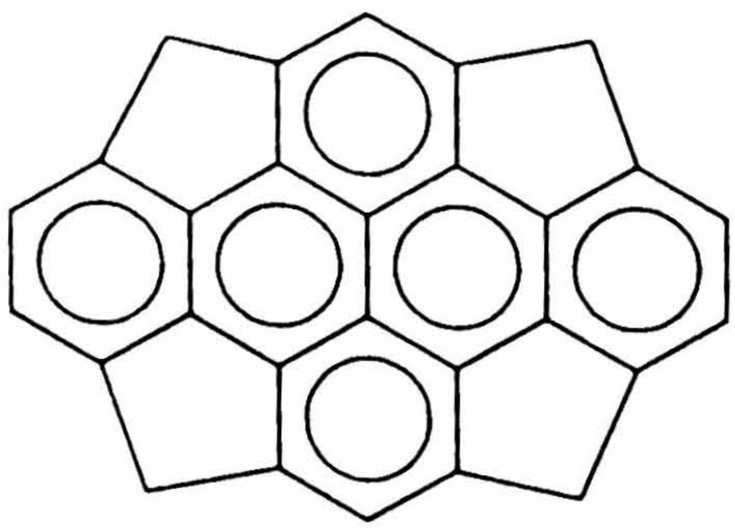

9, $C_{28}H_{14}$

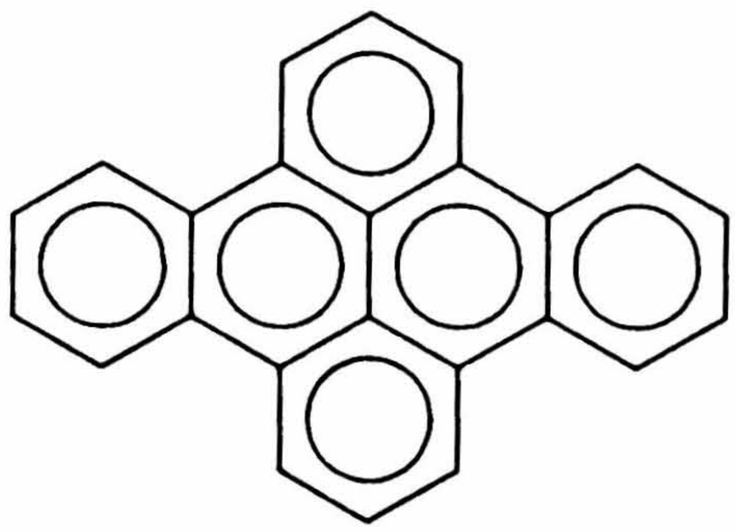

10, $C_{24}H_{14}$

pathways and evaluate the energies and structures of several key fragments enroute.

a. Molecular mechanics and MNDO calculations on sumanene and related substructures of C_{60}.

Strain energies of the hydrocarbons derived from the fragments of C_{60} along the C_5, C_3 and C_2 symmetry pathways indicate that the strain energy per carbon increases gradually along the C_3 and C_2 paths, but has a maximum at $C_{40}H_{10}$ along the C_5 path. Sumanene, 7, has been recognized as a possible fragment along C_3 route with an inversion barrier of 24.2 kcal mol^{-1} and a bowl depth of 1.15 A at MNDO level. This is to be contrasted with corannulene, 8, which is a more shallow bowl with a lower inversion barrier. The bond alternation in the central six membered ring of sumanene resembles that of C_{60}. The higher fragments have higher barriers. (J. Chem. Soc. Perkin Trans 2, 1993, 1867).

b. Molecular mechanics and MNDO calculations on pinakene and related substructures of C_{70}.

Possible synthetic avenues to C_{70} along different symmetry pathways are also carried out in this section . The fragment pinakene, $C_{28}H_{14}$, 9, is taken as a key fragment in C_{70}. The strain energy build up in the sequential placement of methylene bridges starting from $C_{24}H_{14}$, 10, to pinakene, 9, is estimated by using MMX and MNDO calculations. (J. Chem. Soc., Perkin Trans., 1994, 0000).

Chapter 1

Introduction

1.1 Introduction

Chemistry is an experimental science. Understanding molecular structures, evaluating molecular properties and effecting chemical transformations are of fundamental importance in Chemistry. Conceptual models based on the existing information to organize and understand the experimental observations and also to rationally design new experiments, are necessary for the progress of chemistry. Such frameworks at various levels constitute most of theory in chemistry.

Quantum mechanics provides the mathematical formalism to calculate properties of chemical interest.[1] However, exact solutions to the quantum mechanical formulation of any realistic system (with more than two electrons) cannot be obtained. One then resorts to approximate methods. Extensive work by theoretical chemists resulted in program packages to perform quantum chemical calculation at various levels of approximation. The tremendous progress in computer hardware and software is instrumental in making, slowly but surely, theoretical chemistry as an alternative approach for "doing chemistry".

The role of theory in the development of chemistry has been ever increasing. Not all experiments go along the planned paths. A number of strategies may be thought of for executing a specific experiment. A theoretical chemist using quantum mechanical methods and new generation computers, can in principle scrutinize quickly various possible mechanistic paths to effect a particular chemical

transformation and suggest what is the best approach. Experiments carried out along these suggested lines will prove the validity of the theoretical models. Occasionally, new models are necessary for explaining the observations. Interplay of experiment and theory help in developing deeper insight into a given problem. Theory has one special advantage: one need not synthesize a molecule to determine its properties! Similarly, understanding intermediates in a reaction, local minimum on a Potential Energy Surface, etc. which are often elusive for experimental verification can be calculated by theoretical methods with as much ease as is possible for a stable molecule. Thus, theory has transformed into a valuable adjunct to experiment in studying molecular structure and reactions.

Traditionally chemistry is divided into many branches such as organic, inorganic, organometallic etc. Extension of the concepts available in one branch to another is a way of building bridges between them. For example, the isolobal analogy helps building bridges between organic and inorganic chemistry.[2] A lot of new insights can be obtained by this process.

A brief discussion of various theoretical methods used in this thesis is given below.

Ab Initio Molecular Orbital Theory

The Schroedinger equation can be solved using the variational theory.[1] A variational calculation involves three steps: (i)

constructing the hamiltonian for the system, (ii) selecting a trial wave function containing variable parameters and (iii) minimizing the expectation value of energy with respect to the parameters constituting the wave function. The complete hamiltonian describing a system is very complicated and hence it is a general practice to use the hamiltonian derived from the Born-Oppenheimer approximation[3] for electronic structure calculations. The trial wave function is usually represented by the anti-symmetrized product of one-electron functions obtained from a single Slater determinant. The spatial part of the one electron functions are called molecular orbitals. These one-electron functions are further constructed using an appropriate basis set. Minimizing the total energy of the system with respect to the one electron functions results in Hartree-Fock equations. When these equations are derived using the linear combination of atomic orbitals (LCAO) for the MOs, Roothan MO equations are obtained which are relatively simpler to solve.[4] Rigorous solution of the Hartree-Fock-Roothan equations with no empirical parameters is known as ab initio MO theory.[5] The solutions of the Hartree-Fock-Roothan equations are self consistent and the method of solving is referred to as the self consistent field method.The results obtained from this methodology depend on the basis set employed. Various types of basis sets have been examined. Slater type orbitals (STO's) simulated by gaussian functions have been in use commonly.[6] Increasing the basis gives a better expectation value for energy. The limit at which the increase of basis set does not change the energy is known as Hartree-Fock limit. Often, Hartree-Fock approximation is

inadequate in obtaining the particular property of interest. Inclusion of electron correlation is essential in instances where major electron reorganization is expected. Two standard approaches are used to incorporate electron correlation. The first is configuration interaction, in which the wave function is constructed from many Slater determinants. Configuration Interaction can be used at various levels depending on the type of excited configurations included. The second is perturbation theory in which the perturbation series is truncated at the desired order.[7] The quality of the basis set also affects the calculations at the post Hartree-Fock levels.[8]

Semiempirical SCF methods

Although ab initio MO theory has proved to be extremely useful, it requires immense computational power for large systems. Evaluation of all the one and two electron integrals takes a large part of CPU time in ab initio calculations. Semiempirical approaches avoid the evaluation of many difficult integrals by making extensive use of the experimental information.[9] Electron repulsion integrals involving the overlap distribution are considered to be very small and are often ignored. This is called Zero Differential Overlap (ZDO) approximation.[10] There are a number of modified theories based on this idea. They differ mainly in the extent to which ZDO approximation is invoked in evaluating electron repulsion integrals. The most popular and reliable among them are MNDO[11] and AM1,[12] and hence only these two methods are employed in this thesis.

Extended Huckel calculations and Fragment Molecular Orbital Approach

Extended Huckel method,[13] pioneered by Hoffmann, has been developed into an extremely powerful method for doing electronic structure calculations on large molecules. The inherent simplicity and usefulness in constructing explanations makes this method extremely useful. Very valuable insights into chemical binding can be obtained by minimum computational effort.[14] The analysis of extended Huckel results relies mainly on symmetry, overlap, electron count and electronegativity and not as much on the sum of the one electron energies. Fragment Molecular Orbital[15] approach involves the construction of the MOs of a complex molecule from simpler and easily understood fragment MOs. This is best used within the extended Huckel formalism. Fragment Molecular Orbital approach within extended Huckel formalism is widely used in this thesis.

Frontier Molecular Orbital Theory

Frontier molecular orbital theory of Fukui, is one of the most successful qualitative theories to explain the feasibility of reactions in organic chemistry.[16] In addition to answering the basic question whether the reaction is allowed or forbidden, it also provides qualitative information about several other key features of the reaction. The shape, size and energy of frontier orbitals are helpful in predicting regio- and stereo-chemistries and also the rates of the reaction. It is most widely used in the

study of electrocyclic reactions. These ideas are extensively used in the next chapter.

Empirical Force Field Calculations

The empirical force field methods (Molecular Mechanics) within the classical mechanics are useful in solving many problems in chemistry[17]. These calculations use potential functions from classical mechanics to calculate the geometry of the molecules. Vibrational Force fields, which are used in these calculations, are taken from the experimental data from a large number of related molecules. Recently, force fields generated from the ab initio calculations have also been actively pursued.[18] The basis for Molecular Mechanics calculations is a generally accepted concept that many characteristics of bonds are transferable from molecule to molecule in a given family of molecules Deviation from these natural bond parameters brings in strain in the molecules. Molecular Mechanics has been a highly successful method in the study of molecular geometries, heats of formation and strain energies of hydrocarbons. Bond stretching, angle bending, torsion and van der Waals interactions are the most important terms included in the force fields. Additional terms are added to give the best possible fit to the available experimental values, such as geometries, heats of formation, dipole moments etc. In this study, we have used the MM2 force field, whose performance in predicting the structure and properties of hydrocarbons is well documented in the literature.[17-19]

Molecular Mechanics in general ignores the presence of electrons in the molecules. Subsequently, no information can be obtained about the details of the electronic structure. Therefore quantum mechanical procedures are to be adopted which give the electronic structure in addition to the molecular structure and energetics. There are attempts to include the results of Huckel model to Molecular Mechanics.[19]

The scope of the present investigation

Various theoretical methods of diverse sophistication are used in the present study. We have chosen the best method available to solve the problems in this thesis within the facilities available. When more demanding calculations were necessary, collaboration was sought from people with better computer facilities and their contributions are acknowledged appropriately. We have also performed collaborative studies with experimental groups to rationally design substrates that would undergo a desired reaction. A brief description of the problems studied is given below.

Chapter 2 deals with the effect of disubstitution on the relative stabilities and reactivity of cyclobutadienes. Cyclobutadiene has been a center of both theoretical and experimental investigations for a long time. While the chemistry of cyclobutadiene is rigorously explored theoretically, the effect of substitution on cyclobutadiene is not well understood. Cyclobutadiene and most of its derivatives are extremely reactive.

14-Electron transition metal fragments such as $Fe(CO)_3$ stabilize and release them easily on oxidation. These transition metal complexes have proved to be extremely useful in providing an easy access to cyclobutadiene for chemical transformations. The relative stabilities of the vicinal disubstituted cyclobutadienes play crucial role in deciding the regiochemistry of the Diels-Alder adducts. Cyclobutadiene and its derivatives dimerize quickly. However, further oligomerizations are not reported. Based on Frontier Molecular Orbital theory and semiempirical calculations, substitution of electron withdrawing groups in the vicinal position on cyclobutadienes is suggested to promote oligomerization by decreasing the HOMO-LUMO energy differences. Based on these suggestions Prof. Mehta and co-workers of our school have successfully carried out the oligomerization of 1,2-dicarbomethoxycyclobutadiene. [4+2]-Cycloaddition of 1,2-dicarbomethoxycyclobutadienes with quinones gives a mixture of regioisomers. We used the FMO and other arguments to rationalize the observed regiochemistry of [4+2]-cycloaddition 1,2-cyclobutadieneester with quinones. The role of transition metal fragments such as $Fe(CO)_3$ is confined to generate cyclobutadienes in the reaction, with no control over how the reaction takes place further. The reaction of a ligand as a part of the metal complex is very different from its reaction in isolation. In chapter 3, a transition metal mediated C-C bond formation via dyotropic rearrangements is studied. The chemistry of zirconocene complexes is very rich as these complexes are versatile reagents which promote many organic reactions. Here we rationalize the experimental results of the dyotropic

rearrangements and account for the observed reactivity. The intricacies involved in assigning the migratory aptitudes to the groups independent of the reaction is highlighted. Some new experiments were suggested based on the extended Huckel calculations.

The second section of chapter 3 deals with the electronic structure and reactivity of $Cp_2Zr=E$ (E = O, S, NH and PH) ligand complexes. These are very reactive species and are trapped by organic ligands such as acetylene. These can be classified as ME (M = transition metal fragment and E = main group element) complexes. Addition of another metal presents many new problems as exemplified by MEM complexes which are studied in chapter 4. In this chapter, we have seen how different geometrical arrangements are adapted by the compounds with the same number of valence electrons. Observing two structures with a variation in the length of a single bond is known as bond stretch isomerism. This is not yet unequivocally established in transition metal chemistry. Some of the examples suggested here could turn out to be the first examples of bond stretch isomerism. Chemistry of these cluster compounds involving transition metal fragments and bare main group elements is flourishing and many new structural features and bonding patterns are realized. However, the chemistry of clusters is revolutionized by the discovery of fullerenes. The unprecedented structures of C_{60}, a new allotropic form of carbon, have generated a lot of interest at the interfaces of chemistry, physics and material science. While there are numerous studies available on the properties of fullerenes, the synthetic

strategies towards them are relatively less studied.

Chapter 1 discusses the strain energy analysis of various fragments of C_{60} and C_{70}. The fragments of C_{60} and C_{70} are interesting in their own right. The detailed understanding of the smaller fragments is essential as they provide the stepping stones towards their syntheses in a stepwise manner. We discuss the strain energy build-up in symmetry imposed stepwise synthetic pathways towards these interesting molecules. Bond localization in C_{60} is explained by taking smaller fragments as models. We have also performed detailed MNDO calculations on sumanene[20] and pinakene[21] which are the key sub-structures of C_{60} and C_{70}. The strain energy build-up in the formation of the methylene bridges in sumanene and pinakene from triphenylene and 1,8-dehydro[5]phenanthracene is estimated

1.2 References

1. E. Schroedinger, Ann. Physik, **1926**, 79, 361.

2. R. Hoffmann, Angew. Chem. Int. Ed. Engl., **1982**, 21, 711.

3. (a) M. Born and J.R. Oppenheimer, Ann. Physik, **1927**, 84, 457.
   (b) A. Szabo and N.S. Ostlund, Modern Quantum Chemistry, McGraw-Hill, New York, **1982**.

4. (a) C.C.J. Roothan, Rev. Mod. Phys., **1951**, 23, 69.
   (b) C.C.J. Roothan, Rev. Mod. Phys., **1960**, 32, 179.

5. W.J. Hehre, L. Radom, P.v.R. Schleyer and J.A. Pople, Ab Initio Molecular Orbital Theory, John Wiley and Sons, New York, 1986.

6. J.C. Slater, Phys. Rev., **1930**, 36, 57.

7. C. Moller and M.S. Plesset, Phys. Rev., **1934**, 46, 618.

8. (a) E.R. Davidson and B. Feller, Chem. Rev., **1986**, 86, 681.
   (b) J. Almlof, T. Helgaker and P.R. Taylor, J. Phys. Chem., **1988**, 92, 3029.

9. J.A. Pople and D.L. Beveridge, Approximate Molecular Orbital Theory, McGraw-Hill, New York, **1970**.

10. (a) J.A. Pople, D.P. Santry and G.A. Segal, J. Chem. Phys, **1965**, 43, s129.
    (b) J. A. Pople and G. A. Segal, J. Chem. Phys, **1966**, 43, s136; 44, 3289.

11. M.J.S. Dewar and W. Thiel, J. Am. Chem. Soc., **1977**, 99, 4899, 4907.

12. M.J.S. Dewar, E.F. Healy, J.J.P. Stewart and E.G. Zoebisch, J. Am. Chem. Soc., **1977**, 107, 3902.

13. (a) R. Hoffmann and W.N. Lipscomb, J. Chem. Phys., **1962**, 36,

2179.

(b) R. Hoffmann, J. Chem. Phys., **1963**, 38, 1397.

(c) M. Wolfsberg and L. Helmholz, J. Chem. Phys., **1952**, 20, 837.

14. (a) P.J. Hay, J.C. Thibeault and R. Hoffmann, J. Am. Chem. Soc., **1975**, 97, 4884.

(b) B.M. Gimark, Molecular Structure and Bonding, Academic Press; New York, **1979**, 216.

15. H. Fujimoto and R. Hoffmann, J. Phys. Chem., **1974**, 78, 1167.

16. (a) I. Fleming, Frontier Orbitals and Organic Reactions, John Wiley: New York, 1976.

(b) R.B. Woodward and R. Hoffmann, The conservation of Orbital Symmetry, Academic Press, New York, 1970.

(c) A. Streitwieser, Molecular Orbital Theory for Organic Chemists, John Wiley and Sons, Inc., New York, 1961.

(d) M.J.S. Dewar, The Molecular Orbital Theory of Organic Chemistry, McGraw-Hill, New York, 1969.

17. (a) U. Burkert and N.L. Alliger, Molecular Mechanics; ACS Monograph, Washington, D.C., 1982, vol. 177.

(b) N.L. Allinger, J. Am. Chem. Soc., **1977**, 99, 8127.

(c) N.L. Allinger, Adv. Phys. Org. Chem., **1986**, 13.

18. "Special issue on Molecular Mechanics" in Chem. Rev., **1993**, 93, #7.

19. (a) N.L. Allinger and J.T. Sprague, J. Am. Chem. Soc., **1973**, 95, 3893.

(b) N.L. Allinger and J. Kao, J. Am. Chem. Soc., **1977**, 99, 975.

20. G. Mehta, S.R. Shah and K. Ravikumar, J. Chem. Soc., Chem. Com., **1993**, 1006.

21. E.D. Jemmis, G.N. Sastry and G. Mehta, J. Chem. Soc., Perkin Trans. 2, **1994**, 0000.

Chapter 2

Disubstituted cyclobutadienes: relative stabilities and reactivity

2.0 General Introduction

The structure of cyclobutadiene has been debated for a long time.[1] There is now general agreement that the ground state is a singlet with rectangular geometry, which automerizes rapidly at room temperature.[1,2] Cyclobutadiene and most of its derivatives are extremely reactive and isolating them is very difficult under ordinary conditions. 14-electron transition metal fragments such as $Fe(CO)_3$ stabilize cyclobutadiene and release them when necessary by oxidative decomposition.[3] A large number of substituted cyclobutadienes are synthesized as $Fe(CO)_3$ complexes allowing easy access to free cyclobutadiene for chemical transformations.[4] The C-C bond lengths of cyclobutadienes in transition metal complexes are nearly equal. In the free state it adopts thermodynamically more stable rectangular form.

The first section of the chapter deals with the relative stabilities of disubstituted cyclobutadienes. The second section deals with reactivity of these disubstituted cyclobutadienes in some [4+2]-cycloaddition reactions. The Frontier orbital control on the oligomerization of cyclobutadienes as a function of substituents is presented. The regiochemistry of the adducts with quinones observed experimentally are rationalized based on the Frontier Molecular Orbital theory.

2.0 General Introduction

The structure of cyclobutadiene has been debated for a long time.[1] There is now general agreement that the ground state is a singlet with rectangular geometry, which automerizes rapidly at room temperature.[1,2] Cyclobutadiene and most of its derivatives are extremely reactive and isolating them is very difficult under ordinary conditions. 14-electron transition metal fragments such as $Fe(CO)_3$ stabilize cyclobutadiene and release them when necessary by oxidative decomposition.[3] A large number of substituted cyclobutadienes are synthesized as $Fe(CO)_3$ complexes allowing easy access to free cyclobutadiene for chemical transformations.[4] The C-C bond lengths of cyclobutadienes in transition metal complexes are nearly equal. In the free state it adopts thermodynamically more stable rectangular form.

The first section of the chapter deals with the relative stabilities of disubstituted cyclobutadienes. The second section deals with reactivity of these disubstituted cyclobutadienes in some [4+2]-cycloaddition reactions. The Frontier orbital control on the oligomerization of cyclobutadienes as a function of substituents is presented. The regiochemistry of the adducts with quinones observed experimentally are rationalized based on the Frontier Molecular Orbital theory.

2.1 Relative Stabilities of Disubstituted Cyclobutadienes. An Ab initio Molecular Orbital Study

2.1.1 Abstract

Ab initio molecular orbital calculations are carried out on the disubstituted cyclobutadienes, **I-III**, X = Me, OH, CN, $CH=CH_2$, CH_2^+ and CH_2^- to estimate their relative isomer stabilities. All the structures are optimized at HF/3-21G, HF/6-31G* and MP2/6-31G* levels of theory. Single point calculations are performed at QCISD(T)/6-31G* level of theory on the MP2/6-31G* optimized geometries. Two distinct minima are characterized for the vicinal disubstituted system, for X = Me, OH, CN and $CH=CH_2$. The relative energy ordering is **III** < **II** < **I**, for all the substituents except for $CH=CH_2$. For vinyl substituent the ordering is **I** < **III** < **II**. The dependence of relative energies on (a) the basic tendency of ethylene to add on substituents, (b) the repulsive interaction between the double bonds and (c) the electrostatic interaction is described. The loss of cyclobutadiene character is encountered with the extreme substituents, CH_2^+ and CH_2^-. Various conformational isomers corresponding to the Me, OH and $CH=CH_2$ substitution are analyzed. The calculated conformational preferences highlight the limited delocalization of the double bonds in cyclobutadienes.

2.1.2 Introduction

Vicinal disubstituted cyclobutadienes have a choice of two rectangular forms, **I** and **II**. Only one 1,3-disubstituted derivative is possible. Both the substituents are formally on the same double bond in **I**. In **II**, the substituents are on two different double bonds. Experiments on vicinal diphenylcyclobutadienes indicate the existence of an equilibrium mixture of two distinct rectangular forms, **I** and **II** (X = Ph).[5] Based on the distribution of Diels-Alder adducts with quinones[5] and semiempirical calculations[6], 1,2-diphenylcyclobutadiene, **I**, is judged to be thermodynamically more stable than the 1,4 isomer, **II**. In contrast, the regiochemistry of some of the adducts obtained from dicyano[7] and dimethylester derivatives[8] suggest **II** to be more stable than **I**. Semiempirical AM1

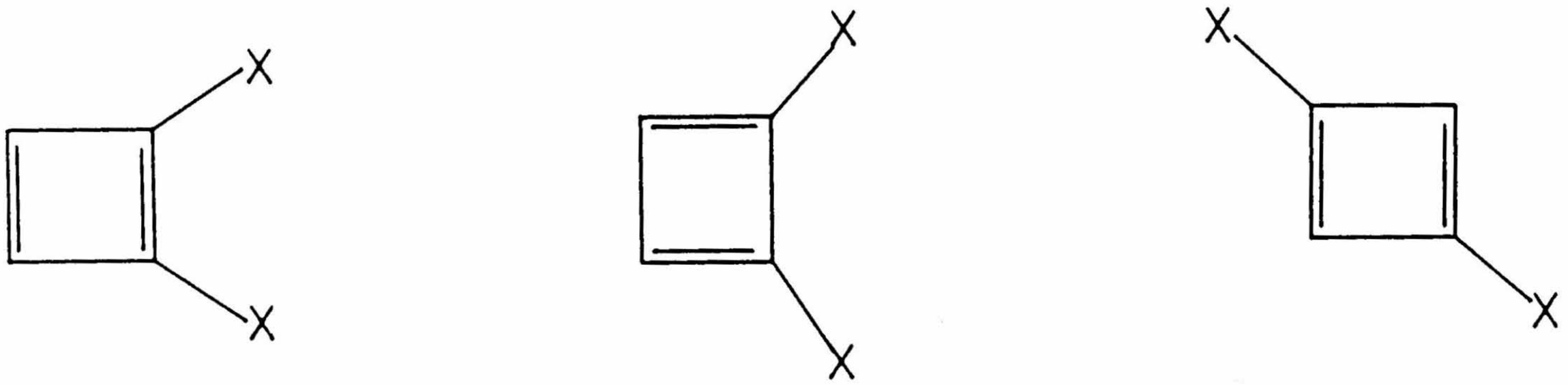

I II III

	a	b	c	d	e	f
X	CH_3	OH	CN	$CH{=}CH_2$	CH_2^+	CH_2^-

calculations confirm that II is more stable than I for X = COOMe.[9] A mixture of adducts are obtained in the above reactions and diverse regiochemistries are observed.[6-9] Obviously, relative stabilities of I and II depend on the substituents and play a key role in governing the regioselectivities. The only theoretical study involved a CNDO estimate of relative stabilities of dihalo cyclobutadienes.[10] It is ideal to have a qualitative and quantitative understanding of the substituent effect in designing synthetic strategies involving cyclobutadienes profitably.

The effect of substituents (X = CN, CH_3, OH, $CH{=}CH_2$, CH_2^+ and CH_2^-) on the relative stabilities of the three isomeric forms I, II and III is discussed here. The factors controlling the relative stabilities as well as the conformational preference of the substituents (Me, OH and $CH{=}CH_2$ derivatives) within a given isomeric form are also analyzed.

2.1.3 Method of calculations

The geometries of I, II and III are fully optimized employing standard procedures[11] at the HF/3-21G,[12] HF/6-31G*[13] and MP2(FC)/6-31G*[14] levels of theory. Single point calculations at the QCISD(T)/6-31G*[15] level are done on MP2/6-31G* optimized geometries. For a given isomeric form, several conformers are possible with Me, OH and $CH{=}CH_2$ substituents. Only the most favourable conformational isomers are studied at all levels. The relative energies and the nature of the stationary points of the less stable conformational isomers are evaluated only at the HF/3-21G level. Fragment Molecular Orbital approach[16] explains

most of the relative energy orderings. The relative energies obtained at the QCISD(T)/6-31G*//MP2/6-31G* level of theory and geometries at the MP2/6-31G* level are used in the discussion unless otherwise specified. The calculations are done using Gaussian92 program package.[17] QCISD(T) calculations are done using MOLPRO package.[18]

2.1.4 Results and discussion

The structure and relative energies of the isomers are given first. Various factors that might contribute to the relative stabilities are discussed next. Conformational preferences of Me, OH and $CH=CH_2$ substituents are discussed at the end. The total energies are given in Table 2.1.1 along with zero point energies at HF/6-31G* level. Table 2.1.2 gives the relative energies of the three isomeric forms for X = Me(**Ia-IIIa**), OH(**Ib-IIIb**), CN(**Ic-IIIc**), $CH=CH_2$(**Id-IIId**), CH_2^+(**IIe-IIIe**) and CH_2^-(**IIf-IIIf**). The two types of vicinal disubstituted isomers (**I** and **II**) are minima, for X = Me, OH, CN and $CH=CH_2$. In general isomeric form **III** is the most stable, except for vinyl substitution. The energy differences among the methyl derivatives, **Ia**, **IIa** and **IIIa**, are very low (Table 2.1.2). The 1,3-dihydroxy cyclobutadiene, **IIIb**, is more stable than **Ib** and **IIb** by 9.04 and 3.90 kcal mol^{-1} respectively. In the dicyano derivatives the relative energy differences are very low. The stability ordering of the isomeric forms for these substituents is the same (**III** > **II** > **I**). The extra conjugating group, $CH=CH_2$, reverses the general trend; **Id** is the most stable isomer.

TABLE 2.1.1: Absolute energies (in hartrees) and Zero Point Energies (in kcal mol^{-1}) of substituted cyclobutadienes.

No.	HF/3-21G	HF/6-31G*	MP2/6-31G*	QCISD(T)/6-31G*// MP2/6-31G*	ZPE (NIMAG)
Ia	-230.42531	-231.72830	-232.49707	-232.58736	79.3(0)
IIa	-230.42567	-231.72882	-232.49749	-232.58772	79.3(0)
IIIa	-230.42643	-231.73001	-232.49782	-232.58817	79.2(0)
Ib	-301.65386	-303.35012	-304.21017	-304.27802	48.2(0)
IIb	-301.65941	-303.35714	-304.21789	-304.28450	48.1(0)
IIIb	-301.66954	-303.37085	-304.22515	-304.29091	48.0(0)
Ic	-335.21076	-337.11059	-338.17763	-338.25497	40.9(0)
IIc	-335.21202	-337.11266	-338.17780	-338.25597	41.0(0)
IIIc	-335.21353	-337.11435	-338.17635	-338.25681	40.9(0)
Id	-305.70049	-307.42910	-308.44128	-308.55372	87.1(0)
IId	-305.69487	-307.42341	-308.43593	-308.54856	87.0(0)
IIId	-305.69950	-307.42874	-308.43910	-308.55259	86.9(0)
IIe	-228.51921	-229.83278	-230.53064	-230.61685	63.3(0)
IIIe	-228.55842	-229.87054	-230.54890	-230.63728	63.9(0)
IIf	-228.93674	-230.23406	-231.01662	-231.09690	55.5(4)
IIIf	-228.98297	-230.28311	-231.05003	-231.130225	56.7(2)

TABLE 2.1.2 : Relative energies (kcal mol^{-1}) of substituted cyclobutadienes.

No.	HF/3-21G	HF/6-31G*	MP2/6-31G*	QCISD(T)/6-31G*// MP2/6-31G*
Ia	0.79	1.17	0.55	0.59
IIa	0.55	0.83	0.29	0.36
IIIa	0.00	0.00	0.00	0.00
Ib	9.49	13.00	13.00	9.04
IIb	5.91	8.49	4.45	3.90
IIIb	0.00	0.00	0.00	0.00
Ic	1.84	2.37	0.12	1.15
IIc	1.15	1.15	0.00	0.62
IIIc	0.00	0.00	-0.81	0.00
Id	0.00	0.00	0.00	0.00
IId	3.54	3.71	3.49	3.37
IIId	0.62	0.27	1.43	0.77
IIe	25.22	23.91	11.67	13.03
IIIe	0.00	0.00	0.00	0.00
IIf	33.83	29.74	19.90	19.82
IIIf	0.00	0.00	0.00	0.00

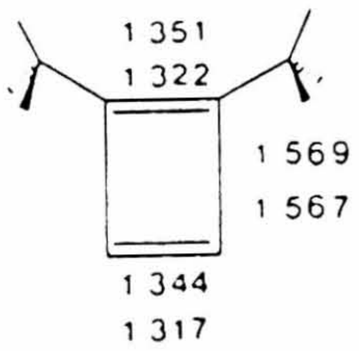

Ia, C_{2v}

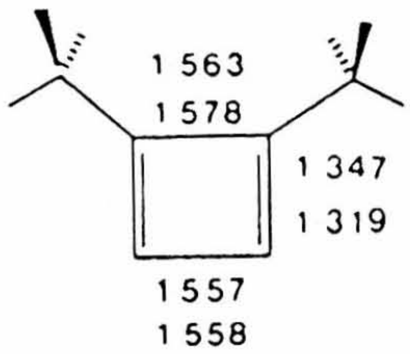

IIa, C_{2v}

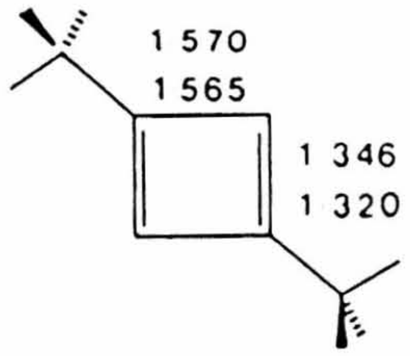

IIIa, C_{2h}

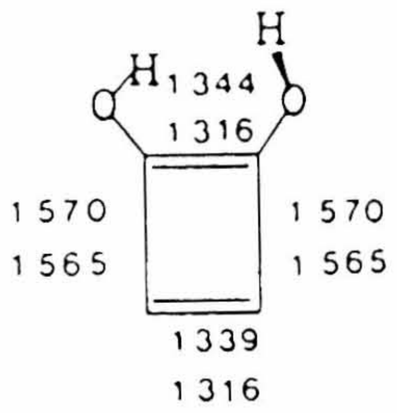

Ib, C_1

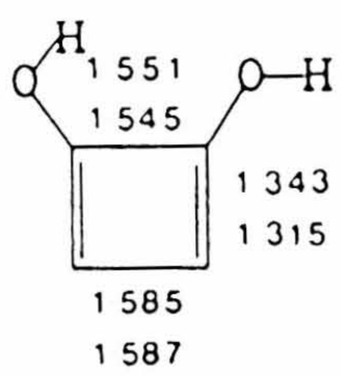

IIb, C_s

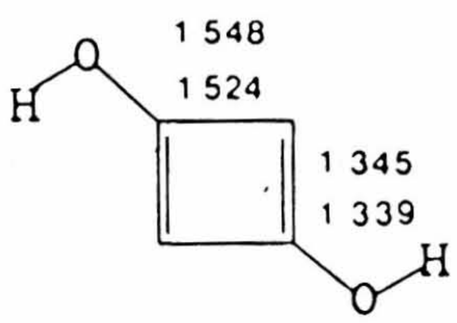

IIIb, C_{2h}

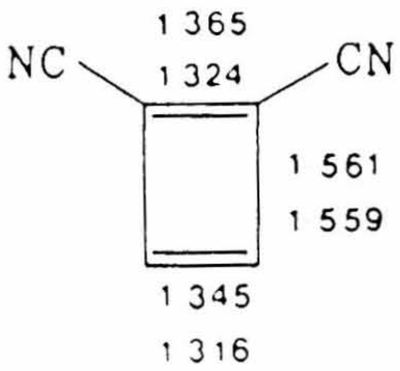

Ic, C_{2v}

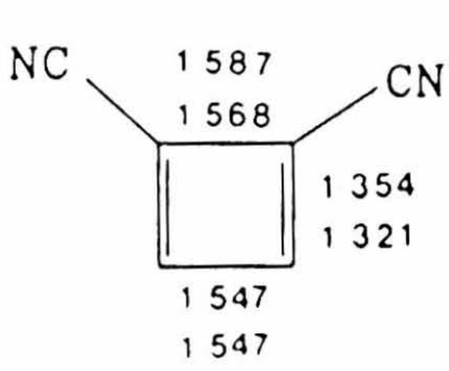

IIc, C_{2v}

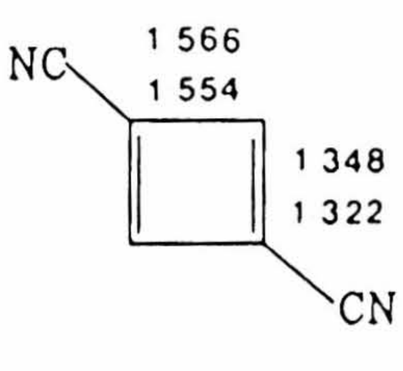

IIIc, C_{2h}

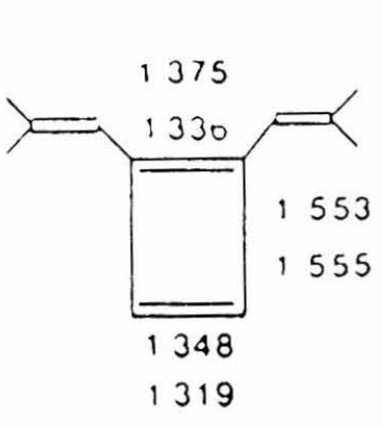

Id, C_{2v}

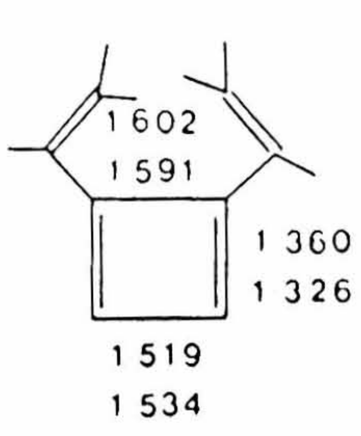

IId, C_2

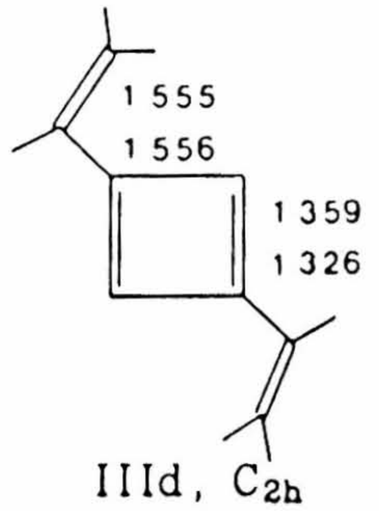

IIId, C_{2h}

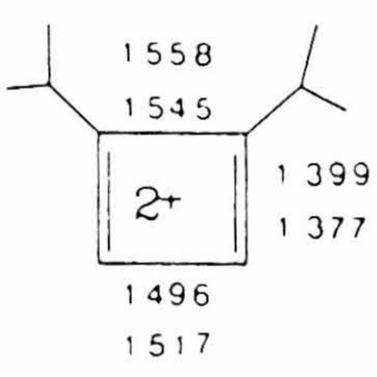

IIe, C_{2v}

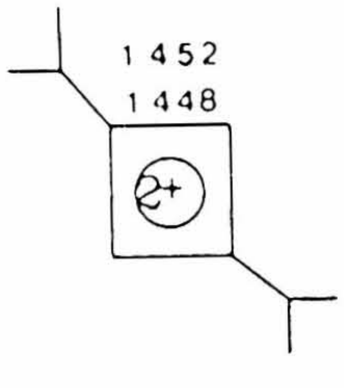

IIIe, D_{2h}

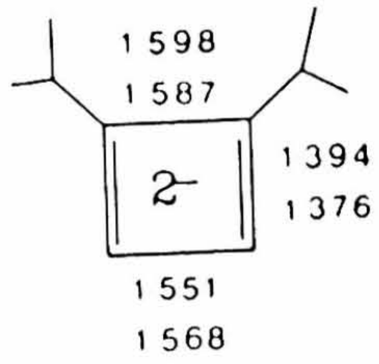

IIf, C_{2v}

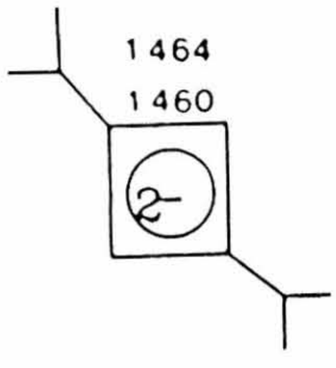

IIIf, D_{2h}

Fig. 2.1.1: Structures of **I, II** and **III** (X = CN, Me, OH, $HC{=}CH_2$, CH_2^+ and CH_2^-) with MP2/6-31G* (first entry) and HF/6-31G* (second entry) bond lengths.

The important bond lengths of the structures considered in this study are depicted in Figure 2.1.1. The single and double bond lengths in the parent cyclobutadiene are 1.568 and 1.317 (HF/6-31G*), 1.565 and 1.343 (MP2/6-31G*) and 1.549 and 1.349 Å (MCSCF(DZP)) respectively.[2,19] We observe a significant change in the double bond length (0.026 Å) going from HF to MP2 level while there is virtually no change in the single bond length. This may be a direct consequence of mixing in LUMO which has strong antibonding interaction across the short C-C bond. The optimized double bond length of cyclobutadiene at MP2 level compares closely with MCSCF(DZP) values, but there is a small change in the single bond length (0.016 Å). Figure 2.1.2 leads to the general observation that the substituents have only minor effect on the bond alternation in cyclobutadiene.[1,2] The C-C bonds with two substituents, except for **IIb**, are slightly elongated compared to that between the two unsubstituted carbon atoms whether these are single or double bonds. The π-delocalization on substitution is mainly responsible for the calculated changes in the bond lengths. The effect of π-delocalization is the highest with the vinyl substitution. As a result, in **IId** the bond lengths are 1.602 and 1.519 Å for substituted and unsubstituted single bond respectively (Fig. 2.1.1). In **IIb** the disubstituted single bond has shorter bond length (1.551 Å) compared to the unsubstituted one (1.585 Å). This may be attributed to the hydrogen bonding present in this molecule. The electrostatic effects between the adjacent carbons in the C_4 ring also contribute to the observed structure.

The ultimate electron withdrawing and electron donating

substituents based on carbon, CH_2^+ and CH_2^-, remove the rectangular nature of cyclobutadiene when these are at the 1,3 positions. When these two substituents, CH_2^+ and CH_2^-, are at vicinal positions there exists only one isomer, **II**. The 1,2-bismethylenecyclobutadiene dication (**Ie**) and dianion (**If**) on optimization goes to **IIe** and **IIf** respectively. **IIe** is a minimum while **IIf** is a higher order stationary point. **IIIe** and **IIIf** on optimization collapse to D_{2h} symmetry. **IIIe** is a minimum, but **IIIf** has two imaginary frequencies corresponding to the out-of-plane motions of the C-H bond. IIIe has been considered as an alternative for benzene dication in addition to the other structures considered previously and is higher in energy by 31.5 kcal mol^{-1} than $C_6H_6^{2+}(C_{5v})$ at HF/6-31G* level.[20] Both the methylene groups are in the plane of the molecule in **IIe**, **IIIe**, **IIf** and **IIIf**.

Methyl, OH and $CH=CH_2$ substituents bring additional conformational isomers and they are discussed separately below. The structures presented in Figure 2.1.2 for Me, OH and $CH=CH_2$ are the most stable conformers within a given isomeric structure.

Possible factors controlling relative stabilities

There are several ways of analyzing the relative stabilities of **I**, **II** and **III**. The basic tendency of ethylene to add on substituents is considered first by the following isodesmic equation (eq. 2.1.1).[17,21] This gives a measure of one of the factors that control the relative stabilities of **I** and **II**. The exothermicity of the equations shows that in general the

stabilization obtained by the first substitution is greater than that from the second substitution on ethylene. In other words, given a choice this preference is least for the vinyl substituent which extends the π-conjugation. Eq. 2.1.1 would lead one to conclude that **II** will always be more stable than **I**. This is true for all substituents except vinyl. Despite the large difference in relative energies between **I** and **II** for CN and OH (0.52 and 5.14 kcal mol^{-1}) the exothermicities of eq. 2.1.1. for X = CN and OH differ by 1.42 kcal mol^{-1} only. Clearly there would be additional factors that control the relative stabilities of **I**, **II** and **III**.

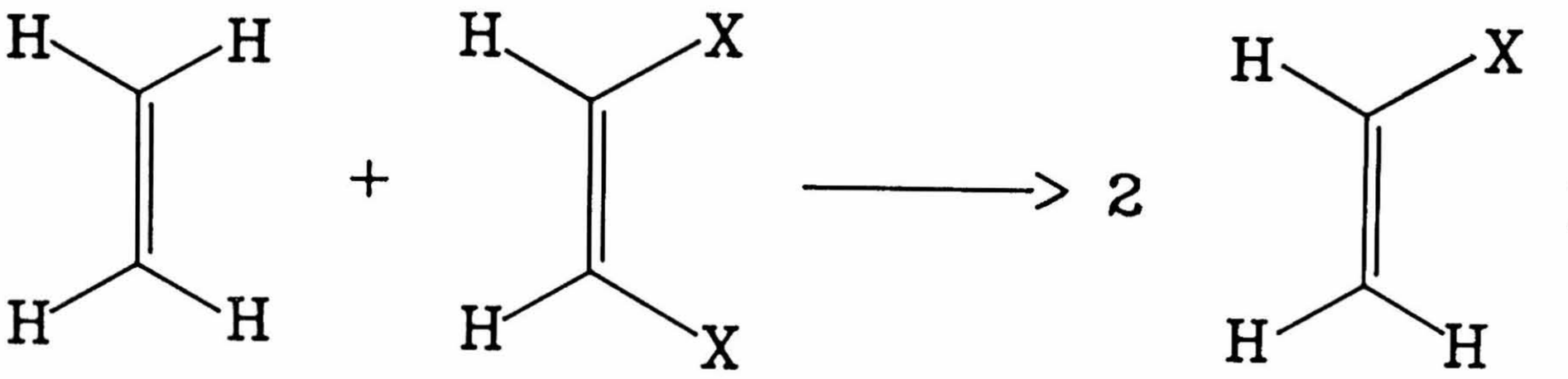

Eq. 2.1.1

X	E (kcal/mol)
Me	−1.20
CN	−5.34
OH	−3.92
$CH{=}CH_2$	−0.81

Cyclobutadiene can be viewed as two double bonds, interacting with each other. If the repulsive, four electron-two orbital, interaction is reduced between the double bonds, the

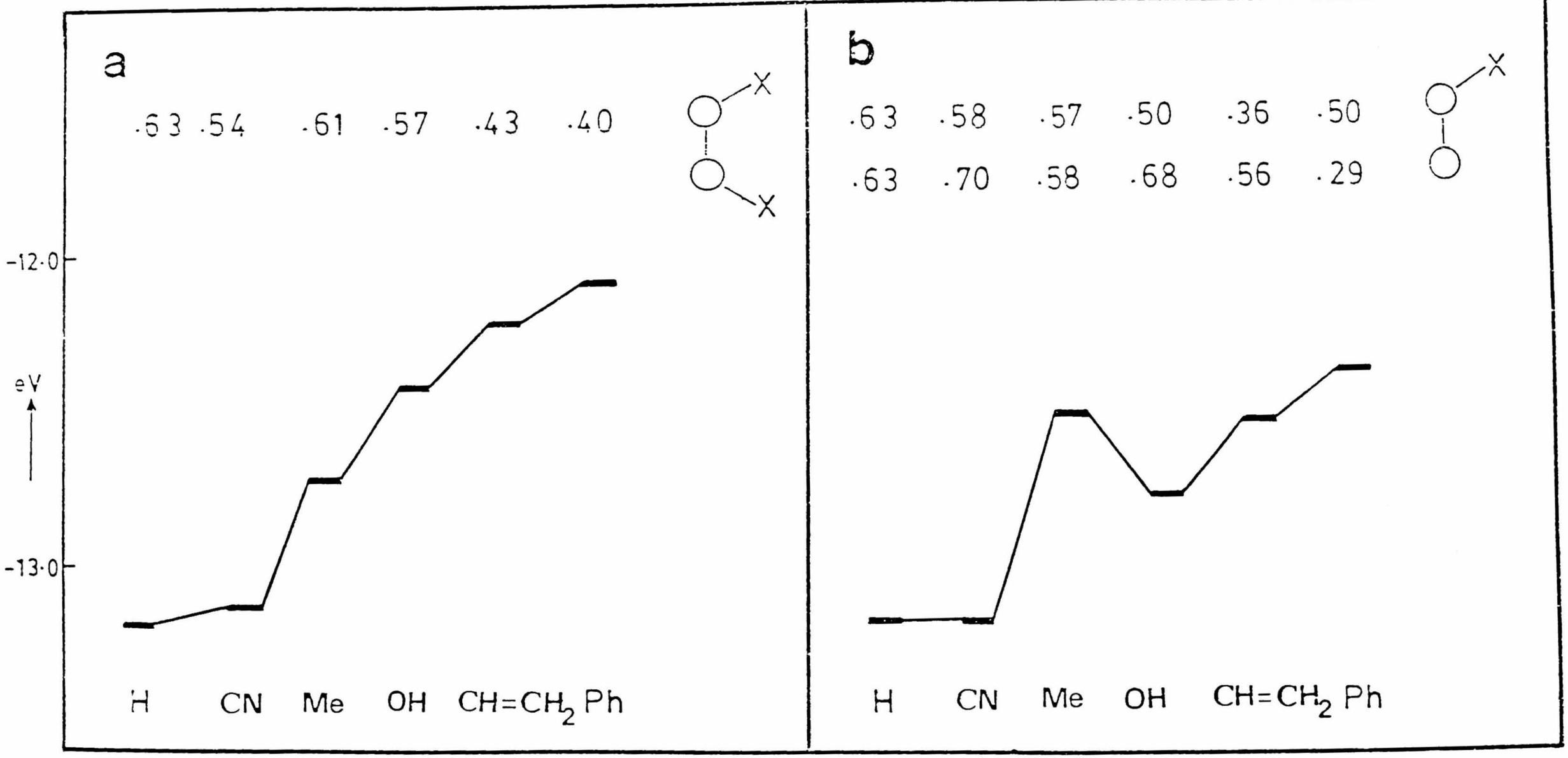

Fig. 2.1.2: The energy levels and the magnitudes of the coefficients of the π molecular orbitals of the bent acetylene with (a) two and (b) one substituents.

molecule becomes more stable. Different substituents change this repulsive interaction in the three isomeric forms differently. The Fragment Molecular Orbital approach within the extended Huckel formalism is employed to understand this interaction in detail. Cyclobutadienes may be visualized as constructed from two bent acetylenes. The energies and the size of the coefficients of the π orbitals of the di- (Figure 2.1.2a) and monosubstituted bent acetylenes (Figure 2.1.2b) should contribute to the strength of the π interaction. The difference in the energy between the π orbitals of the disubstituted acetylene and unsubstituted one is very high for X = $CH{=}CH_2$ and hence the interaction between the two double bonds should be very small. The size of the π-orbital coefficients at the interacting carbons is also reduced. Therefore, repulsion between the two double bonds is the lowest with the extra conjugating group, vinyl, compared to the other substituents. We have also calculated the energies of the fragments with phenyl substituents and found that the difference between the π molecular orbitals considered here is even higher (Figure 2.1.1b). Thus, according to this **I** with vinyl or phenyl as substituent would be amongst the least destabilized. The two occupied π orbitals of the acetylenes leading to **II** are essentially at the same energy. The two isoenergetic double bonds repel each other more strongly than that in **I**. This is a head-to-head interaction. A head-to-tail interaction leads to **III**. The head-to-head interaction is stronger with more overlap between the double bonds.[22] In **III** the two double bonds repel less strongly compared to that of **II**, independent of the substituent.

Thus the stabilization found in eq. 2.1.1 for monosubstituted ethylene is opposite to the effect found in the model that considers the repulsive interaction of 2 π bonds. The calculated relative energies between **I** and **II** is a result of these effects. In the process vinyl derivative which has the largest difference between the π levels (Fig. 2.1.1a) is more stable in structure **I** than in **II**. This is also the substituent that gave least exothermicity for eq. 2.1.1.

Electrostatic forces play a major role when the electronegativity difference between the substituent and carbon is significant.[23] The head-to-head interaction that leads to **II** brings maximum electrostatic repulsion. This would explain the large difference in the relative energies with hydroxy substitution, **Ib-IIIb** (Table 2.1.2).

Conformational preference for Me, OH and $CH=CH_2$ substitutions

The choice of most stable conformer among methyl, hydroxy and vinyl derivatives is not clear. Therefore, various conformers are studied in detail. The nature of the stationary points are identical at HF/3-21G and HF/6-31G* levels for the molecules previously studied in this chapter (Fig. 2.1.1). Hence, all the conformers which are higher in energy are studied only at HF/3-21G level. For the sake of uniformity, in this section, results obtained at HF/3-21G level are used throughout. Qualitative arguments and analogies to previously known structures are used to account for the calculated conformational preferences.

Fig 2.1.3 gives the conformations considered for the methyl derivatives. The most stable structures, **Ia**, **IIa** and **IIIa**, have C-H bond syn (i.e., eclipsed) with the double bond. The situation is similar to that found in propene and related molecules.[24] The conformations where one or both methyl groups are not syn to the double bond are higher in energy and are not minima. The relative energies indicate that for each unfavourable conformation, there is a destabilization of about 2 kcal mol^{-1}, and one imaginary frequency corresponding to the motion of the hydrogens in the methyl groups. Accordingly, structures **1**, **3** and **5** have one imaginary frequency while **2**, **4** and **6** have two imaginary frequencies. There is only one minimum on the methyl rotational potential.

The factors controlling the conformational stabilities of hydroxy derivatives are many fold. Figure 2.1.4 gives the conformations considered for OH substitution and their relative energies with respect to **IIIb**. The number of imaginary frequencies are given in the parenthesis. Although hydroxy derivatives are not synthetically accessible, corresponding alkoxy derivatives are realistic targets to be stabilized as transition metal complexes. The conformational preferences of methoxy and ethoxy derivatives should be similar to those of hydroxy derivatives.

Let us start from the 1,3-dihydroxycyclobutadiene, **III**, which is the easiest to explain. None of the conformations with

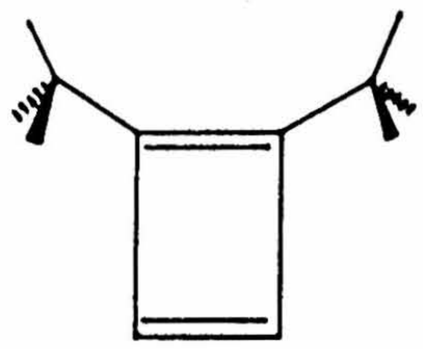

Ia, C_{2v}, 0·79 (0)

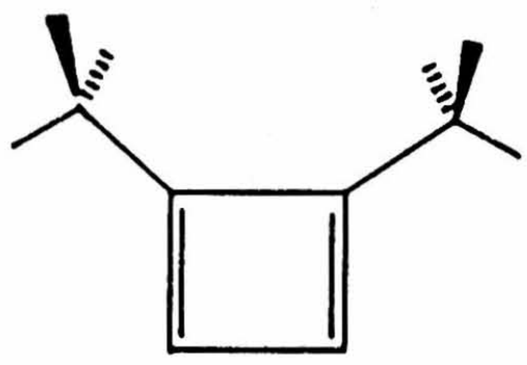

IIa, C_{2v}, 0·55 (0)

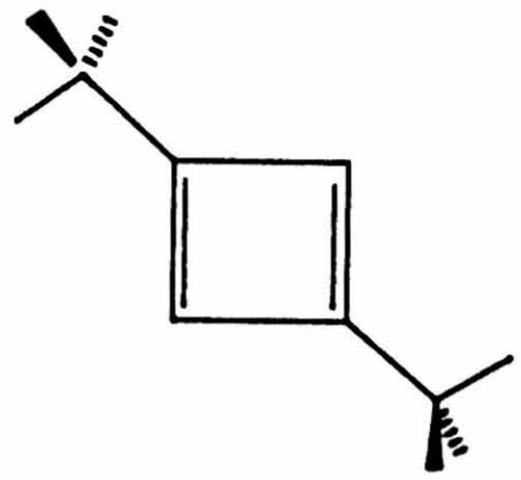

IIIa, C_{2h}, 0·00 (0)

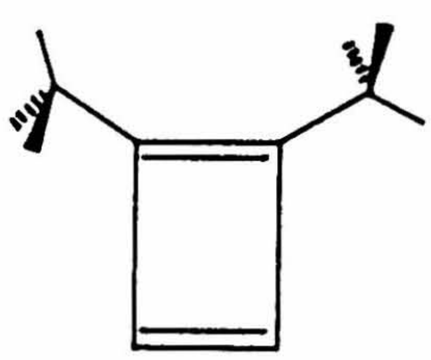

1, C_s, 2·44 (1)

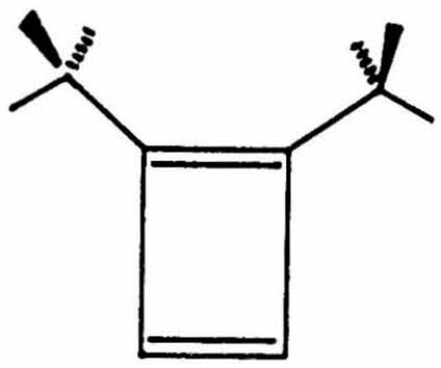

2, C_{2v}, 3·78 (2)

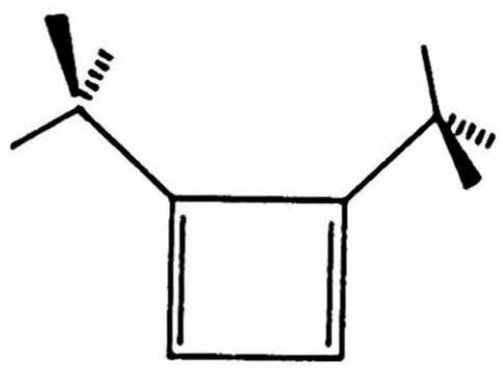

3, C_s, 2·13 (1)

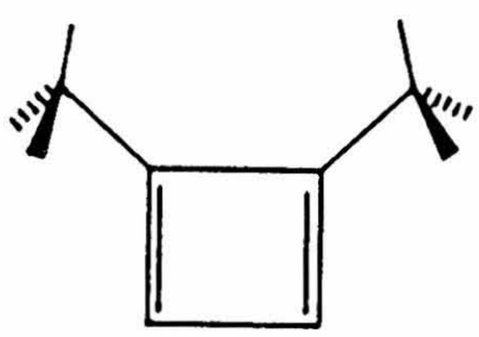

4, C_{2v}, 3·99 (2)

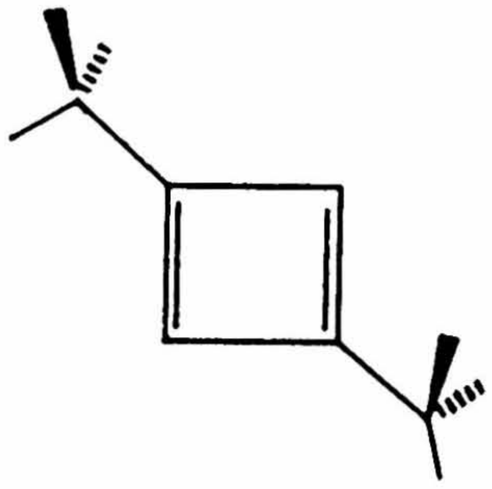

5, C_s, 1·91 (1)

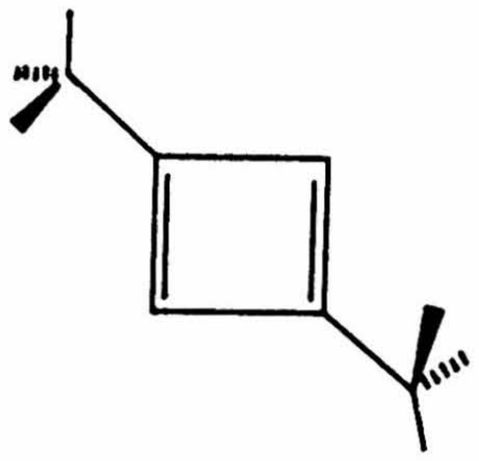

6, C_{2h}, 3·71 (2)

Fig. 2.1.3: Relative energies (kcal mol^{-1}) of conformational isomers **Ia-IIIa** at HF/3-21G level. The number of imaginary frequencies are given in the parentheses.

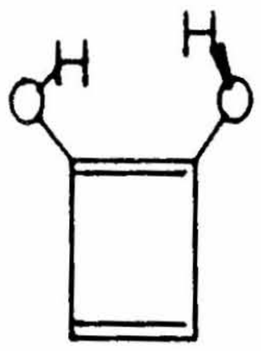

Ib, C_1, 9·49 (0)

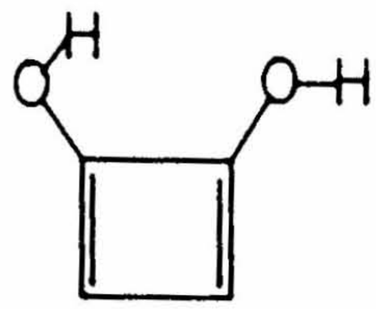

IIb, C_s, 5·91 (0)

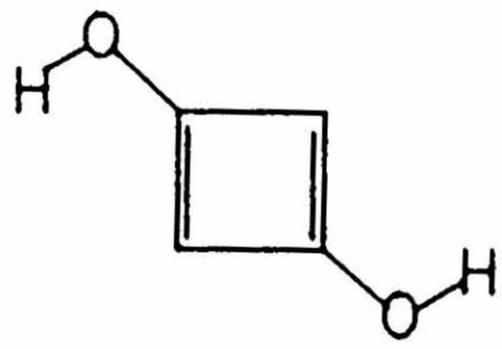

IIIb, C_{2h}, 0·00 (0)

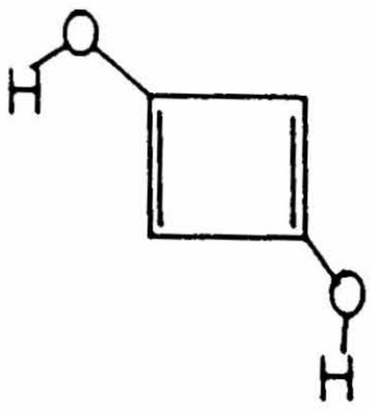

7, C_s, 1·39 (0)

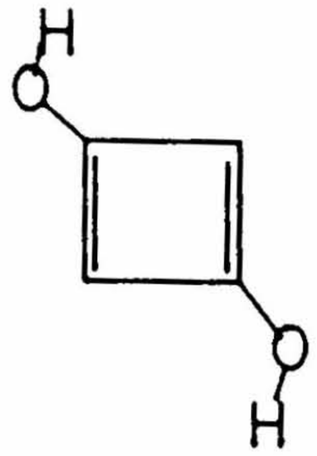

8, C_{2h}, 2·25 (0)

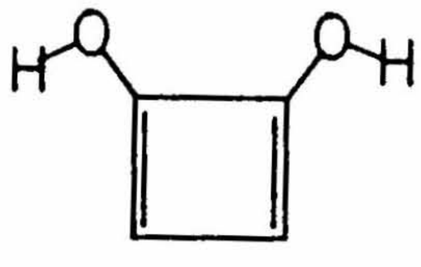

9, C_{2v}, 6·24 (0)

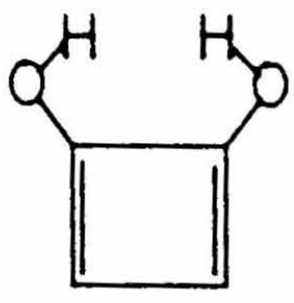

10, C_{2v}, 11·19 (2)

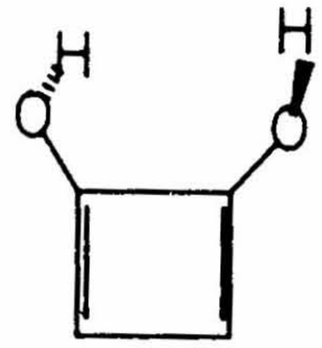

11, C_2, 10·35 (1)

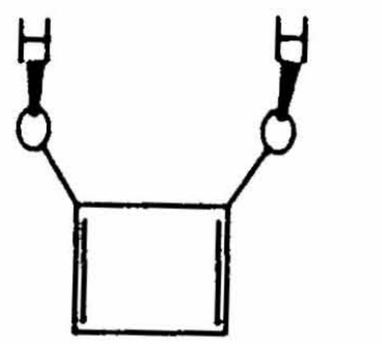

12, C_2, 11·69 (1)

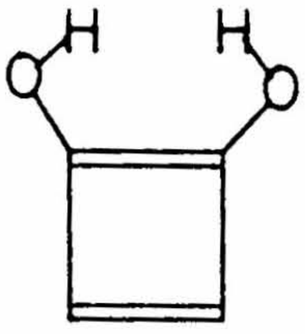

13, C_{2v}, 13·20 (1)

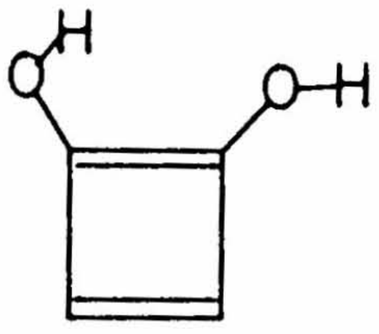

14, C_s, 11·33 (1)

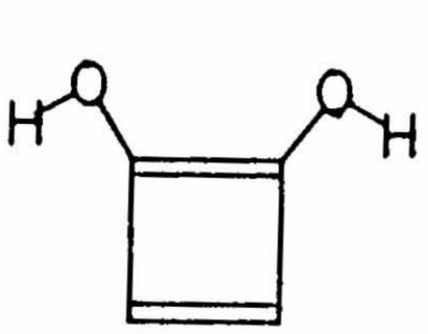

15, C_{2v}, 14·99 (2)

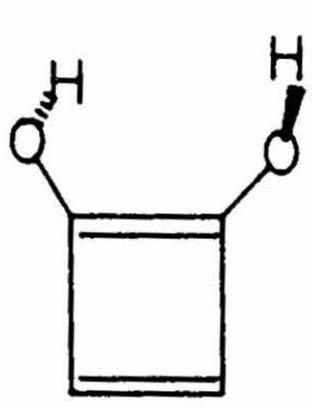

16, C_2, 10·42 (0)

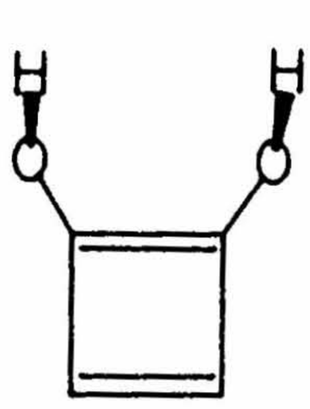

17, C_s, 11·64 (1)

Fig. 2.1.4: Relative energies (kcal mol^{-1}) of conformational isomers **Ib-IIIb** at HF/3-21G level. The number of imaginary frequencies are given in the parentheses.

hydroxy group perpendicular to the molecular plane corresponds to stationary point. All the three structures (**IIIb**, **7** and **8**) are local minima. Among all the conformations of 1,3 dihydroxy derivatives, the conformation where O-H bond is syn to the double bond, as observed in vinyl alcohol, is the one most preferred.[25]

7 and **8** with one and two unfavourable conformations of OH are about 1.2 and 2.5 kcal mol^{-1} less stable respectively than the most stable conformer **IIIb**. In **IIb** and **IIIb** the delocalization of the oxygen lone pairs with the double bonds is reminiscent of the situation in allyl anion and hence isomeric structures with both the hydroxy groups in the C_4-plane are generally more stable.Among the 1,4 isomers **IIb** is only marginally more stable than **9** which has the preferred conformation, O-H syn to the double bond. Hydrogen bonding, present in **IIb** (O...H distance 3.00 Å), is responsible for its higher stability over **9**. Both **IIb** and **9** are minima. The other C_{2v} structure, **10**, has both O-H bonds trans to the double bond. This is a higher order stationary point and higher in energy. The conformations with hydroxy groups perpendicular to the C_4 plane, **11** and **12**, are higher in energy.

Conformations **13-15** have two π-type lone pairs in conjugation with the double bond and are similar to butadiene dianion and are not minima. The imaginary frequencies correspond to the out of plane motions of the OH bonds. The imaginary frequencies lead to **16** and **17**. There is repulsion between the two oxygen lonepairs in **17** which is a transition state. **16** in the absence of this repulsive interaction, is a minimum. The best conformation of the 1,2-derivative should have only one π-type lone pair of oxygen delocalized to the double bond (similar to

allyl anion). The most stable conformer, **Ib**, has one hydroxy group in the plane and the other almost perpendicular (the C-C-O-H torsional angle is 108°) to it.

The vinyl substituent prefers to have its C-C double bond trans to that of cyclobutadiene (Fig. 2.1.5).[21b,c] Hence the choice of conformations for **Id** and **IIId** are obvious and are not discussed here. For the isomeric form **II** with X = $CH=CH_2$ the trans double bond conformation, **19**, is a transition state (Fig. 2.1.5). The conformation with cis double bonds, **18**, is also not a minimum. The imaginary frequencies in **18** and **19** correspond to the out-of-plane motions of the vinyl group, and lead to the minima at **IId** and **20** respectively. **IId** is more stable as the two double bonds are roughly trans to each other.

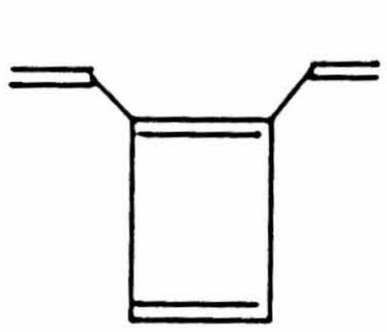

Id, C_{2v}, 0·00 (0)

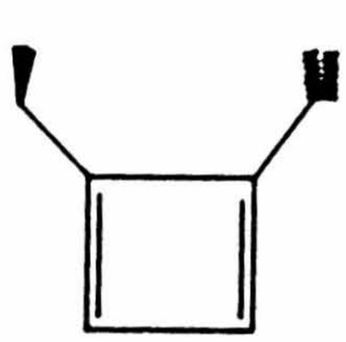

IId, C_2, 3·54 (0)

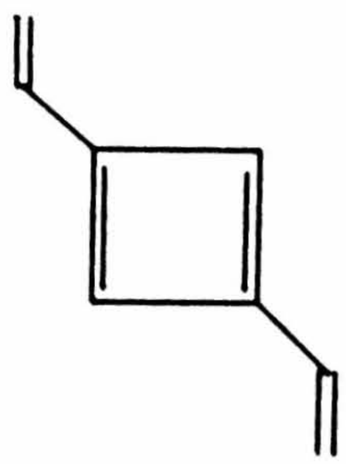

IIId, C_{2h}, 0·62 (0)

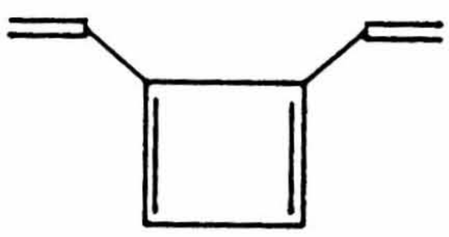

18, C_{2v}, 5·88 (2)

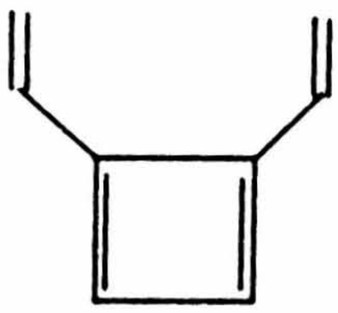

19, C_{2v}, 3·99 (1)

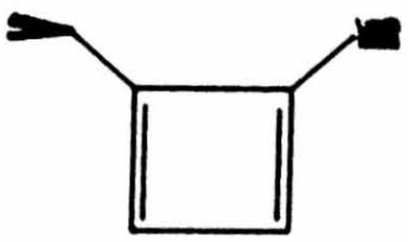

20, C_2, 5·81 (0)

Fig. 2.1.5: Relative energies (kcal mol^{-1}) of conformational isomers of **IId** at HF/3-21G level. The number of imaginary frequencies are given in the parenthesis.

2.1.5 Conclusions

The existence of two distinct isomeric forms for the vicinal disubstituted cyclobutadienes , **I** and **II**, is established by ab initio molecular orbital calculations. The relative stabilities obtained for X = CH_3, OH and CN are opposite to those obtained for X = $CH{=}CH_2$. The latter substituent is similar to phenyl. Thus the reversal of relative stabilities observed between X = CN and Ph is confirmed by the present study. Three major contributors to the relative energy viz. the basic tendency of ethylene to add on substituents, the repulsive interaction between the double bonds in cyclobutadiene and the electrostatic interaction explain the calculated results. The substituents CH_2^+ and CH_2^- remove the "cyclobutadiene character" of the parent system. The conformational preference exhibited by Me, OH and $CH{=}CH_2$ derivatives are understood by treating the double bonds in the cyclobutadiene as localized. A knowledge of the relative stabilities of the cyclobutadiene derivatives should help in selecting the appropriate substituents in achieving a specific Diels-Alder reaction.

2.2 Vicinal disubstituted cyclobutadienes: oligomerization and reactivity with quinones

2.2.1 Abstract

Parent cyclobutadiene dimerizes quickly. Further oligomerization is hindered by high HOMO-LUMO energy differences. Electron withdrawing substituents such as CN or COOH at 1 and 2 positions decrease the HOMO-LUMO energy differences and hence are suitable precursors for the synthesis of higher ladderanes. The regiochemistry of the ladderanes is predicted by the Frontier Molecular Orbital theory. In the second part of this section, the observed regioselectivity in the [4+2]-cycloaddition between 1,2-dicarbomethoxycyclobutadienes and quinones (benzoquinone and naphthoquinone) are rationalized based on FMO theory. The formation of the mixture of symmetric and unsymmetric regioisomers is due to the low energy difference between the two forms of cyclobutadienes, **2e** and **3e**. The difference between the two symmetric adducts is attributed to the product development control.

2.2.2 Introduction

This section deals with the reactivity of vicinal disubstituted cyclobutadienes in [4+2]-cycloaddition reactions. Firstly, the frontier molecular orbital control on the oligomerization of cyclobutadiene is analyzed. The second part accounts for the observed regioselectivity in the cycloaddition of 1,2-dicarbomethoxycyclobutadiene with quinones.

It has been synthetically challenging to assemble a linear array of four membered rings, known as [n]-ladderanes.[27,28] Oligomerization of cyclobutadienes is conceptually the simplest approach to the higher ladderanes. However, parent cyclobutadiene and its derivatives dimerize rapidly and does not proceed beyond this stage.[1] We want to understand why the oligomerization doesn't go beyond the dimerization stage and further explore the substituted systems that may exhibit enhanced propensity towards further [4+2]-cycloaddition and thus promote a cycloaddition cascade leading to higher ladderanes. Vic-disubstituted cyclobutadiene can adopt two isomeric forms when released from iron complex, **1**.[1,3-5] The two isomeric forms will be in dynamic equilibrium with each other as shown in Scheme 1. For electron withdrawing substituents, **2** is more stable than **3** by a few kcal mol^{-1}. Semiempirical AM1[29] calculations and Frontier Molecular Orbital theory[30] are used to predict the reactivity trends as a function of vic-substituents (a-d).

Scheme 1

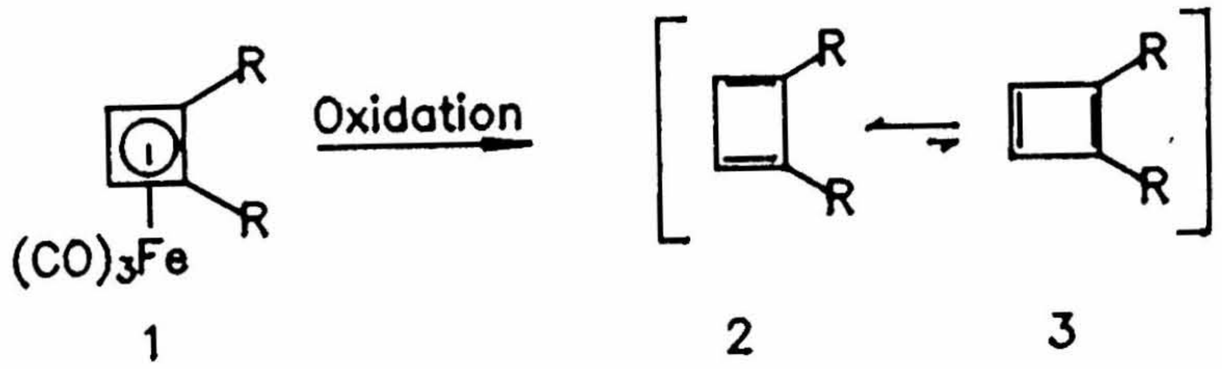

1 2 3

	a	b	c	d	e
R	H	Me	CN	COOH	COOMe

Vic-dicarbomethoxycyclobutadienes react with benzoquinone and naphthoquinone to give a mixture of [4+2] adducts as shown in Scheme 2. These experiments, performed by Mehta and Viswanath, are designed to yield functionalized cubanes eventually.[9] Liberation of 1,2-dicarbomethyoxycyclobutadiene from its iron tricarbonyl complex **1** in the presence of benzoquinone **4** furnished three regioisomeric 1:1 adducts **5**, **6** and **7** in the ratio 16:4:1, (Scheme 2). Similarly with naphthoquinone, **8**, the 4+2 adducts **9**, **10** and **11** are formed in 11:1:2 ratio. We have examined the energy difference of the two forms of vic-dicarbomethoxycyclobutadienes, **2e** and **3e**, at AM1 level and explained the observed regioselectivities using Frontier Molecular Orbital theory.[30]

Scheme 2

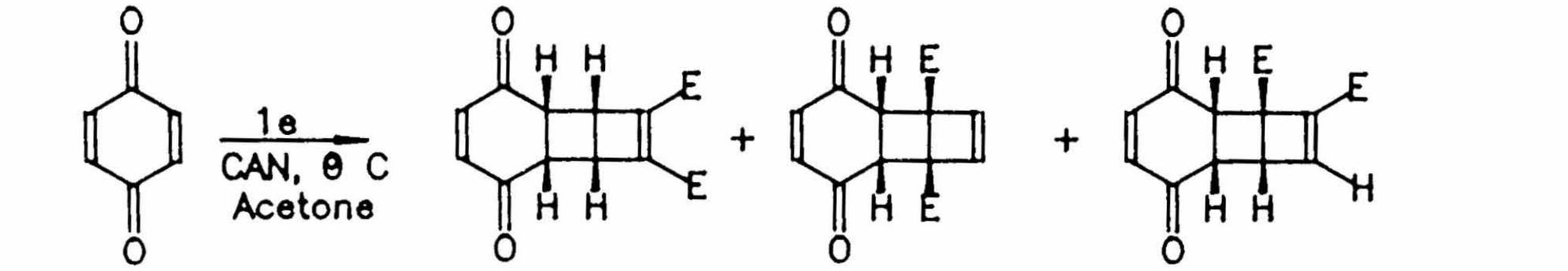

4 5 6 7

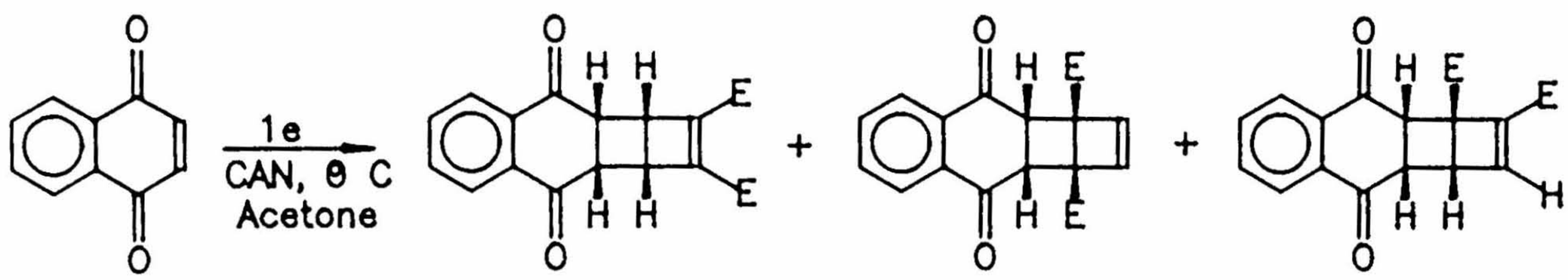

8 9 10 11

2.2.3 Results and Discussion

Oligomerization of cyclobutadienes

Of the two forms of cyclobutadiene, **2** and **3**, we consider the reactivity of the more stable isomeric form **2**. AM1 calculations are performed on **2**, **12** and **13** (R = a-d). Scheme 3 gives the HOMO-LUMO and LUMO-HOMO energy difference calculated for oligomerization process for **2a**. The HOMO-LUMO gaps of 8.46 eV for the dimerization of **2a** is within the range of successful [4+2]-cycloaddition reactions. The reaction of the dimer **12a** with

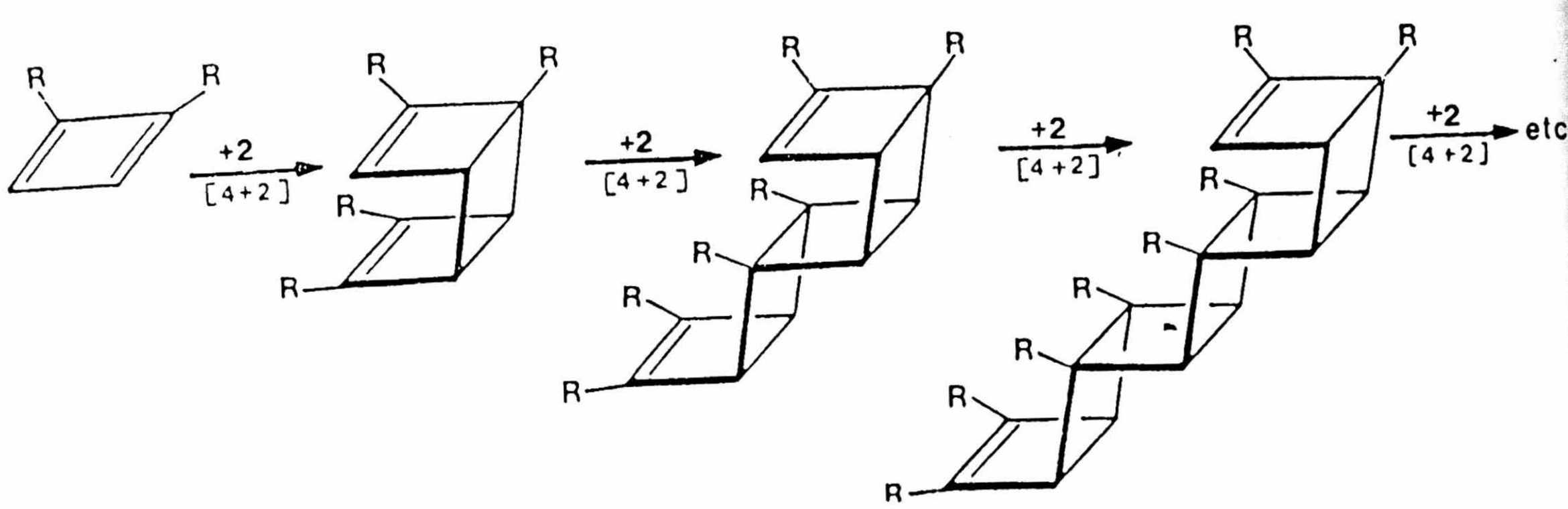

2 12 13 14

Reaction	HOMO-LUMO (LUMO-HOMO) eV			
	R = H	R = Me	R = CN	R = COOH
Dimerization	8.46	8.33	7.83	8.12
Trimerization	9.64(9.70)	8.92 (9.43)	7.98 (9.06)	8.37 (9.29)
Tetramerization	9.68 (9.64)	8.94 (9.41)	8.00 (9.07)	8.35 (9.29)

2a has a HOMO-LUMO or LUMO-HOMO gap considerably larger (9.64 or 9.70 eV). Similarly, the formation of the tetramer **14a** from **13a** and **2a** also has large HOMO-LUMO(LUMO-HOMO) gap of 9.68 (9.64 eV). These HOMO-LUMO energy differences are on higher sides and hence the oligomerization process doesn't proceed beyond the dimerization stage. In the dimerization process the HOMO and LUMO are from the same molecule. The HOMO and LUMO necessarily have to be from different molecules for trimerization onwards. It is likely that some substituted systems may bring down the HOMO-LUMO (or LUMO-HOMO) energy difference corresponding to the trimerization and tetramerization substantially.

Accordingly, the methyl (**2b**, **12b** and **13b**), cyano (**2c**, **12c** and **13c**) and carboxylicacid derivatives (**2d**, **12d** and **13d**) were optimized at the AM1 level. Scheme 3 shows that the dimerization of all the complexes **2b-c** has HOMO-LUMO energy differences which are within the feasible region. For methyl substitution, the HOMO-LUMO and LUMO-HOMO gaps calculated for trimerization are 8.92 and 9.43 eV respectively. Similar HOMO-LUMO energy differences are observed for the tetramerization. The methyl substitution decreases the HOMO-LUMO gap slightly. What is more encouraging is that the HOMO-LUMO gap calculated for the trimerization and tetramerization for dicyano derivatives are 7.98 and 8.00 eV respectively. Similarly for dicarboxylicacid derivatives, the HOMO-LUMO gap is 8.37 and 8.35 eV for trimerization and tetramerization respectively. These are more than 1 eV lower than those calculated for the parent cyclobutadiene and also its methyl derivative. Therefore, **2c** and **2d** can be considered as good candidates for oligomerization.

SCHEME 4a

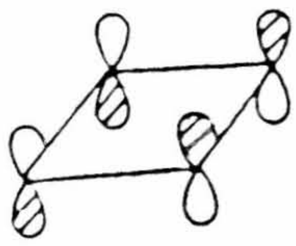

8·56 eV

2a

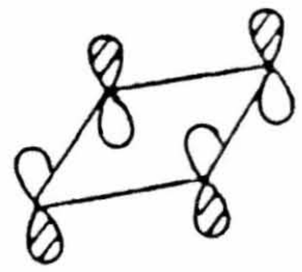

0·10 eV

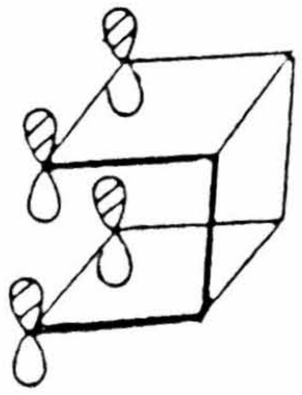

9·54 eV

12a

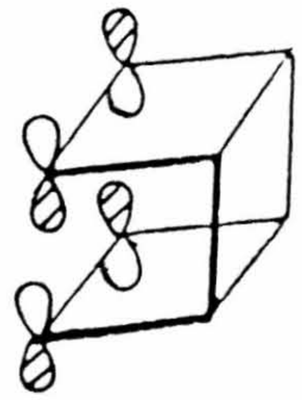

1·14 eV

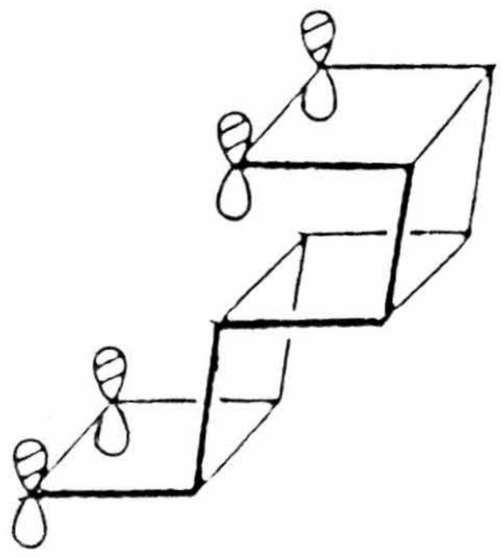

9·58 eV

13a

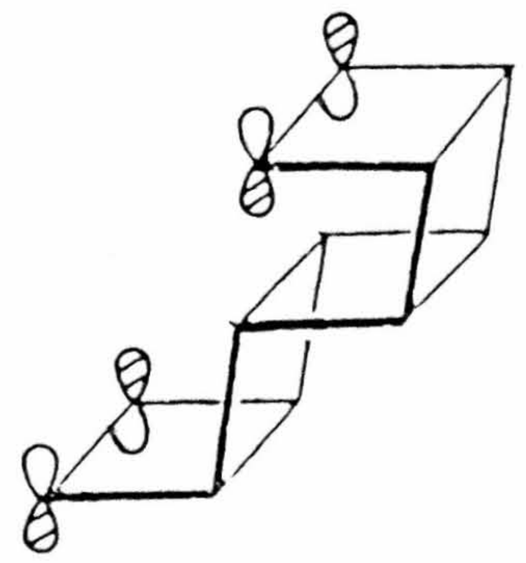

1·08 eV

SCHEME 4b

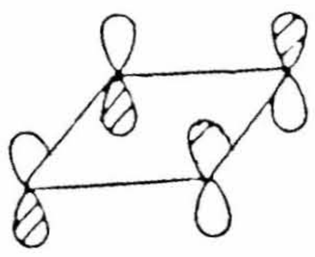

9·71 eV

2d

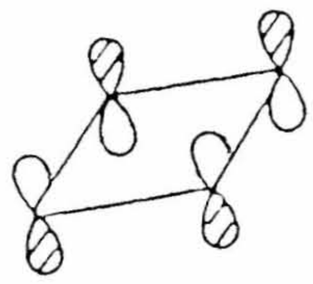

1·59 eV

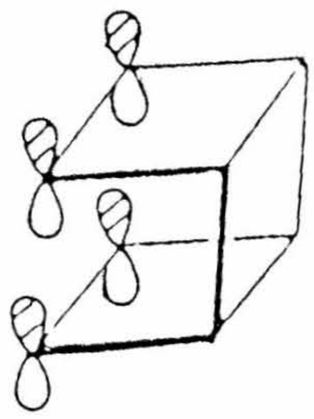

10·88 eV

12d

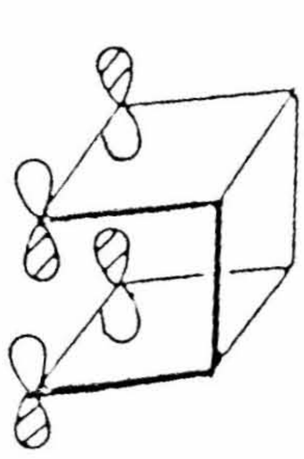

1·34 eV

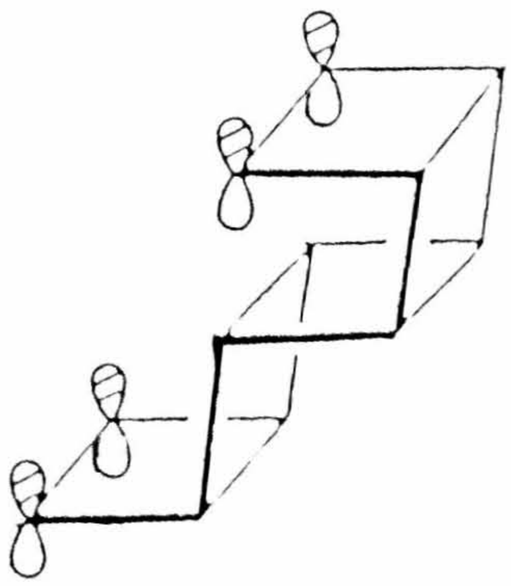

10·88 eV

13d

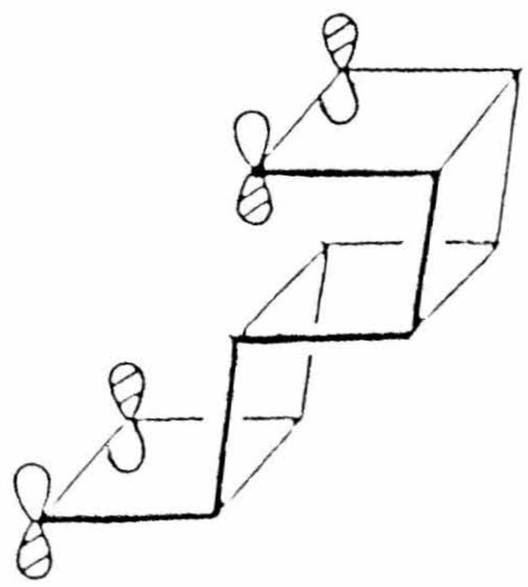

1·30 eV

These studies indicate that 1,2-disubstitution by electron withdrawing groups promote oligomerization of cyclobutadienes.

Scheme 4a gives the frontier orbitals, HOMO and LUMO, of parent ladderanes (**2a**, **12a** and **13a**) and Scheme 4b gives those of dicarboxylicacid derivatives (**2d**,**12d** and **13d**). The regio- and stereochemistry of **12d** follows from the rationalization based on the calculated MO's and their energies in the model coefficients of HOMO and LUMO of **2d** and secondary orbital interactions available during the dimerization (Scheme 4b). Similarly, regiochemistry of **13d** is dictated by the LUMO of **12d** which is localized on the more substituted double bond. The stereochemistry of **13d** in the absence of any secondary orbital interaction, is determined by steric considerations. The reaction is controlled by the HOMO of **2** and the LUMO of **12** and **13** for trimerization and tetramerization respectively. The regiochemistry of **12d**, **13d** and **14d** is dictated by the product development control. Similar observations have been made previously, and this aspect is discussed in detail below. The formation of **14d** follows the same pattern.

Reactivity with Quinones

Vic-dicarbomethoxycyclobutadienes disengaged from $Fe(CO)_3$ gives two isomers **2e** and **3e** which are in dynamic equilibrium. AM1 calculations indicate that **2e** is more stable than **3e** by 1.1 kcal mol^{-1}. In both the isomeric forms, the COOMe groups are not coplanar with the four membered ring. If one of the COOMe groups is kept in the plane the other COOMe group is almost at right

angles to the plane. The frontier orbitals, HOMO and LUMO, of the two forms of cyclobutadienes are depicted in Scheme 5. Both the isomeric forms have very similar frontier orbital pattern. This indicates that, in the given situation the availability of a particular isomeric form in the equilibrium mixture decides the percentage of products. Hence, the energy difference in turn decides the regioselectivity.

The HOMO of benzoquinone is a π MO based on benzene ring with no coefficient on quinone double bond and hence can have little interaction with cyclobutadiene molecule. LUMO is a π^* of quinone double bond and suitable to interact with the cyclobutadiene molecule. The energy difference (HOMO (of **2e**) - LUMO (of **4**)) is 8.13 eV. The HOMO+1 of **4** has the right symmetry to interact but the energy difference (LUMO - HOMO+1 = 9.64 eV) is very large. Similarly, in naphthoquinone only LUMO has the appropriate symmetry to interact with the cyclobutadiene orbitals, HOMO (of **2e**) - LUMO (of **8**) is 8.34 eV. The HOMO of naphthoquinone does not have the right symmetry. HOMO+3, the orbital of right symmetry, is energetically not favourable (LUMO of **2e** - HOMO+3 of **8** = 9.57 eV). Scheme 5 gives the LUMOs of benzoquinone, **4**, and naphthoquinone, **8**, which have the right symmetry to interact with the cyclobutadiene orbitals. The adducts formation is essentially controlled by the interaction between LUMO of quinone and the HOMO of cyclobutadiene. On [4+2]-cycloaddition with quinones, **2e** gives symmetrical adducts and **3e** gives unsymmetric adducts. As **2e** is more stable than **3e** by 1.1 kcal mol^{-1}, the former is present in excess at equilibrium. This may explain the preferential formation of

SCHEME 5

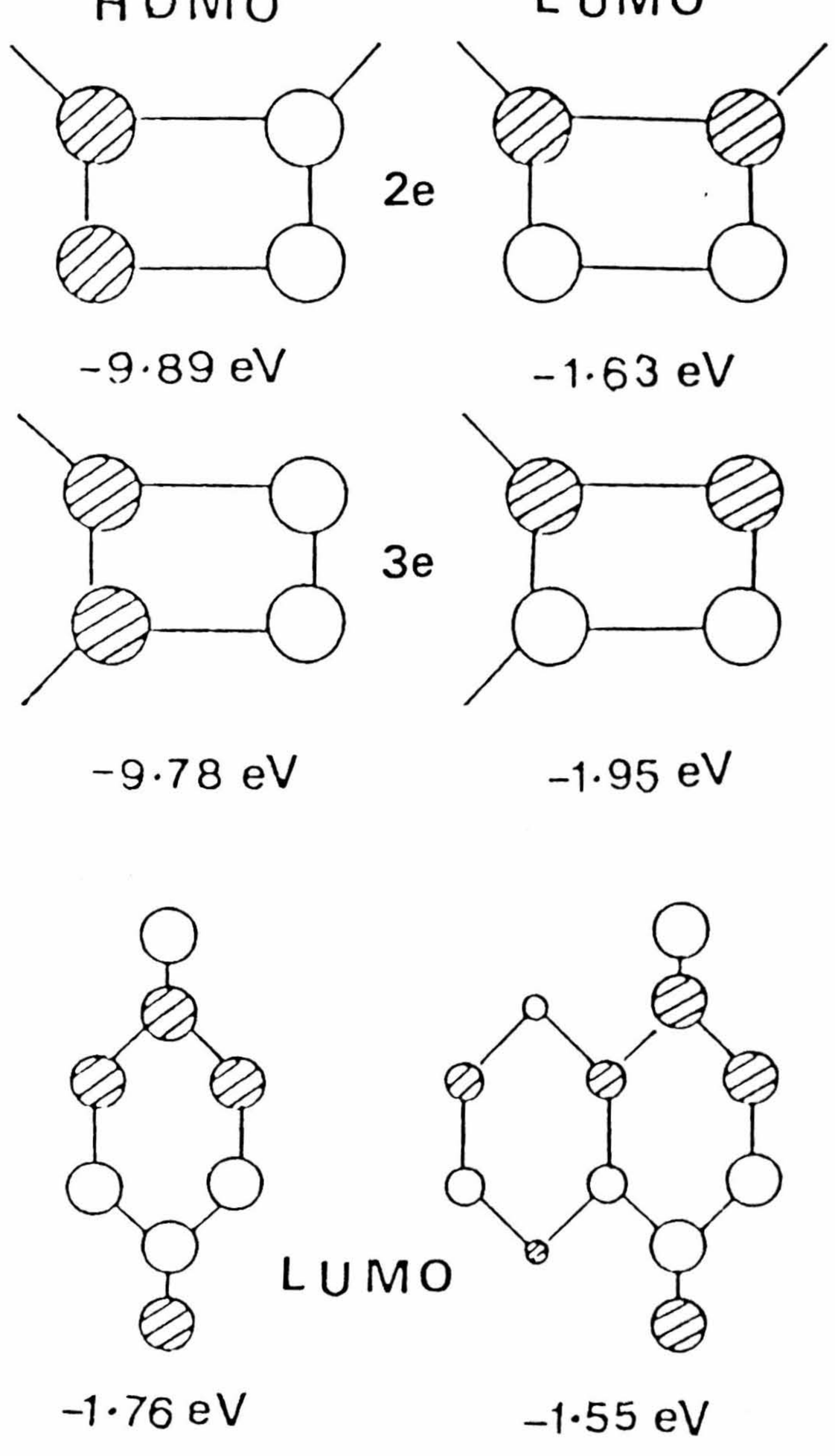

symmetric products (**5**, **6** and **9**, **10**) in comparison to unsymmetrical products (**7** and **11**). All the cycloadditions benefit from the secondary orbital interactions roughly to the same extent.

While the difference between the symmetric and the unsymmetric adducts are mainly due to the energy difference between **2e** and **3e**, from FMO theory we are not able to get a clear explanation for the ratio of the symmetrical adducts obtained. The transition states energies calculated by Molecular Mechanics (MM2)[31] corresponding to **5** and **9** are less favoured by about 4 kcal mol^{-1} than those corresponding to **6** and **10**. This rules out the possibility of steric effect deciding the observed selectivity. AM1 calculations show that **5** and **9** are more stable than **6** and **10** by 12.2 and 11.8 kcal mol^{-1} respectively. While we haven't located the transition states at the AM1 level, in the absence of any clear preference based on FMO theory, the product development control should be the deciding factor.

2.2.4 Conclusions

Parent cyclobutadienes dimerize because of the small HOMO-LUMO differences. Further reactivity is precluded based on the forbidden HOMO-LUMO energy differences. Electron withdrawing groups at 1,2 positions decrease the HOMO-LUMO energy differences considerably i.e., by about 1 eV. Hence, the 1,2-disubstituted cyclobutadienes are good candidates to effect oligomerization reaction. The small energy difference between **2** and **3** is responsible for the mixture of regioisomers observed. The vic-disubstituted cyclobutadienes exist in two different isomeric forms, **2** and **3**. The higher percentage of symmetric adducts in comparison with the unsymmetric adducts in [4+2]-cycloaddition reactions with quinones is due to the higher stability of **2** over **3**. The regioselectivity among the symmetric adducts is attributed to the product development control, after examining the role played by frontier orbital control and steric interactions.

2.3 References

1. (a) B. Arnold, and B. Michl, *In Kinetics and Spectroscopy of Carbenes and Biradicals;* M.S. Platz, Plenum: New York, NY, **1990**; Chapter 1.

   (b) G. Maier, Angew. Chem. Int. Ed. Engl., **1988**, 27, 309.

   (c) T. Balley, and S. Masamune, Tetrahedron, **1980**, 36, 343.

2. (a) B.A. Hess, Jr., P. Carsky and L.J. Schaad, J. Am. Chem. Soc., **1983**, 105, 695.

   (b) G. Maier, R. Wolf, and H.-O. Kalinowski, Angew. Chem. Int. Ed. Engl., **1992**, 31, 738.

   (c) J.D. Dunitz, C. Kruger, H. Irngartinger, E.F. Maverich, Y. Wang, Y.; Nixdorf, M. Angew. Chem. Int. Ed. Engl., **1988**, 27, 387.

   (d) P. Carsky, V. Spirko, B.A. Hess, Jr. and L.J. Schaad, J. Chem. Phys., **1990**, 92, 6069.

3. (a) L. Watts, J.D. Fitzpatrick and R. Pettit, J. Am. Chem. Soc., **1965**, 87, 3253.

   (b) G.F.Emerson, L. Watts and R. Pettit, J. Am. Chem. Soc., **1965**, 87, 131.

4. (a) C.M. Adams, S.A. Joslin, E.S. Crawford and J.E. Schemenaur, Organometallics, **1993**, 12, 656.

   (b) C.M. Adams, J.E. Schemenaur, E.S. Crawford and S.A. Joalin, Synth. Commun., **1992**, 22, 1385.

   (c) J.E.C. Wiegelmann and U.H.F. Bunz, Organometallics, **1993**, 12, 3792.

   (d) G. Berens, F. Kaplan, R. Rimerman, B.W. Roberts and A. Wissner, J. Am. Chem. Soc., **1975**, 97, 7076.

5. P.T. Reeves, J. Devon, and R. Pettit, J. Am. Chem. Soc.,

1969, 91, 5890.

6. M.J.S. Dewar, M.C. Kohn and N.J. Trinajstic, J. Am. Chem. Soc., **1971**, 93, 3437.

7. B. Witulski, L. Ernst, P.G. Jones and H. Hopf, Angew. Chem. Int. Ed. Engl., **1989**, 28, 1279.

8. (a) G. Mehta, M.B. Viswanath, M. Nethaji and K. Venkatesan, J. Chem. Soc., Chem. Commn., **1992**, 82.

(b) G. Mehta, M.B. Viswanath, G.N. Sastry, E.D. Jemmis, D.S.K. Reddy and A.C. Kunwar, Angew. Chem. Int. Ed. Engl., **1992**, 31, 1488.

9. G. Mehta, M.B. Viswanath, E.D. Jemmis and G.N. Sastry, J. Chem. Soc., Perkin Trans. 2, **1994**, 0000.

10. O.M. Herrera and I. Brinn, J. Chem. Soc., Perkin Trans. 2, **1986**, 1683.

11. W.J. Hehre, L. Radom, P.v.R. Schleyer and J.A. Pople, *Ab initio Molecular Orbital Theory*; Wiley: New York, 1986.

12. J.S. Binkley, J.A. Pople and W.J. Hehre, J. Am. Chem. Soc., **1980**, 102, 939.

13. (a) P.C. Hariharan and J.A. Pople, Theor. Chim. Acta., **1973**, 28, 213.

(b) M.M. Francl, W.J. Pietoro, W.J. Hehre, J.S. Binkley, M.S. Gordon, D.J. DeFrees and J.A. Pople, J. Chem. Phys., **1982**, 77, 3654.

14. (a) C. Moller and M.S. Plesset, Phys. Rev., **1934**, 46, 618.

(b) J.A. Pople, J.S. Binkley and R. Seeger, Int. J. Quant. Chem., **1976**, s10, 1.

15. C. Hampel, K. Peterson and W.-J. Werner, Chem. Phys. Lett., **1992**, 190, 1 and references therein. The program to compute the perturbative triples corrections has been developed by M.

Deegan and P.J. Knowles (1992).

16. (a) H. Fujimoto and R. Hoffmann, J. Phys. Chem., **1974**, 78, 1167.

(b) R. Hoffmann, J. Chem. Phys., **1963**, 39, 1397.

(c) R. Hoffmann and W.N. Lipscomb, J. Chem. Phys., **1962**, 36, 2179,3489.

17. Gaussian 92: M.J. Frisch, G.W. Trucks, M. Head-Gordon, P.M.W. Gill, M.W. Wong, J.B. Foresman, B.G. Johnson, H.B. Schlegel, M.A. Robb, E.S. Replogle, R. Gomberts, J.L. Andres, K. Raghavachari, J.S. Binkley, C. Gonzalez, R.L. Martin, D.J. Fox, D.J. Defrees, J. Baker, J.J.P. Stewart and J.A. Pople, Gaussian Inc., Pittsburgh PA, 1992.

18. MOLPRO is a package of ab initio programs written by H.-J. Werner and P.J. Knowles, with contributions of J. Almlof, R. Amos, S. Elbert, K. Hampel, W. Meyer, K. Peterson, R. Pitzer and A. Stone.

19. W.W. Schoeller and T. Busch, Angew. Chem. Int. Ed. Engl., **1993**, 32, 617.

20. (a) P.N.V. PavanKumar and E.D. Jemmis, J. Am. Chem. Soc., **1988**, 110, 125.

(b) K. Krogh-Jespersen, J. Am. Chem. Soc., **1991**, 113, 417.

21. (a) R.A. Whiteside, M.J. Frisch and J.A. Pople, The Carnegie-Mellon Quantum Chemistry Archive, Department of Chemistry, Carnegie-Mellon University, Pittspurgh, P.A., **1983**.

(b) P.G. Szalay, A. Karpten and H. Lischka, J. Chem. Phys., **1982**, 87, 3530.

(c) R. Liu and X. Zhou, J. Phys. Chem., **1993**, 97, 1950.

22. I. Fleming, *Frontier orbitals and organic chemical*

2.4 Appendix

MP2/6-31G* optimized Cartesian coordinates of the substituted cyclobutadines.

Ia, Standard orientation:

Center Number	Atomic Number	Coordinates (Angstroms) X	Y	Z
1	C	0.000000	0.792593	0.015196
2	C	0.000000	-0.792593	0.015196
3	C	0.000000	-0.778292	1.361859
4	C	0.000000	0.778292	1.361859
5	H	0.000000	-1.539254	2.135635
6	H	0.000000	1.539254	2.135635
7	C	0.000000	-1.814319	-1.059763
8	C	0.000000	1.814319	-1.059763
9	H	0.000000	-2.821123	-0.630894
10	H	0.000000	2.821123	-0.630894
11	H	0.881847	-1.715056	-1.704246
12	H	-0.881847	-1.715056	-1.704246
13	H	-0.881847	1.715056	-1.704246
14	H	0.881847	1.715056	-1.704246

IIa, Standard orientation:

Center Number	Atomic Number	Coordinates (Angstroms) X	Y	Z
1	C	0.000000	0.675436	-0.083260
2	C	0.000000	-0.675436	-0.083260
3	C	0.000000	-0.672343	1.486009
4	6	0.000000	0.672343	1.486009
5	H	0.000000	-1.441987	2.250840
6	H	0.000000	1.441987	2.250840
7	C	0.000000	-1.758541	-1.096381
8	C	0.000000	1.758541	-1.096381
9	H	0.000000	-1.342793	-2.108672
10	H	0.000000	1.342793	-2.108672
11	H	0.881935	-2.402012	-0.990188
12	H	-0.881935	-2.402012	-0.990188
13	H	-0.881935	2.402012	-0.990188
14	1	0.881935	2.402012	-0.990188

IIIa, Standard orientation:

Center Number	Atomic Number	Coordinates (Angstroms) X	Y	Z
1	C	-1.034196	-0.039623	0.000000
2	C	0.118413	1.026483	0.000000
3	C	1.034196	0.039623	0.000000
4	C	-0.118413	-1.026483	0.000000
5	H	2.118984	0.001325	0.000000
6	H	-2.118984	-0.001325	0.000000
7	C	0.118413	2.508530	0.000000
8	C	-0.118413	-2.508530	0.000000
9	H	1.141876	2.894876	0.000000
10	H	-1.141876	-2.894876	0.000000
11	H	-0.401365	2.903056	0.881463
12	H	-0.401365	2.903056	-0.881463
13	H	0.401365	-2.903056	0.881463
14	H	0.401365	-2.903056	-0.881463

Ib, Standard orientation:

Center Number	Atomic Number	Coordinates (Angstroms) X	Y	Z
1	C	-0.667575	-0.124475	-0.037108
2	C	0.675595	-0.158880	-0.002089
3	C	0.704079	1.410795	0.018962
4	C	-0.634184	1.445075	-0.015929
5	H	1.502059	2.140746	0.049471
6	H	-1.387685	2.222077	-0.025776
7	O	1.701230	-1.044093	0.013543
8	O	-1.658700	-1.071160	-0.075520
9	H	1.312028	-1.939220	-0.010674
10	H	-2.234129	-0.936667	0.699778

IIb, Standard orientation:

Center Number	Atomic Number	Coordinates (Angstroms) X	Y	Z
1	C	-0.052866	-0.788789	0.000000
2	C	0.000000	0.761988	0.000000
3	C	1.288437	-0.846536	0.000000
4	C	1.342717	0.737688	0.000000
5	O	-1.080963	-1.669404	0.000000
6	O	-1.050298	1.619108	0.000000
7	H	2.043406	-1.618916	0.000000
8	H	2.147586	1.459641	0.000000
9	H	-1.908134	-1.155317	0.000000
10	H	-0.702503	2.530854	0.000000

IIIb, Standard orientation:

Center Number	Atomic Number	Coordinates (Angstroms) X	Y	Z
1	C	1.067958	-0.068253	0.000000
2	C	-0.075366	0.976195	0.000000
3	C	-1.067958	0.068253	0.000000
4	C	0.075366	-0.976195	0.000000
5	H	-2.146448	0.039851	0.000000
6	H	2.146448	-0.039851	0.000000
7	O	0.075366	2.313498	0.000000
8	O	-0.075366	-2.313498	0.000000
9	H	-0.813815	2.717247	0.000000
10	H	0.813815	-2.717247	0.000000

Ic, Standard orientation:

Center Number	Atomic Number	Coordinates (Angstroms) X	Y	Z
1	C	0.000000	0.682671	0.277941
2	C	0.000000	-0.682671	0.277941
3	C	0.000000	-0.672347	1.838986
4	C	0.000000	0.672347	1.838986
5	H	0.000000	-1.455626	2.586228
6	H	0.000000	1.455626	2.586228
7	C	0.000000	-1.673252	-0.721500
8	C	0.000000	1.673252	-0.721500
9	N	0.000000	-2.509812	-1.565542
10	N	0.000000	2.509812	-1.565542

IIc, Standard orientation:

Center Number	Atomic Number	Coordinates (Angstroms) X	Y	Z
1	C	0.000000	0.793534	0.336865
2	C	0.000000	-0.793534	0.336865
3	C	0.000000	-0.768098	1.690603
4	C	0.000000	0.768098	1.690603
5	H	0.000000	-1.530131	2.460841
6	H	0.000000	1.530131	2.460841
7	C	0.000000	-1.778633	-0.668361
8	C	0.000000	1.778633	-0.668361
9	N	0.000000	-2.609789	-1.516498
10	N	0.000000	2.609789	-1.516498

IIIc, Standard orientation:

Center Number	Atomic Number	Coordinates (Angstroms) X	Y	Z
1	C	-1.039024	0.070675	0.000000
2	C	0.083451	-1.022021	0.000000
3	C	1.039024	-0.070675	0.000000
4	C	-0.083451	1.022021	0.000000
5	H	2.122129	-0.048691	0.000000
6	H	-2.122129	0.048691	0.000000
7	C	0.083451	-2.435679	0.000000
8	C	-0.083451	2.435679	0.000000
9	N	0.083451	-3.621337	0.000000
10	N	-0.083451	3.621337	0.000000

Id, Standard orientation:

Center Number	Atomic Number	Coordinates (Angstroms) X	Y	Z
1	C	0.000000	0.687511	0.049546
2	C	0.000000	-0.687511	0.049546
3	C	0.000000	-0.674133	1.602710
4	C	0.000000	0.674133	1.602710
5	H	0.000000	-1.438500	2.372217
6	H	0.000000	1.438500	2.372217
7	C	0.000000	-1.719683	-0.933558
8	C	0.000000	1.719683	-0.933558
9	H	0.000000	-1.415867	-1.980703
10	H	0.000000	1.415867	-1.980703
11	C	0.000000	-3.036137	-0.621215
12	C	0.000000	3.036137	-0.621215
13	H	0.000000	-3.370639	0.412138
14	H	0.000000	3.370639	0.412138
15	H	0.000000	-3.802938	-1.388548
16	H	0.000000	3.802938	-1.388548

IId, Standard orientation:

Center Number	Atomic Number	Coordinates (Angstroms) X	Y	Z
1	C	0.000000	0.801090	0.544375
2	C	0.000000	-0.801090	0.544375
3	C	0.000000	-0.759285	1.903522
4	C	0.000000	0.759285	1.903522
5	H	0.000000	-1.516426	2.681191
6	H	0.000000	1.516426	2.681191
7	C	0.000000	-1.863598	-0.418876
8	C	0.000000	1.863598	-0.418876
9	H	-0.307705	-2.840471	-0.042720
10	H	0.307705	2.840471	-0.042720
11	C	0.358404	-1.744820	-1.715948
12	C	-0.358404	1.744820	-1.715948
13	H	0.343708	-2.601912	-2.381086
14	H	-0.343708	2.601912	-2.381086
15	H	0.671246	-0.796063	-2.135826
16	H	-0.671246	0.796063	-2.135826

IIId, Standard orientation:

Center Number	Atomic Number	Coordinates (Angstroms) X	Y	Z
1	C	-1.016988	0.183204	0.000000
2	C	0.317689	0.981755	0.000000
3	C	1.016988	-0.183204	0.000000
4	C	-0.317689	-0.981755	0.000000
5	H	2.071253	-0.441070	0.000000
6	H	-2.071253	0.441070	0.000000
7	C	0.629225	2.379761	0.000000
8	C	-0.629225	-2.379761	0.000000
9	C	-0.317689	3.341309	0.000000
10	C	0.317689	-3.341309	0.000000
11	H	1.684107	2.654214	0.000000
12	H	-1.684107	-2.654214	0.000000
13	H	-1.374647	3.091293	0.000000
14	H	-0.059844	4.394983	0.000000
15	H	1.374647	-3.091293	0.000000
16	H	0.059844	-4.394983	0.000000

IIe, Standard orientation:

Center Number	Atomic Number	Coordinates (Angstroms) X	Y	Z
1	C	0.000000	0.779004	-0.134289
2	C	0.000000	-0.779004	-0.134289
3	C	0.000000	-0.748107	1.264251
4	C	0.000000	0.748107	1.264251
5	H	0.000000	-1.503052	2.054186
6	H	0.000000	1.503052	2.054186
7	C	0.000000	-1.856937	-1.015185
8	C	0.000000	1.856937	-1.015185
9	H	0.000000	-1.701146	-2.095491
10	H	0.000000	-2.884573	-0.647358
11	H	0.000000	1.701146	-2.095491
12	H	0.000000	2.884573	-0.647358

IIIe, Standard orientation:

Center Number	Atomic Number	Coordinates (Angstroms) X	Y	Z
1	C	0.000000	0.000000	1.040575
2	C	0.000000	1.012463	0.000000
3	C	0.000000	-1.012463	0.000000
4	C	0.000000	0.000000	-1.040575
5	C	0.000000	0.000000	2.417924
6	C	0.000000	0.000000	-2.417924
7	H	0.000000	0.934751	2.979773
8	H	0.000000	-0.934751	2.979773
9	H	0.000000	0.934751	-2.979773
10	H	0.000000	-0.934751	-2.979773
11	H	0.000000	2.107910	0.000000
12	H	0.000000	-2.107910	0.000000

IIf, Standard orientation:

Center Number	Atomic Number	Coordinates (Angstroms) X	Y	Z
1	C	0.000000	0.799068	-0.041177
2	C	0.000000	-0.799068	-0.041177
3	C	0.000000	-0.775368	1.352845
4	C	0.000000	0.775368	1.352845
5	H	0.000000	-1.554971	2.123910
6	H	0.000000	1.554971	2.123910
7	C	0.000000	-1.676947	-1.136960
8	C	0.000000	1.676947	-1.136960
9	H	0.000000	-1.311996	-2.166714
10	H	0.000000	-2.761514	-1.005444
11	H	0.000000	1.311996	-2.166714
12	H	0.000000	2.761514	-1.005444

IIIf, Standard orientation:

Center Number	Atomic Number	Coordinates (Angstroms) X	Y	Z
1	C	0.000000	0.000000	1.029000
2	C	0.000000	1.041508	0.000000
3	C	0.000000	-1.041508	0.000000
4	C	0.000000	0.000000	-1.029000
5	C	0.000000	0.000000	2.415797
6	C	0.000000	0.000000	-2.415797
7	H	0.000000	0.926101	2.997782
8	H	0.000000	-0.926101	2.997782
9	H	0.000000	0.926101	-2.997782
10	H	0.000000	-0.926101	-2.997782
11	H	0.000000	2.131977	0.000000
12	H	0.000000	-2.131977	0.000000

Chapter 3

Dyotropic rearrangements of Cp_2ZrL_n complexes and the electronic structure and reactivity of $Cp_2Zr=E$ complexes (E = S, O, NH and PH)

Chapter 3

Dyotropic rearrangements of Cp_2ZrL_n complexes and the electronic structure and reactivity of $Cp_2Zr=E$ complexes (E = S, O, NH and PH)

3.0 General Introduction

The success of organometallic synthesis lies in the ability of transition metals to stabilize reactive organic fragments and activate stable molecules. Rearrangements of organic moieties at transition metal centers is of fundamental importance in organometallic chemistry. Zirconocene, Cp_2Zr has been one of the most useful transition metal fragments in this regard. In this chapter we discuss two problems dealing with Cp_2Zr chemistry. The carbon-carbon bond formation reaction via dyotropic rearrangements is discussed first. The second section deals with the electronic structure and reactivity of $Cp_2Zr{=}E$ (E = O, S, NH and PH) compounds.

3.1 Dyotropic rearrangements of Cp_2ZrL_n complexes

3.1.1. Abstract

The dyotropic rearrangements in Cp_2Zr ligand complexes such as $Cp_2Zr(X)(CH_2\text{-}SR)$ (3) are studied using molecular orbital theory. The greater reactivity for X = Ph in comparison to X = Me, Cl and CH_2-Ph depends on the energy match of the migrating fragment MO's with those of the rest of the fragment along an assumed reaction coordinate (eq. 3.1.2). The ease of reactivity of $Cp_2Zr(C_4H_3O)_2$ (5) to give Zirconacycle (6) follows from a similar argument. New substitutents that should render the above reactions fast are suggested from these studies. A general discussion on the migratory aptitudes and the difficulties involved in assigning migratory aptitudes to groups independent of reactions are given.

3.1.2 Introduction

Isomerisations in which two groups migrate intramolecularly around a bond are called dyotropic rearrangements.[2] Eq. 3.1.1 represents the prototype of the dyotropic rearrangements, where two vicinal groups 'a' and 'd' migrate around the b-c bond. Formation of a three membered intermediate such as a-b-c-d or a-b-c-d decreases the activation barrier effectively.[3] Most of the dyotropic rearrangements are known to take place around C-C bonds.[2]

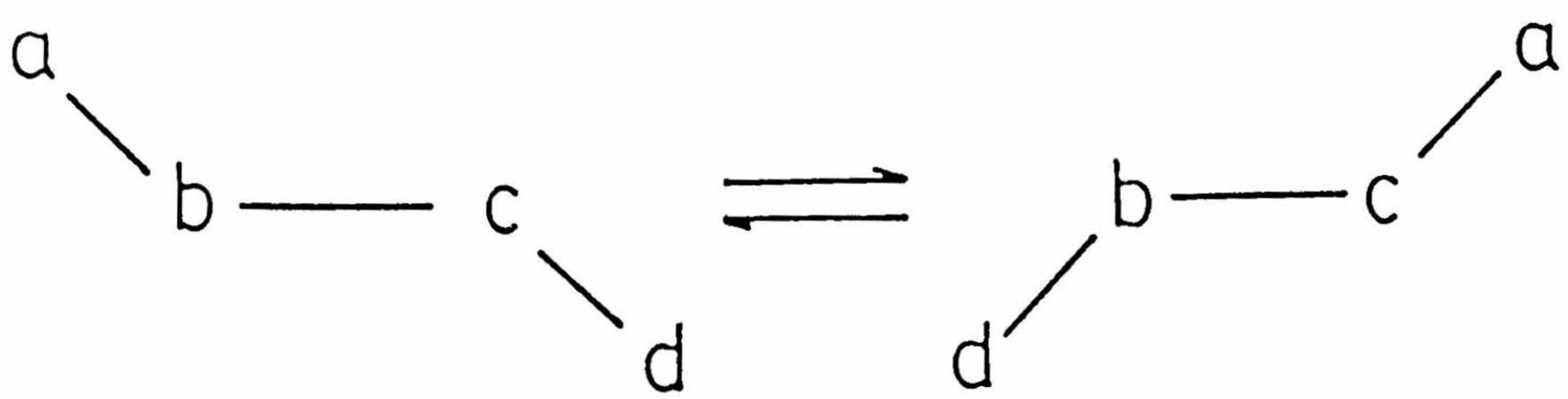

Eq. 3.1.1

1 2

Dyotropic rearrangements are also observed in organotransition metal chemistry. Mintz and coworkers reported a novel dyotropic rearrangement in zirconocenyl thioethers, where a = X, b = Cp_2Zr, c = $CH(SiMe_3)$, d = SCH_3 (eq. 3.1.2).[4] The reaction proceeds smoothly only for X = Ph. Kinetic data and labelling and cross over experiments indicate that it is an intramolecular reaction. A mechanism involving the intramolecular

nucleophilic attack of phenyl group on the methylene carbon has been proposed.[4] The facile reaction with X = Ph is attributed to the higher migrating ability of the phenyl groups. When a p-C_6H_4OMe group is substituted for the Ph group, the reaction is found to take place five times faster.[4] Attempts to get the reaction going with X = Cl, Me or CH_2Ph were futile under similar reaction conditions.

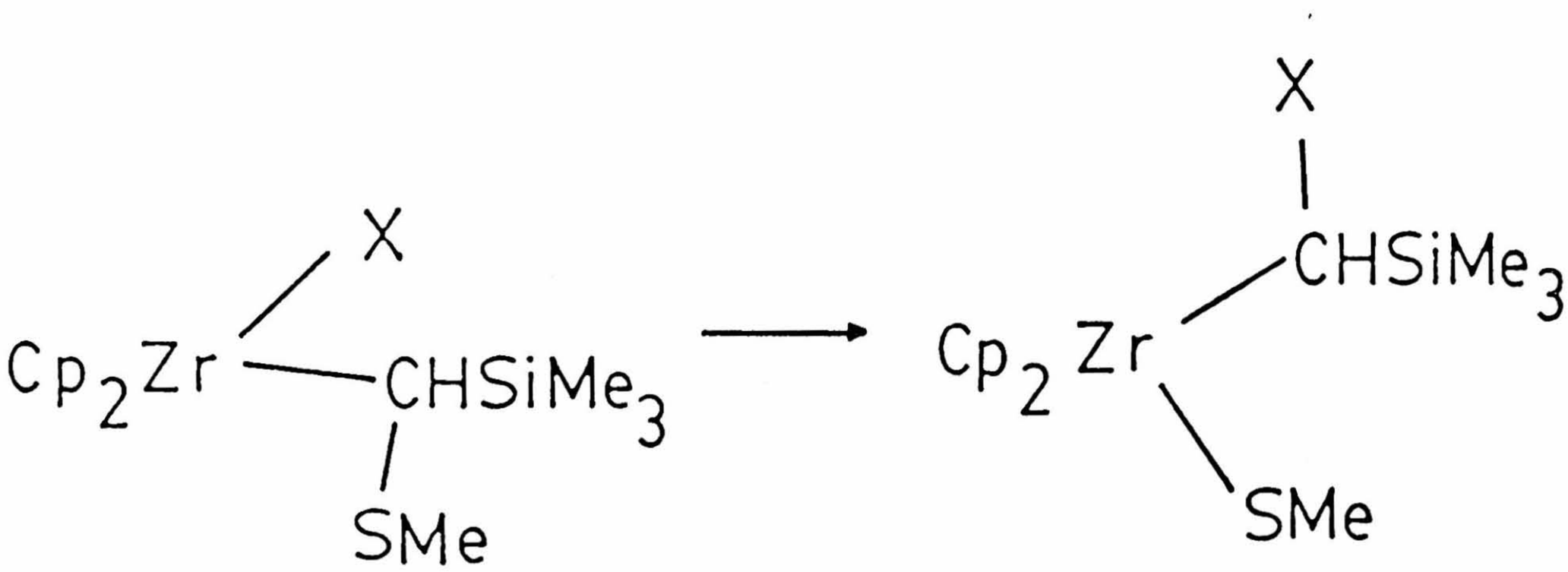

3 4 Eq. 3.1.2

a b c d

X = Ph Me CH_2Ph Cl

Though there is an analogy between Cp_2Zr and CH_2[5], larger number of orbitals of various symmetry are available in the frontier range for Cp_2Zr.[6] The two migrating groups in the eq. 3.1.2a are SMe and Ph. The migration of the SMe group is not strictly similar to the migration represented in eq. 3.1.1,

because the lone pair on sulfur is involved in the beginning stages of the reaction. The migration of the phenyl group completes the process. Despite the involvement of the lone pair on sulfur the reaction may be called as dyotropic rearrangement.

A similar reaction has been reported recently by Erker and coworkers (eq. 3.1.3).[3] In the above two reactions (eq. 3.1.2 and eq. 3.1.3) all the changes may be assumed to be taking place in one plane, referred to as the reaction plane in this chapter. This plane is orthogonal to the plane formed by the two Cp centroids and Zr.

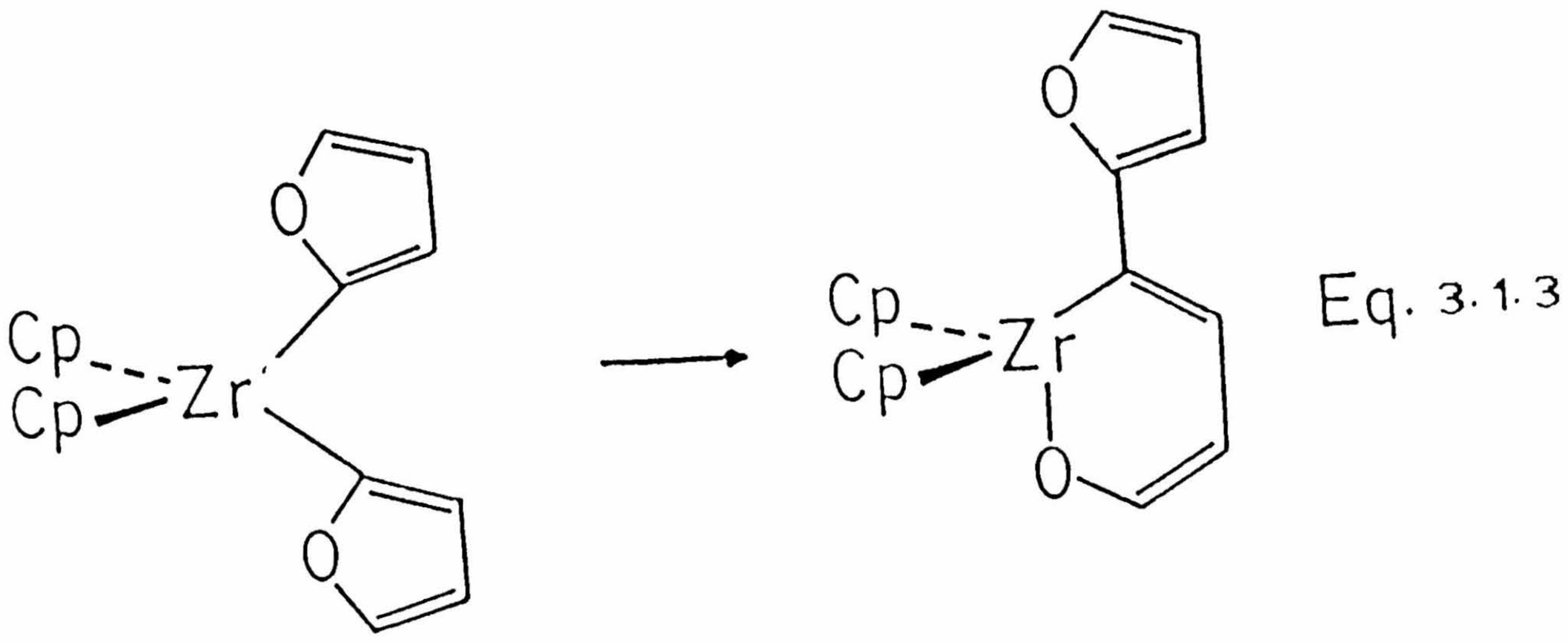

5 6 Eq. 3.1.3

The degenerate rearrangement between 7 and 8 is also an example for the dyotropic rearrangement in organotransition metal chemistry.[7] The two migrating groups are the Cp_2Zr units. There exists already an interaction in the ground state between the migrating group and the terminus. This reduces the barrier for

migration considerably. The structures 7 and 8 are close to 9 which is characterized by X-ray diffraction studies, and a qualitative molecular orbital picture is available for 9.[8]

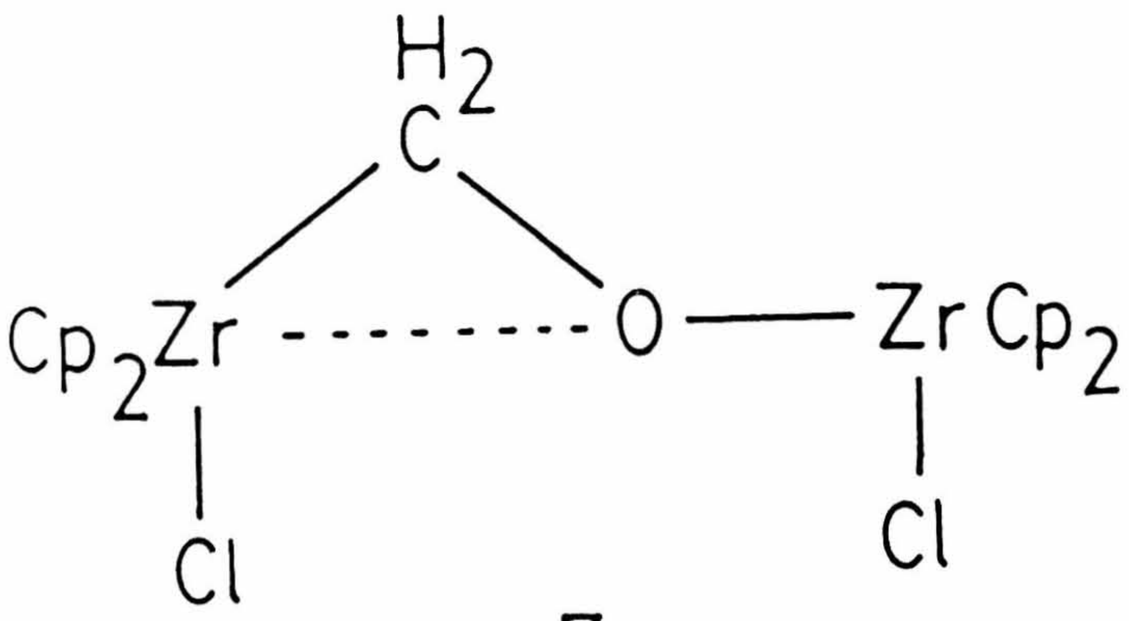

7

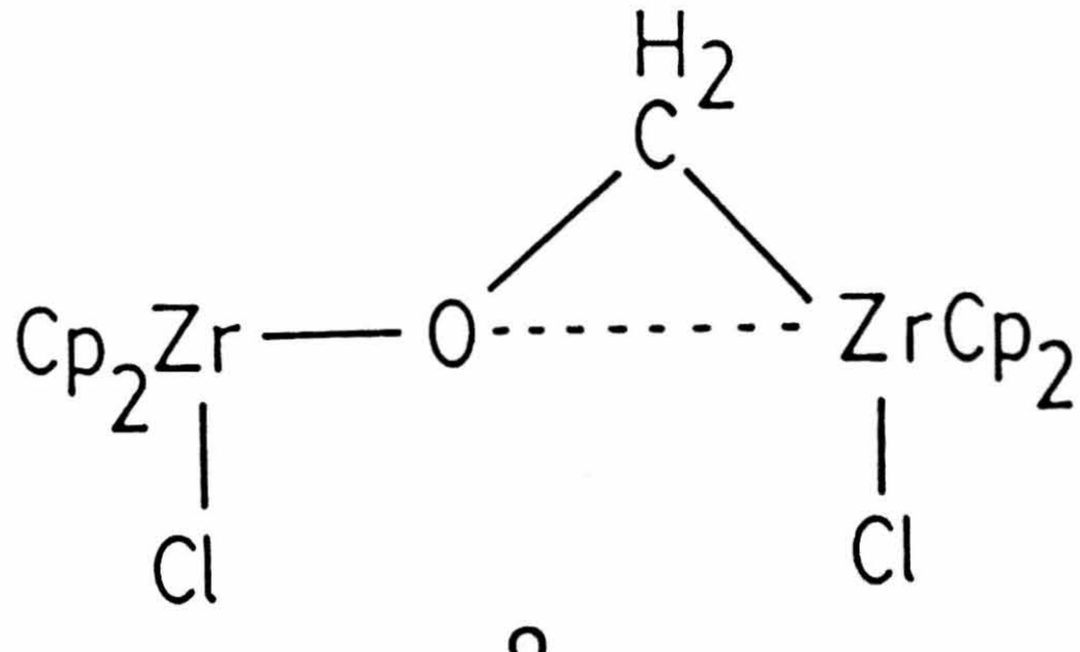

8

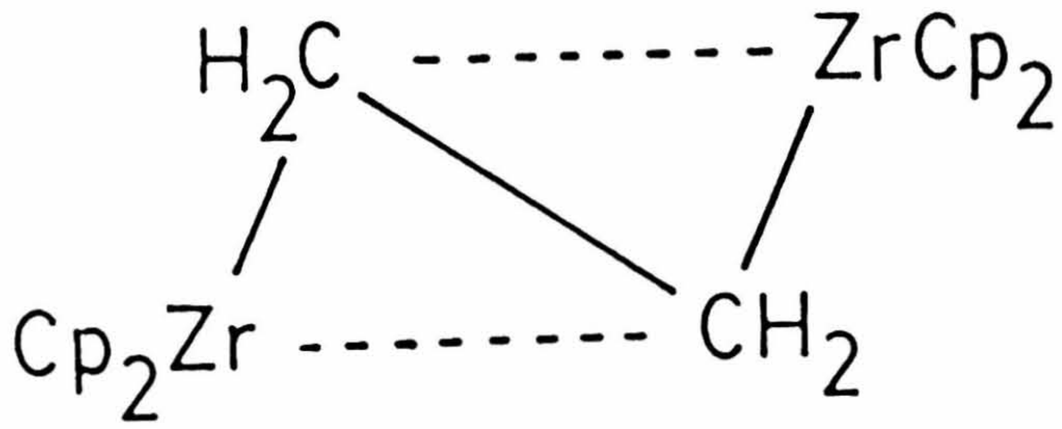

9

A molecular orbital study of the variations in the barriers of these reactions, as a function of the migrating groups is presented in this chapter. This also leads us to a discussion of migratory aptitudes in general.

Electronic structure studies are done using fragment molecular orbital approach[9] within the extended Huckel approximation.[10] The geometric parameters used in the calculations

are adopted from the X-ray structures of the various related complexes and are given in the appendix along with the atomic parameters.

3.1.3 Results and discussion

The reaction of $Cp_2Zr(X)$-$CH(SiMe_3)SR$ complexes (Eq. 3.1.2):

The rearrangement indicated by eq. 3.1.2 is modelled using the complex $Cp_2Zr(Ph)(CH_2SH)$ in the calculation. Experimental and theoretical studies on several related complexes had shown that the CH_2-SR group can bind to the Zr centre in three possible ways, "η^1-outside" (**10**), "η^2- inside" (**11**), "η^2- outside" (**12**).[11] Out of these only η^2- outside conformation (**12**) serves as the starting point for eq. 3.1.2. An NMR study accounts for the existence of η^2-outside structure for **3**,[12] hence this conformation is taken as the starting point in the calculations. To understand the electronic structure of the initial complex, **3a**, an interaction diagram is constructed between the fragments Cp_2Zr-CH_2 and Ph...SH. Cp_2Zr-CH_2 fragment orbitals are obtained from the familiar Cp_2Zr [6] and CH_2 [13] fragment orbitals (left side of Fig. 3.1.1). All the fragment orbitals are labelled according to C_s symmetry. In Cp_2Zr-CH_2 fragment, 1a′ and 3a′ are largely Cp_2Zr based orbitals and didn't change substantially from Cp_2Zr fragment orbitals after interacting with the CH_2 group orbitals. These are the ones that interact strongly with the phenyl group (Fig. 3.1.1). Due to the low symmetry of the resulting molecule (**12**)

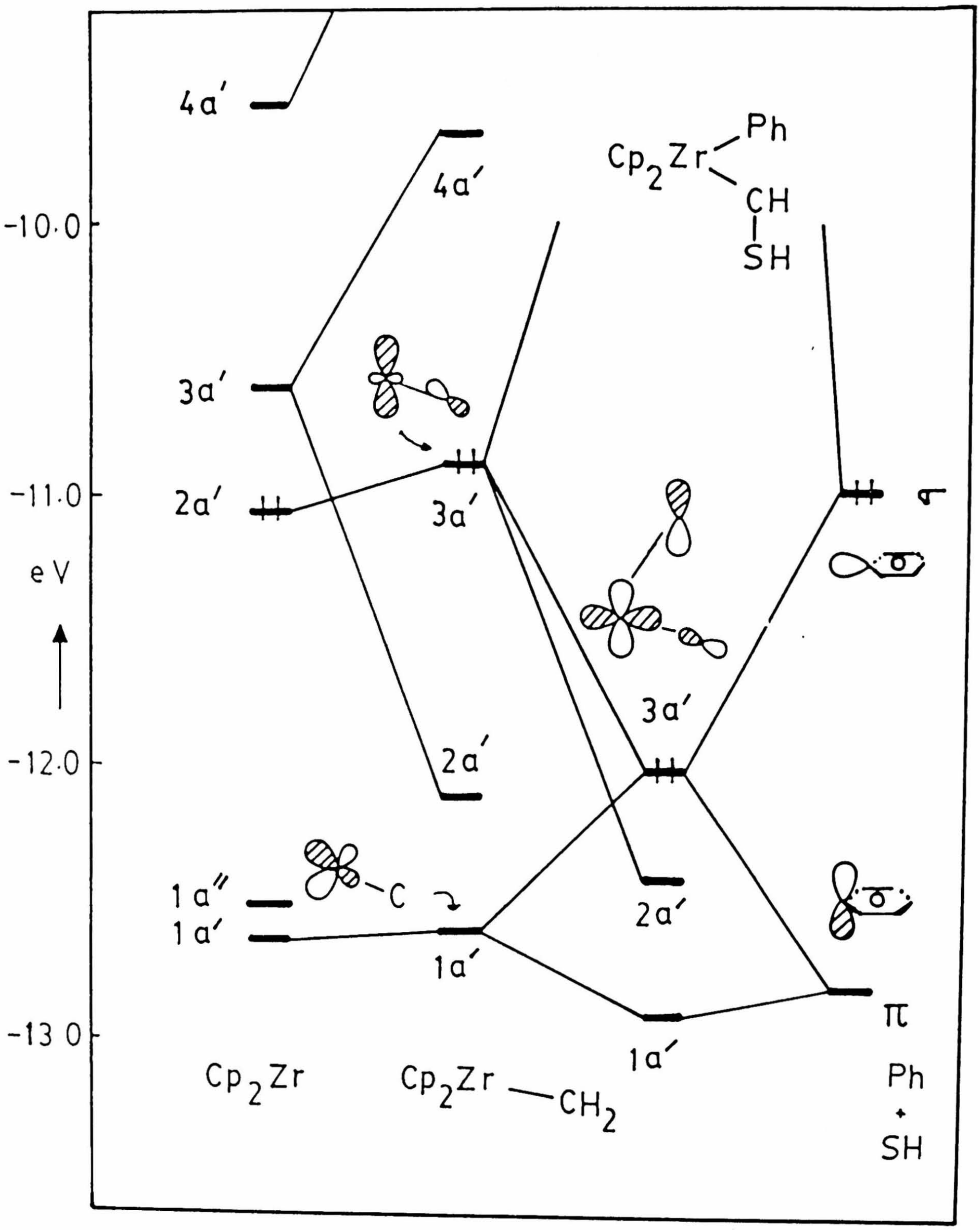

Fig. 3.1.1: Construction of the molecular orbitals of $Cp_2Zr(Ph)(CH_2\text{-}SH)$ (4) from the fragment orbitals of $Cp_2Zr\text{-}CH_2$ and Ph...SH (right). The $Cp_2Zr\text{-}CH_2$ fragment orbitals are in turn obtained from the group orbitals of Cp_2Zr and CH_2 fragments (left). Only Cp_2Zr orbitals are shown, the CH_2 orbitals are not shown in the Figure.

several multicentre interactions are seen. The HOMO of **12**, 3a′, is a part of the four orbital-six electron interaction as shown in Fig. 3.1.1. 3a′ is an antibonding combination of the Zr-C bonding orbital and the Ph π orbital. The frontier orbitals of SH group are at relatively lower energy. The sulfur atom of the SH group is

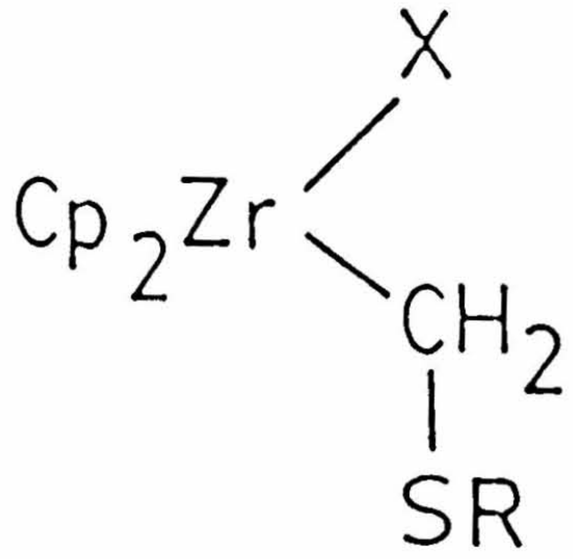

10

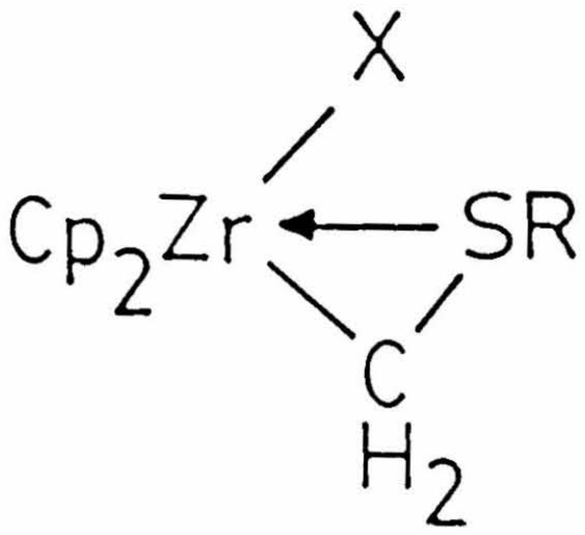

11

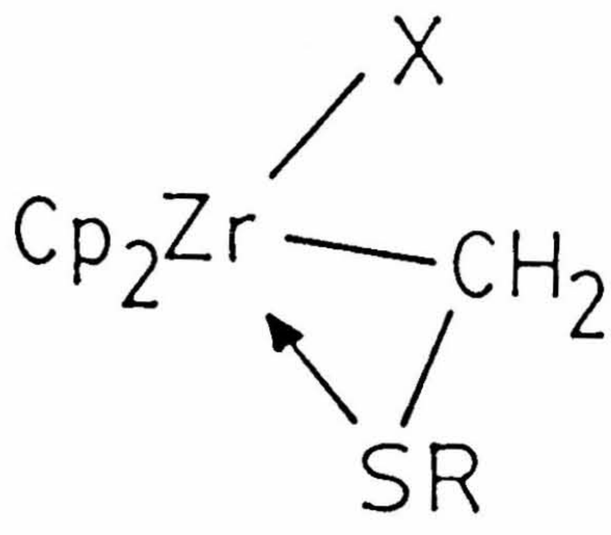

12

bound to C(1) in a σ fashion and at the same time the lone pair on sulfur is donated to the Zr centre.

A reaction coordinate is constructed for eq. 3.1.2 which connects the initial structure (**3**) and the final structure (**4**) in equal increments of all the geometric parameters. The Ph group is

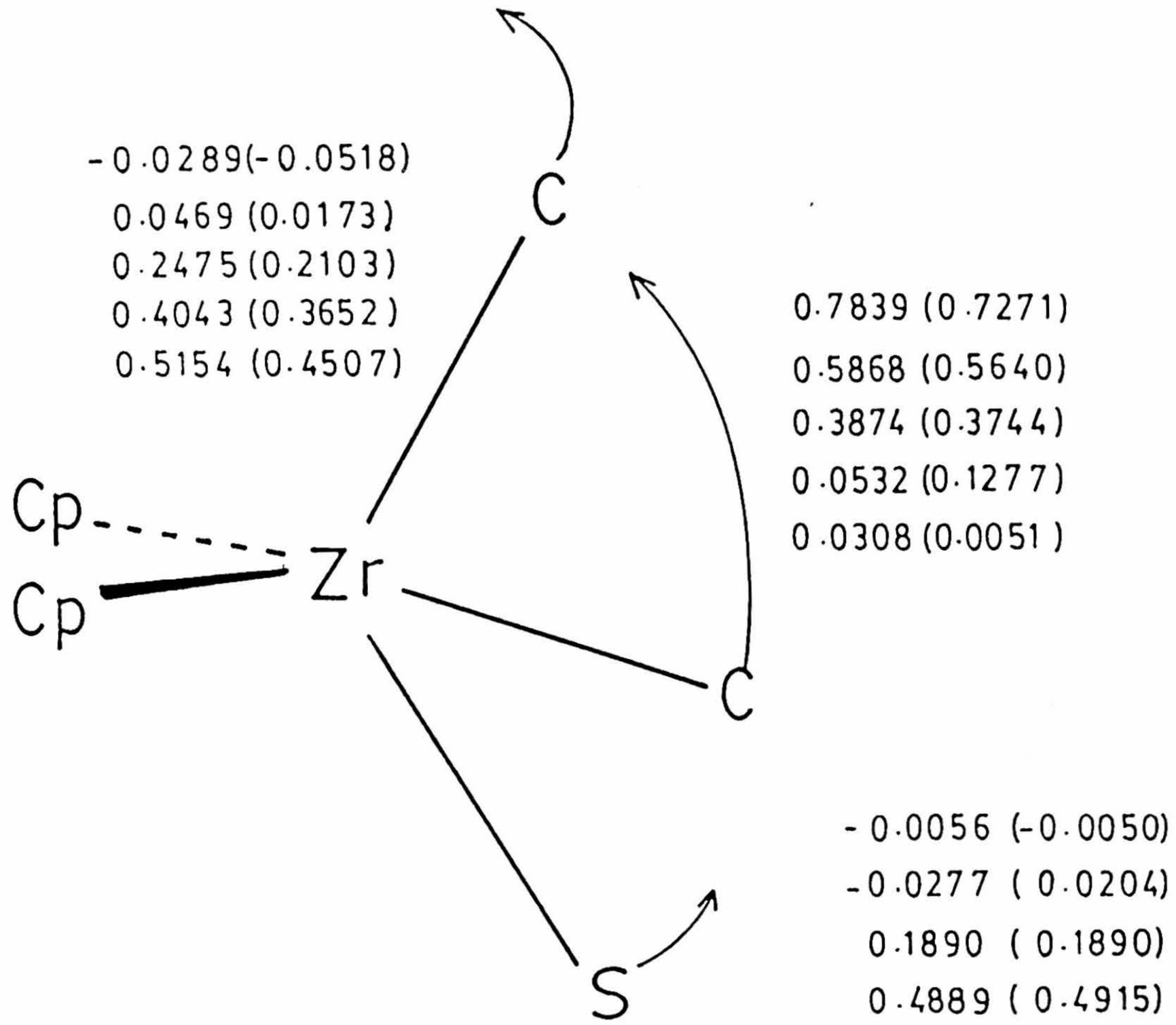

Fig. 3.1.2: Positional changes of C(1), C(2) and S along the reaction coordinate as in eq. 3.1.2 for $Cp_2Zr(X)(CH_2\text{-}SH)$ going to $Cp_2Zr(CH_2\text{-}X)(SH)$ (eq. 3.1.2a). The corresponding Mullikan overlap population values between Zr-C(2), C(1)-C(2) and C(1)-S along the reaction coordinate are given for X = Ph. The values in the parentheses correspond to X = Me.

kept perpendicular to the reaction plane because in the in-plane geometry there are serious steric factors. The positions of C(1) (the methylene carbon), C(2) (the carbon of the migrating group) and S in the reaction plane at different points along the reaction coordinate are plotted in Fig. 3.1.2. This reveals that C(1) has to move a lot more than that of either C(2) or S during the reaction (since the Cp_2Zr unit is kept rigid during the process). The plot of the sum of one electron energies for eq. 3.1.2a shows a barrier of 16 kcal mol^{-1} (Fig. 3.1.3) for X = Ph. This is comparable to the experimentally observed value of 20 kcal mol^{-1}, for eq. 3.1.2a. The product (**4a**) is calculated to be more stable than the reactant (**3a**) by about 28 kcal mol^{-1}.

The Walsh diagram (Fig. 3.1.3a) for this process shows some of the MO's that change maximum along the reaction coordinate. C_s symmetry is retained during the reaction. HOMO (5a') reproduces the variations of the total energy to some extent. This molecular orbital is initially based on Zr, C(2) and C(1). As the reaction proceeds, the antibonding interaction between Zr-C(2) and C(1) in HOMO gets stronger and an additional Zr-S antibonding interaction develops until the transition state is reached as shown in the Scheme 1. But after reaching a maximum, it comes down as the interaction with S changes from antibonding to bonding with Zr-C(1) bond in the HOMO (Scheme 1). The C-H bonding orbitals of CH_2 (1a'') show a minimum around the transition state which brings down the barrier for the process by about 11.5 kcal mol^{-1}. At the transition state C(1) is more like an sp^2 carbon. One of the

Scheme I

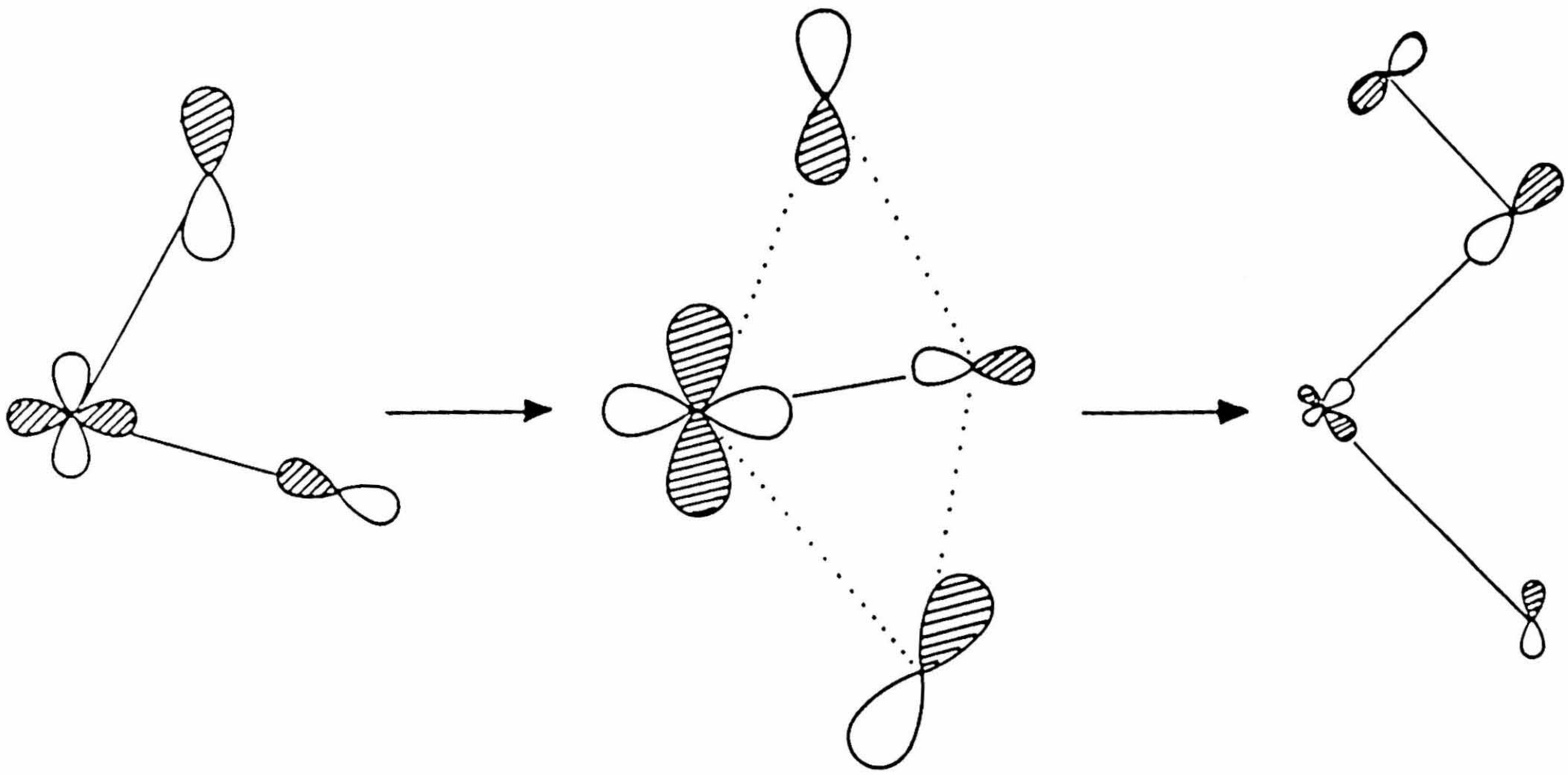

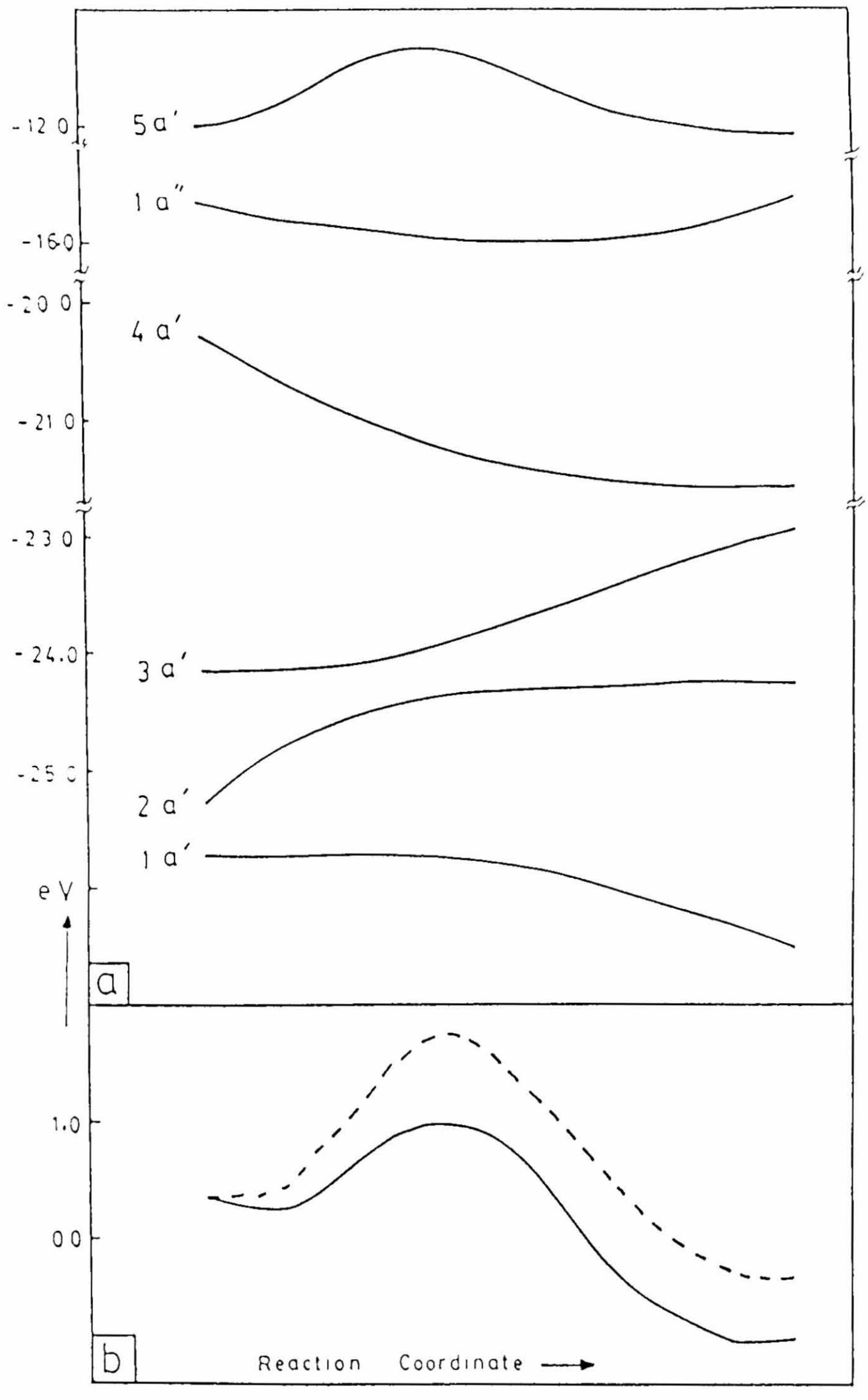

Fig. 3.1.3: (a). Walsh diagram for the transformation of $Cp_2Zr(Ph)(CH_2\text{-}SH)$ (3) to $Cp_2Zr(CH_2\text{-}Ph)(SH)$ (4) (eq. 3.1.2a); only the orbitals undergoing significant changes are shown. (b). Plot of the sum of one electron energies in going from **3a** to **4a** (thick line). Dashed line shows the corresponding plot of for **3b** going to **4b**.

reasons for the minimum is the fact that sp^2 carbon forms stronger C-H bonds than sp^3 carbon. Except for this, molecular orbitals antisymmetric to the reaction plane are the least affected along the reaction coordinate. Low lying orbitals corresponding to the formation of C-C and Zr-S bonds, and to the cleavage of Zr-C and C-S bonds are the most affected as the reaction proceeds.

The ground state electronic structure of the reactants (3) in eq. 3.1.2 when X = Ph or Me is not very different. But a methyl instead of phenyl prevents the reaction to take place. When the potential energy surface is generated for eq. 3.1.2b the barrier comes to about 32 kcal mol^{-1} (Fig. 3.1.3b). This barrier is significantly higher than that calculated for eq. 3.1.2a.

The difference in the barrier with two different substituents arises mostly from the difference in the stabilization of the transition states by the two groups. The highest energy point along the reaction coordinate is regarded as the transition state in this one-electron model study. The product (4) is calculated to be more stable than the reactant (3) only by about 16 kcal mol^{-1} for X = Me as against 28 kcal mol^{-1} for X = Ph.

To explore the differences between Ph and Me in this reaction (eq. 3.1.2), interaction diagrams are constructed at the geometry corresponding to the transition state. Here we consider $Cp_2Zr\text{-}CH_2(SH)$ as one fragment and X as the other, because there is

Indira Gandhi Memorial Library University of Hyderabad

not much of an influence of the SH group orbitals in the frontier levels. The major interactions of Ph and Me with $Cp_2Zr(CH_2)SH$ are shown in Fig. 3.1.4. In both the cases the frontier orbital of the X group interacts with the LUMO and an occupied orbital of the metal fragment leading to a three orbital-four electron interaction. In the ground state the HOMO results from a four orbital-six electron interaction. It has now become three orbital-four electron interaction because the orientation of the π orbital of Ph is not suitable for the interaction with the metal fragment orbitals at this transition state geometry. For the methyl or the phenyl as the migrating group the middle orbital in the three orbital-four electron interaction, HOMO, is chiefly responsible for the barrier. The frontier orbital of the Me group lies lower in energy than that of the Ph group. In the three orbital-four electron interaction, the Ph σ-bonding orbital interacts more strongly with the LUMO of the metal fragment whereas the Me σ-bonding orbitals interact more strongly with the occupied orbital of the metal fragment (Fig. 3.1.4).

Variations in the low lying orbital energies also contribute to the barrier.[14,15a] Both the bonding and the antibonding orbitals resulting from the interaction of the low lying orbitals are occupied so that stronger interactions between these fragment molecular orbitals lead to more destabilisation. There is a strong interaction when X = Me in the low lying MOs. Such strong interactions between the two fragments at the transition state results in higher barrier for the reaction. The relative

A01678

Indira Gandhi Memorial Library
University of Hy

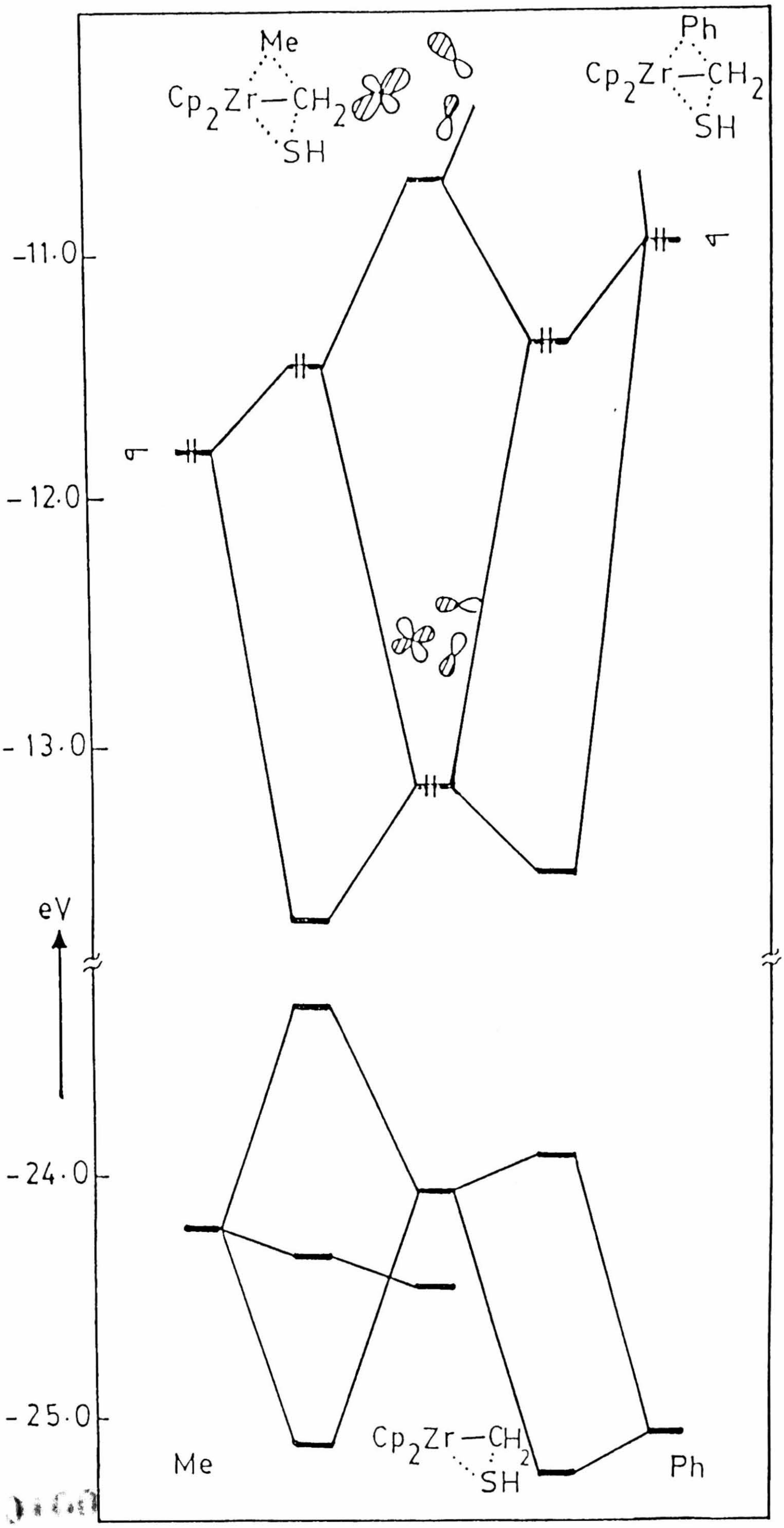

Fig. 3.1.4: The orbital interaction diagram of $CP_2Zr(CH_2\text{-}SH)$ fragment with Ph (right) and Me (left) fragments at the transition state.

importance of the frontier orbitals versus lower lying ones is analyzed by splitting the plot of the sum of one electron energies into two parts. The first part consists of occupied orbitals upto -14.975 eV which includes the two occupied orbitals in the three orbital-four electron interaction (the frontier region) and the second part includes the remaining low lying orbitals. There is a gap of about 1 eV between these two parts in the Walsh diagram and there is no crossing between the levels of the two groups. The first part gives a difference of 7 kcal mol^{-1} and the latter gives 9 kcal mol^{-1} for the barrier of the reaction. This shows that both the frontier as well as the low lying orbitals are equally responsible for the barrier in this reaction.

Mulliken overlap population values at various points along the reaction coordinate reveal that for eq. 3.1.2b, the Zr-C(1) and C(1)-C(2) values are less than their counterparts in eq. 3.1.2a, (Fig. 3.1.2). This implies that Ph group could bind simultaneously with the metal and the CH_2 group more strongly than is possible for the Me group. The C-C bond formation starts much earlier in the case of Ph while retaining considerable bonding interaction with the metal centre (Fig. 3.1.2).

The net charge on the migrating phenyl carbon gradually changes from a high negative value (-0.294) to a positive value (0.088) along the reaction coordinate (eq. 3.1.2a). This shows that an electron donating group on the phenyl ring would favour the reaction. Experimentally, the reaction is found to be five

Table 3.1.1 : Changes in the net charges on C(1), C(2), S and Zr along the reaction coordinate in eq. 3.1.2a.

Points along the reaction coordinate	ATOM			
	C(1)	C(2)	S	Zr
1	-0.304	-0.294	0.175	0.447
2	-0.116	-0.218	0.032	0.302
3	-0.009	-0.087	-0.316	0.225
4	-0.360	-0.020	-0.531	0.626
5	-0.464	0.061	-0.424	0.745
6	-0.402	0.088	-0.348	0.738

times faster for X = p-C_6H_4OMe than for X = Ph. The net charges on Zr, S, C(1) and C(2) are given in Table. 3.1.1. As the reaction proceeds, the negative charge on C(1) decreases gradually up to the transition state and increases afterwards. This would facilitate the nucleophilic attack of the migrating group on C(1).

The above analysis shows that Ph group has many advantages over Me in eq. 3.1.2. Since there is not much of a difference in the frontier orbitals of Me and CH_2Ph we do not find a significant difference between eq. 3.1.2b and eq. 3.1.2c. The Cl substitution also presents a similar picture leading to a high barrier. As expected it is observed that eq. 3.1.2 takes place only with X = Ph. A vinyl group with its π orbital in the reaction plane for X in eq. 3.1.2 provides similar frontier orbitals to that of the Ph group. A potential energy surface for eq. 3.1.2 when X = $-CH=CH_2$ gives a barrier of about 15 kcal mol^{-1}, which is comparable to that with the Ph substituent. Experimental studies in this direction should be rewarding.

The reaction of $Cp_2Zr(C_4H_3O)_2$ to give the zirconacycle (6) (eq. 3.1.3)

Eq. 3.1.3 (formation of Zirconacycle (6)) has a close similarity to eq. 3.1.2. Both involve C-C bond formation, Zr-C bond cleavage and Zr-O or Zr-S bond formation followed by C-O or C-S bond cleavage. The reaction coordinate chosen for study of eq. 3.1.3 is similar to that for eq. 3.1.2. The plot of the sum of one

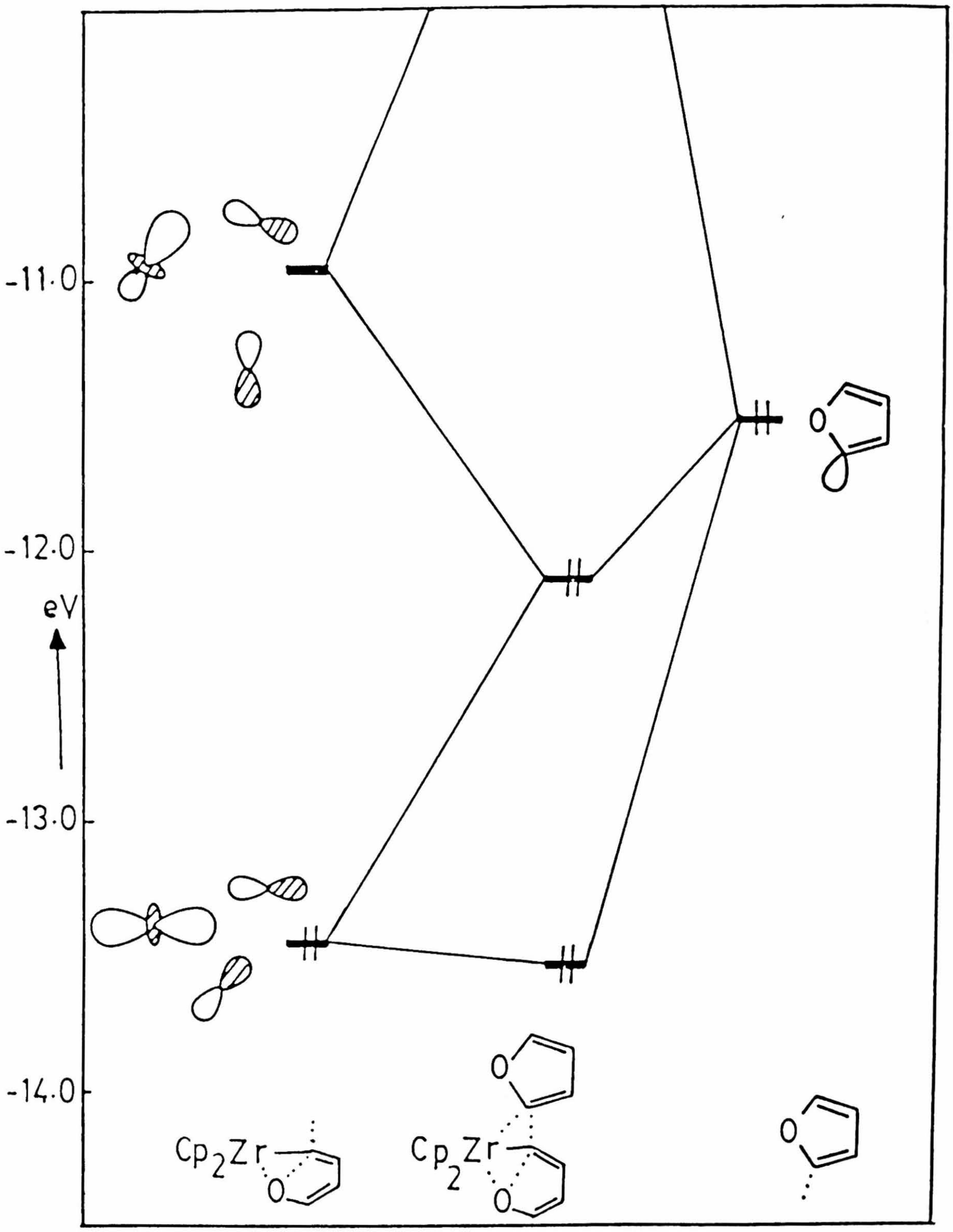

Fig. 3.1.5: The orbital interaction diagram between the fragments $Cp_2Zr(C_4H_3O)$ and C_4H_3O at the transition state.

electron energies shows a barrier of about 10 kcal mol^{-1}.

The Walsh diagram shows that the barrier is reproduced by the HOMO+2 orbital to some extent. An interaction diagram is constructed for this reaction at the transition state using the fragments furanyl and $Cp_2Zr(C_4H_3O)$. Here also the strongest interaction is a three orbital-four electron one involving the HOMO of the migrating group (furanyl), LUMO and an occupied orbital of $Cp_2ZrC_4H_3O$. HOMO+2 which reproduced the total energy is the middle orbital in the three orbital interaction. There are also some interactions among low lying orbitals that add to the effects of the frontier orbitals. In general the controlling factors for eq. 3.1.2 and eq. 3.1.3 appear to be similar. The potential energy surface is generated for eq. 3.1.3 by replacing the migrating furanyl by Ph and Me. The plot of the sum of one electron energies shows no barrier when Ph is the migrating group. Me substitution gives a barrier of about 7 kcal mol^{-1}. The low barrier for eq. 3.1.3 can be traced to the low lying metal fragment LUMO (-10.95 eV). This LUMO interacts strongly with the HOMO of the migrating group and stabilises the lower two orbitals of the three orbital interaction. In eq. 3.1.2 the LUMO of the metal fragment, $Cp_2Zr(CH_2\text{-}SR)$ is at -10.57 eV. Hence for the same migrating groups there is a large difference in the barriers of these two reactions. If the starting compounds with Me and Ph are prepared for eq. 3.1.3, according to this analysis, the formation of Zirconacycles should be facile.

Intrigued by the above suggestions, Erker et al. have experimentally carried out the dyotropic rearrangements with Me and Ph as the substituents.[16] Both methyl and phenyl migration seems to proceed even more slowly than the furanyl shifts contrary to the extended Huckel calculations.[17] However, the differences in rates are not very large. In addition to Me and Ph, they have carried out the reaction with $SiMe_3$, whose migration from Zr to carbon is found to be several orders of magnitude faster than all the substituents, i.e., furanyl, Me and Ph.

On the migratory aptitudes of ligands

Basically any migration involves the cleavage of a bond and the formation of another. Barriers for migration reactions are said to be controlled by the migrating abilities of the groups. What are the factors involved in the migration of a group? What are the conditions that make the process better or worse? Is it possible to talk about the inherent migrating ability of any group independent of the reaction? We attempt to find out the origin of the higher or lower migrating ability of a group in these reactions. Many theoretical and experimental studies are available on the topic of migrations, in organic as well as organometallic chemistry.[14,15] It has not been possible to attribute the migratory aptitudes to groups that can be used from reaction to reaction. We shall see the intricacies involved in giving a rigid value for migrating aptitudes of groups independent of the reaction based on the above results.

The three orbital-four electron interaction noticed at the transition state point is common in the reactions that are studied. The difference in energy between the σ bonding orbital of the migrating group and the LUMO of the metal fragment should be minimum to get the maximum stabilization. The extension in space of the σ bonding orbital of the migrating group is also important. It should be so oriented that there is optimum overlap with the LUMO of the metal fragment.

In addition to this there can be other interactions in the lower lying orbitals. These are two orbital-four electron interactions, which lead to destabilisation. Sometimes these will be determinative as in eq. 3.1.2a. Though the HOMO of the furanyl group lies at a higher energy than that of the Me group, a slightly higher barrier is observed for the furanyl substitution over Me in eq. 3.1.3. This is due to the interactions of low lying orbitals as seen from an interaction diagram for X = Me and $Cp_2Zr(C_4H_3O)$ at the transition state. This analysis indicates that in organometallic migratory reactions it is not possible to talk about the inherent migrating abilities of different groups. Migratory aptitude depends on the total molecule of which the migrating group is a part. What is true of the organometallic compounds should also be applicable to the organic compounds even though the details of the interactions between the migrating group and the organic moiety will differ. This is reflected in the difference in the migratory aptitudes of the same set of groups in

different reactions. In addition to the electronic effects, migrations should also depend on the medium of the reaction. It is not surprising therefore that clear cut answers to the relative migrating tendencies of various groups that are applicable to large sets of reactions are not available.[18]

3.1.4 Conclusions

The feasibility of the reaction $Cp_2Zr(X)(CH_2\text{-}SR)$ going to $Cp_2Zr(CH_2\text{-}X)SR$ with X = Ph and not with X = Me, CH_2-Ph or Cl is attributed to the higher migratory aptitudes of the phenyl groups. Molecular orbital studies using the extended Huckel method has confirmed the general idea that the migratory aptitudes can not be independent of the reaction. However as expected, the method is not able to give quantitative results. The same set of groups would have different relative migratory aptitudes in different reactions. Only the migrating group's σ orbital and not their π orbitals seems to play a major role in these rearrangements.

The Cp_2Zr fragment in these complexes may be treated as the smallest metal template on which various transformations can occur. The two Cp units would be above and below the reaction plane (the plane containing the fragment orbitals) and orthogonal to the plane formed by Zr and the centroids of the Cp rings. The large number of frontier orbitals of differing symmetry and extension in space in the reaction plane help in retaining substantial bonding character throughout the reaction coordinate. This is seen from the Mulliken overlap population values. Hence we feel that Cp_2Zr fragment may be treated as a mononuclear system closest to that of a template.

3.2 Electronic Structure and Reactivity of $Cp_2Zr=E$ (E = S, O, NH and PH) compounds.

3.2.1 Abstract

Extended Huckel calculations are performed on $Cp_2Zr=E$ (E = S, O, NH and PH). Electronic structure of these compounds is similar. Their reactivity is mainly due to the LUMO and LUMO+1. The HOMO of these complexes have Zr-X π^* interaction, which also plays a significant role. Alkynes and alkenes react with $Cp_2Zr=E$ in 2+2 fashion. The electronic structures of the resultant metallacyclobutenes and metallacyclobutanes are studied. Alkenes and alkynes form similar stabilizing interactions with the transition metal fragment, $Cp_2Zr=E$, in the reaction plane. In alkynes the π^* orbital perpendicular to the reaction plane stabilizes the HOMO of $Cp_2Zr=E$. This additional stabilizing interaction is absent in alkenes.

3.2.2 Introduction

Reactions that produce direct adducts between M=E and organic molecules are not common[19]. Recently zirconocene compounds with the terminal sulphido,[20] oxo,[21] imido[22] and phosphido[23] ligands are found to be unusually reactive towards organic molecules. These studies are aimed at activating stable organic molecules and incorporating hetero-atoms into them through transition metal mediated reactions.[20-24] $Cp_2Zr=E$ compounds dimerize easily.[25] The more sterically demanding Cp^* ligands inhibit this dimerization process, forcing $Cp_2Zr=E$ to complex with organic moieties. While $Cp^*_2Zr=E$ compounds are readily trapped with alkynes, nitriles and dative ligands, similar trapping reactions with alkenes are scarce. It is also found that diphenylacetylene reacts faster and form more stable adducts compared to their dialkyl analogs.[24,26] Recently, the formation of 2+2 adduct between $Cp_2Zr=NR$ and ethylene has been reported.[27] However, the reaction is reversible at room temperature.

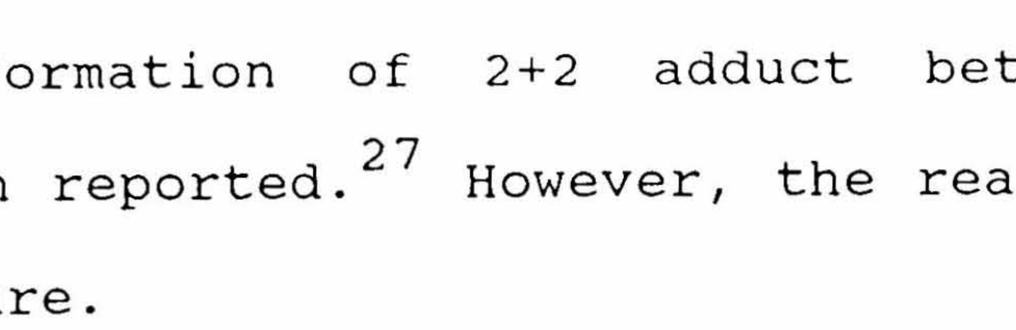

	a	b	c	d
E	S	O	NH	PH

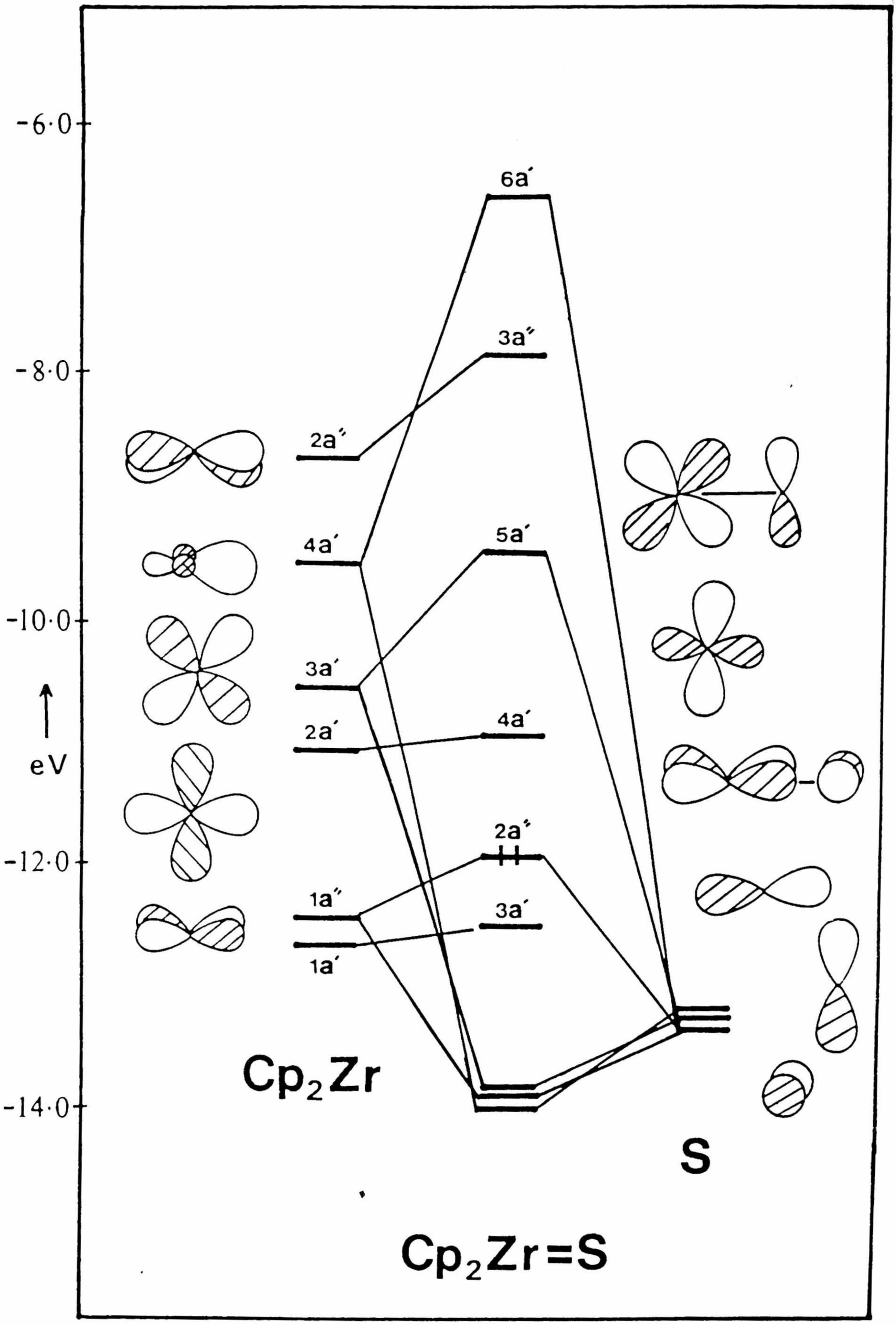

Fig. 3.2.1: Construction of the orbitals of $Cp_2Zr{=}S$ from the fragments Cp_2Zr and S.

In this section, we study the electronic structure of $Cp_2Zr=S$, **1a**, first. The correlation of frontier molecular orbital energy levels of $Cp_2Zr=E$ (E = S, O, NH and PH) is presented next. The difference in the reactivity of $Cp_2Zr=S$ towards alkynes and alkenes is also studied. We modelled Cp^* with Cp in this study. This modelling is quite unlikely to reverse the qualitative arguments that are used in this study. Fragment Molecular Orbital[9] approach within the extended Huckel formalism[10] is used in this study.

3.2.3 Results and Discussion

Electronic Structure of $Cp_2Zr=S$, 1a.

The molecular orbitals of $Cp_2Zr=S$ can be constructed from the well known simpler fragments Cp_2Zr and S (Fig. 3.2.1). C_s symmetry labels are used for convenience, although the molecule has C_{2v} symmetry. The frontier orbitals of Cp_2Zr lie exclusively in the plane perpendicular to the plane formed by the centroids of the two Cp rings and Zr. There is a σ bond (between 4a′ of Cp_2Zr and p_x of S) and an in-plane π bond (between 3a′ of Cp_2Zr and p_y of S) formed between Zr and S. The other π (1a′′) and π^* orbital (2a′′) are occupied. This accounts for the double bond character between Zr and S. The HOMO of $Cp_2Zr=S$ has Zr-S out-of-plane π^* character. However, S atom may not be in the plane containing the two centroids of the Cp rings and Zr. Extended Huckel calculations show that the structure is more stable when sulfur atom is off the

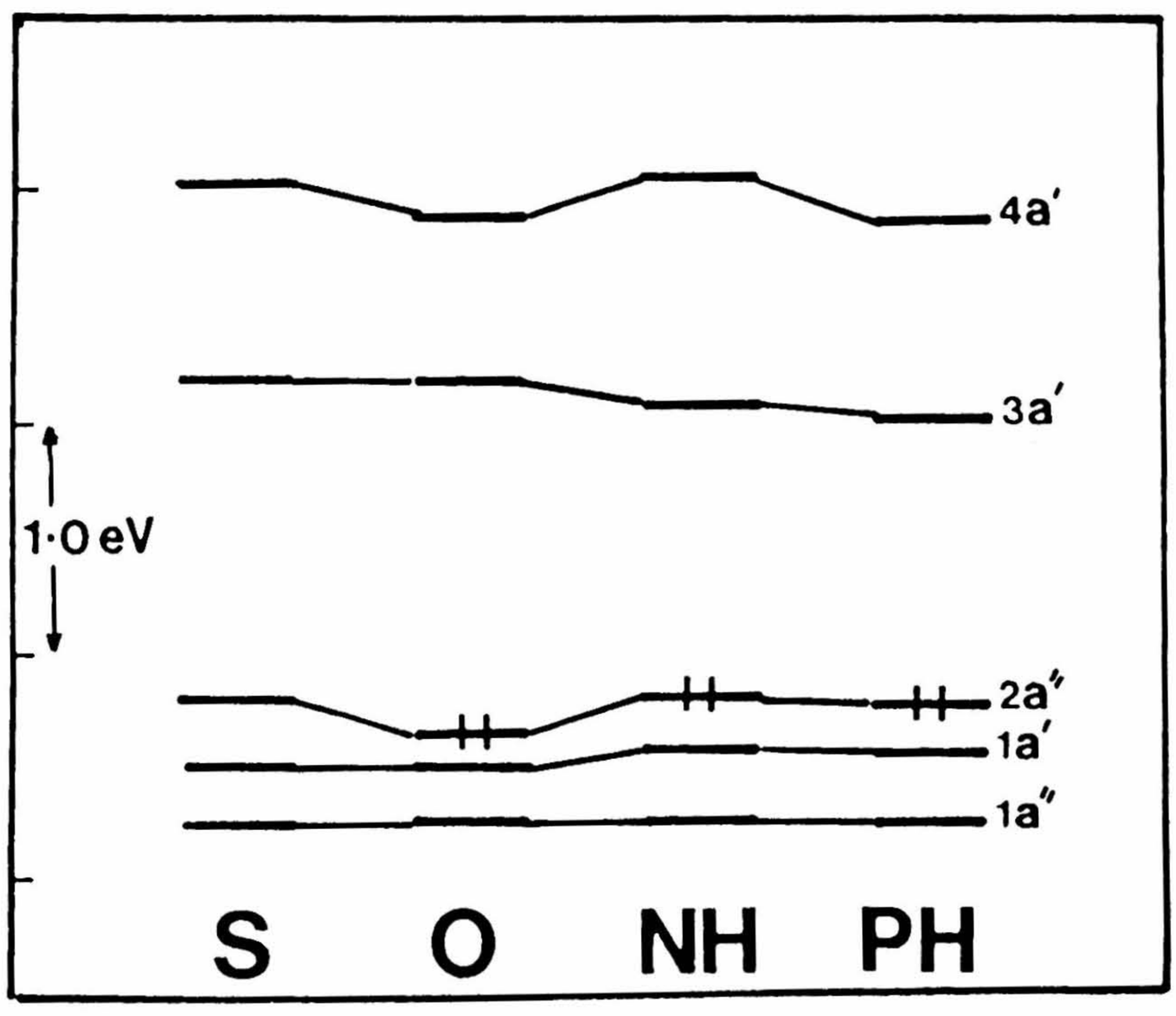

Fig. 3.2.2: Correlation of the energy levels of $Cp_2Zr=E$ (E = S, O, NH and PH) as a function of E.

C_2 axis by 30° in the reaction plane. Scheme 1 gives the change in the frontier orbitals when the S atom is off the C_2 axis by 30°. The potential energy profile for the movement of S atom in that plane is very soft. Such an arrangement of $Cp_2Zr{=}S$ is ideal for reactions with the incoming ligands, as the frontier orbitals, LUMO and LUMO+1, are oriented in the direction of the incoming ligands.

Correlation of $Cp_2Zr{=}E$ (E = S, O, NH and PH) as a function of E

Fig. 3.2.2 gives the correlation of $Cp_2Zr{=}E$ (E = S, O, NH and PH) as a function of E. In **1c**, the conformer with Zr-N-H angle of 180° is calculated to be the most stable, which is in conformity with the experimental observation. **1d** follows the same trend. The reactivity of these $Cp_2Zr{=}E$ complexes is mainly due to the metal based LUMO and LUMO+1. The HOMO, 2a'', has Zr-E π^* character, which is perpendicular to the reaction plane. This orbital, 2a'', could play crucial role when the π interactions perpendicular to the reaction plan is operative, which is not common in Cp_2Zr Chemistry.[1,6] The electronic structures of $Cp_2Zr{=}E$ (E = O, NH and PH) compounds are similar to that of $Cp_2Zr{=}S$ and hence are not discussed in detail. The potential for the movement of E atom in the reaction plane is very soft in all the cases.

Reactivity of $Cp_2Zr{=}S$ with acetylene and ethylene

The molecular orbitals of **2** and **3** can be constructed in two

Scheme 1

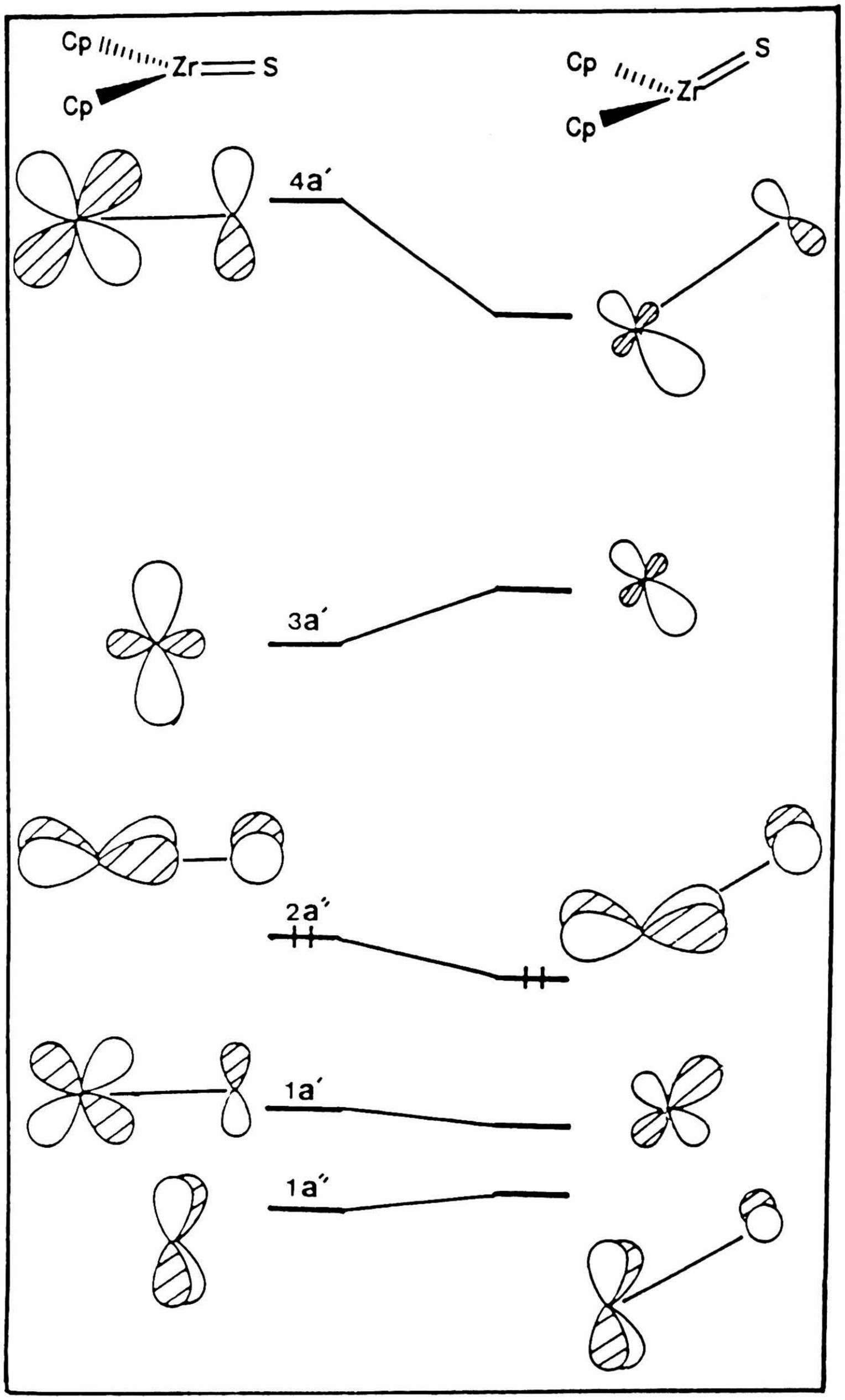

ways. We can consider the interaction of $Cp_2Zr{=}S$ with C_2H_2 and C_2H_4 (Fig. 3.2.3). Alternatively, we can consider the interaction of Cp_2Zr with SC_2H_2 and SC_2H_4. However, the latter fragmentation does not provide any further insight into the bonding and is not presented here.

Fig. 3.2.3 shows the interaction of $Cp_2Zr{=}S$ orbitals with C_2H_2 (right) and C_2H_4 (left) orbitals. The interactions of both the alkyne and the alkene with $Cp_2Zr{=}S$ are similar in the reaction plane. The LUMO and LUMO+1 of **1a** interact with the in-plane π and π^* orbitals of alkynes and alkenes giving a four orbital-two electron interaction. Thus, alkenes and alkynes act as two electron donors. The HOMO of $Cp_2Zr{=}S$ is slightly destabilized by the pseudo-π orbital of C_2H_4 fragment. On the other hand, C_2H_2 has the π^* orbital of the right symmetry to suppress the corresponding destabilization interaction. Although π and π^* orbitals of acetylenes formally belong to the same symmetry, only π^* will have proper overlap with the HOMO of $Cp_2Zr{=}S$ in this case. Effectively, acetylenes have greater stabilizing effect when trapped with $Cp_2Zr{=}S$, compared to alkenes. This has been reflected in the low lying HOMO of **2** compared to **3** (Fig. 3.2.3). The stabilization due to the interaction of acetylene with $Cp_2Zr{=}S$ is calculated to be 2.6 eV. Corresponding stabilization with ethylene is only 2.0 eV. The stabilization interaction is calculated by taking the difference of the sum of one electron energies of the product and individual fragments. Experimentally, the complexes are not found to be easily trapped by alkenes. Similar to the acetylenes,

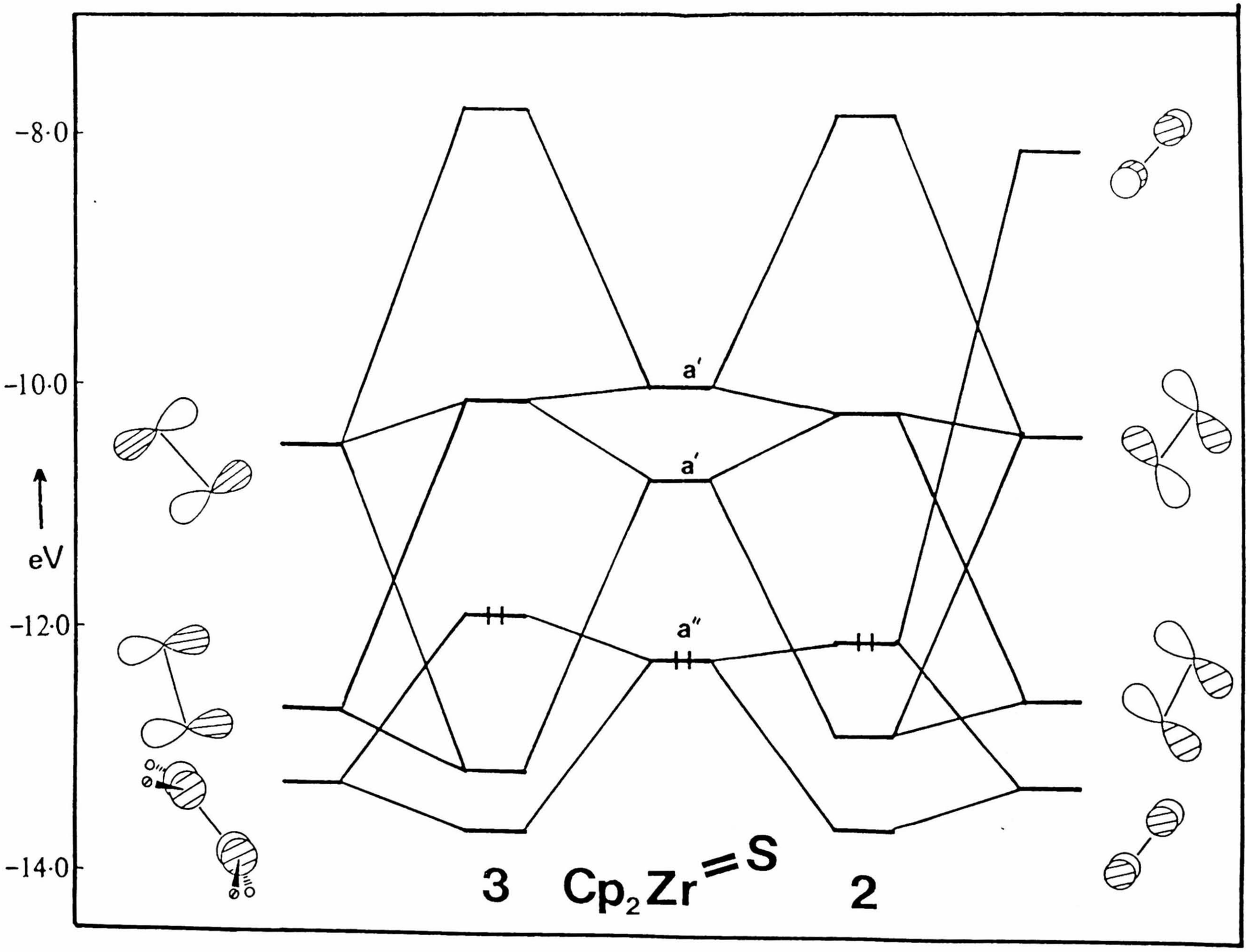

Fig. 3.2.3: The orbital interaction diagram of $Cp_2Zr{=}S$ with C_2H_2 (right) and C_2H_4 (left) fragments.

nitriles (RC=N), which also have two orthogonal π bonds will form stable adducts with $Cp_2Zr=E$ compounds.

This analysis also explains the experimental observation that diphenylacetylene forms more stable adducts with $Cp_2Zr=E$ type complexes compared to simple dialkylacetylenes. This follows from the low lying π^* orbital of diphenylacetylene which is energetically more favourable to interact with the HOMO of $Cp_2Zr=E$. It should be possible to expand this model to understand other reactions of $Cp_2Zr=E$.

3.2.4 Conclusions

The description of the electronic structure of $Cp_2Zr{=}E$ (E = S, O, NH and PH) complexes is helpful in predicting their reactivity. The extreme reactivity of these class of complexes towards organic molecules is due to their low lying LUMO and LUMO+1. The HOMO of $Cp_2Zr{=}E$ complexes have Zr-E π^* (out-of-plane) character, which has the right symmetry to interact with the acetylene (or nitrile) π^* orbital. Such additional stabilization is absent in alkenes. This analysis also accounts for the higher reactivity of diphenylacetylenes in comparison to the simple or dialkyl acetylenes.

3.3 References

1. (a) S.L. Buchwald and R.B. Nielsen, Chem. Rev., **1988**, 88, 1047.

   (b) G. Erker, Angew. Chem. Int. Ed. Engl. **1989**, 28, 387.

   (c) R.F. Jordan, Adv. Organomet. Chem., **1991**, 32, 325.

2. (a) M. T. Reetz, Adv. Organomet. Chem., **1977**, 16, 33.

   (b) M. T. Reetz, Angew. Chem. Int. Ed. Engl., **1972**, 11, 129, 131.

3. G. Erker, J. Chem. Soc., Chem. Commun., **1989**, 345.

4. (a) E. A. Mintz, A. S. Ward and D. S. Tice, Organometallics, **1985**, 4, 1308.

   (b) A. S. Ward, E. A. Mintz and M. P. Kramer, Organometallics, **1988**, 7, 8.

5. (a) H. H. Britzinger and L. S. Bartell, J. Am. Chem. Soc., **1970**, 92, 1105.

   (b) H. H. Britzinger and J. E. Bercaw, J. Am. Chem. Soc., **1970**, 92, 6182.

6. J.W. Lauher and R. Hoffmann, J. Am. Chem. Soc., **1976**, 98, 1729.

7. (a) K. I. Gell, G.M. Williams and J. Schwartaz, J. Chem. Soc., Chem. Commun., **1980**, 550.

   (b) G. Erker and K. Kropp, Chem. Ber., **1982**, 115, 2437.

8. (a) W. Kaminsky, J. Kopf, H. Sinn and H. -J. Vollmer, Angew. Chem., 88 (1976) 688; Angew. Chem. Int. Ed. Engl., **1976**, 15, 629.

   (b) A. J. Kos, E. D. Jemmis, P. v. R. Schleyer, R. Gleiter, U. Fischbach and J. A. Pople, J. Am. Chem. Soc., **1981**, 103, 4996.

9. (a) H. Fujimoto and R. Hoffmann, J. Phys. Chem., **1974**, 78, 1169.

(b) R. Hoffmann, T. R. Swenson and C. -C. Wan, J. Am. Chem. Soc., **1973**, 95, 7644.

10. (a) R. Hoffmann, J. Chem. Phys., **1963**, 39, 1397.

(b) R. Hoffmann and W. N. Lipscomb, J. Chem. Phys., **1962**, 36, 3179; **1962**, 36, 3489.

11. (a) P. Hofmann, P. Stauffert and N. E. Schore, Chem. Ber., **1982**, 115, 2153.

(b) K. Tatsumi, A. Nakamura, P. Hofmann, P. Stauffert and R. Hoffmann, J. Am. Chem. Soc., **1985**, 107, 4440.

12. A. S. Ward, E. A. Mintz and M. R. Ayers, Organometallics, 5 **1986**, 1585.

13. W. L. Jorgensen and L. Salem, *The Organic Chemist's Book of Orbitals*, Academic Press, New York, **1973**.

14. The determinative role played by two centred four electron interactions seen in, S. Shaik, R. Hoffmann, C. R. Fisel and R. H. Summerville, J. Am. Chem. Soc., **1980**, 102, 4555, also see 14a.

15. (a) H. Berke and R. Hoffmann, J. Am. Chem. Soc., **1978**, 100, 7224, and references cited therein.

(b) F. U. Axe and D. S. Marynick, J. Am. Chem. Soc., **1988**, 110, 3728 and references cited therein.

(c) C. Zheng, Y. Apeloig and R. Hoffmann, J. Am. Chem. Soc., **1988**,110, 749.

16. G. Erker, R. Petrenz, C. Kruger, F. Lutz, A. Weiss and S. Werner, Organometallics, **1992**, 11, 1646.

17. G.N. Sastry and E.D. Jemmis, J. Organomet. Chem, **1990**, 388, 289.

18. J. March, *Advanced Organic Chemistry*, 3rd ed., Mc Graw-Hill, New York, **1985**, pp 949-951, and references cited therein.

19. (a) W.A. Nugent and J.A. Mayer, *Metal-Ligand Multiple Bonds;* Wiley-Interscience: New York, **1988**.

(b) R.H. Holm, Chem. Rev., **1987**, 87, 1401.

20. M.J. Carney, P.J. Walsh and R.G. Bergman, J. Am. Chem. Soc., **1990**, 112, 6426.

21. (a) M.J. Carney, P.J. Walsh, F.J. Hollander and R.G. Bergmann, J. Am. Chem. Soc., 1989, 111, 8751.

(b) M.J. Carney, P.J. Walsh, F.J. Hollander and R.G. Bergman, J. Am. Chem. Soc., **1989**, 111, 8751,

22. (a) P.J. Walsh, F.J. Hollander and R.G. Bergmann, J. Am. Chem. Soc., **1988**, 110, 8729.

(b) P.J. Walsh, M.J. Carney and R.G. Bergmann, J. Am. Chem. Soc., **1991**, 113, 6343.

23. (a) Z. Hou and D.W. Stephan, J. Am. Chem. Soc., **1992**, 114, 10088.

(b) Z. Hou, T.L. Breen and D.W. Stephan, Organometallics, **1993**, 12, 3258.

24. (a) M.J. Carney, P.J. Walsh, F.J. Hollander and R.G. Bergman, Organometallics, **1992**, 11, 761.

(b) A.M. Baranger, P.J. Walsh and R.G. Bergman, J. Am. Chem. Soc., **1993**, 115, 2753.

(c) W.A. Howard and G. Parkin, Organometallics, **1993**, 12, 2363.

25. W.E. Hunter, D.C. Hencir, R.V. Buynum, R.A. Pentilla and J.L. Atwood, Organometallics, **1983**,2, 750.

26. A.M. Baranger, P.J. Walsh and R.G. Bergmann, J. Am. Chem. Soc., **1993**, 115, 2753.

27. P.J. Walsh, F.J. Hollander and R.G. Bergman, Organometallics, **1993**, , 3705.

3.4 Appendix

The parameters for extended Huckel calculations for C, H, O and Zr are taken from the previous studies [8,10b].

Geometric parameters used:

Zr-C 2.28A, Zr-C_{Cp} 2.50A, Zr-S 2.48A, C-C 1.40A, C-H 1.09A, Zr-O 2.16A, C-C 1.54A, S-H 1.34A, Cp-Zr-Cp 126°, C(1)-S-H 105°. In 3, C(1)-Zr-C(2) 75°, Zr-C(1)-S 80° and in 4 C(1)-Zr-S 90°. The reaction coordinate is obtained by varying all the geometric parameters which are changing along the reaction coordinate in equal increments. The variations of the positions of the atoms are shown in Fig. 3.1.2 for the eq. 3.1.2a.

Chapter 4

Possibility of bond stretch isomerism in $[Cp(CO)_2M]_2(\mu - E)$ complexes (M = Mn, Re, Cr and W; E = S , Se and Te); a molecular orbital study

Chapter 4

Possibility of bond stretch isomerism in $[Cp(CO)_2M]_2(\mu - E)$ complexes (M = Mn, Re, Cr and W; E = S , Se and Te); a molecular orbital study

4.1 Abstract

Extended Huckel calculations are carried out on $[Cp(CO)_2M]_2(\mu$-E) complexes (M = Mn, Re, Cr and W ; E = S, Se and Te) in linear, bent and triangular geometries. The possibility of double well potential and consequent "Bond stretch isomerism" in these complexes is analyzed. All the complexes with 38 VEC are calculated to have a minimum corresponding to the triangular geometry. The Mn and Cr complexes with tellurido bridge have an additional minimum for the bent geometry: only the bent structure is known experimentally. The triangular isomers of these two complexes are marginally higher in energy, but separated by sizable barriers. Other M_2E combinations studied here exist in the triangular geometry. The difference in the behaviour of these complexes is explained using fragment molecular orbital approach and the atomic radii of M and E involved. Single point ab initio calculations using the LANL1MB basis set on $[Cp(CO)_2M]_2(\mu$-E) (M = Mn and Re; E = S, Se and Te) confirm the relative energy orderings obtained by the extended Huckel calculations. The relation between the M-E bond orders, bond lengths and main-group d orbital participation is also analyzed. Complexes with 36 and 40 VECs should adapt linear and bent geometries respectively.

4.2 Introduction

The number of structural patterns involving transition metals and bare main group elements are rapidly increasing.[1,2] With two transition metal fragments (M) around a central main group element (E) only three basically different arrangements are possible: linear(1), bent(2) and triangular(3). Table 4.1 presents a list of well characterized MEM structures with their valence electron count (VEC), M-E-M angle (θ), M...M and M-E distances. There is a general relationship between the VEC and the structural type. 36 VEC species[3,10] are linear. 38 VEC species[11,15] are found in bent and triangular forms while 40 VEC[16-19] makes them bent. Existence of two different structures which are connected by the variation of one interatomic distance as in 2 and 3 for the same number of electrons constitutes bond

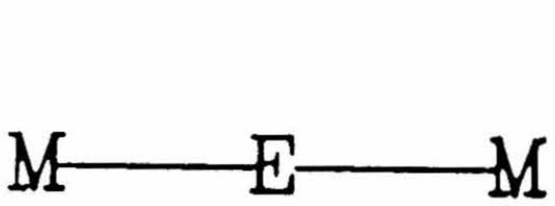

1

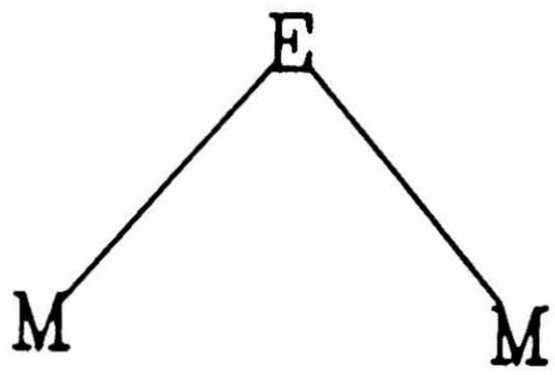

2

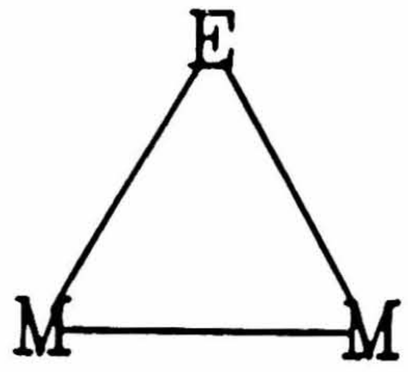

3

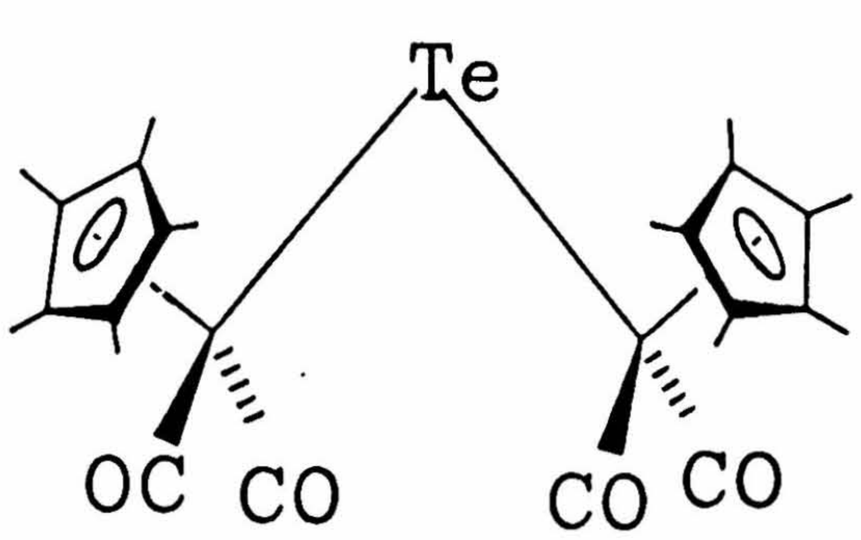

4

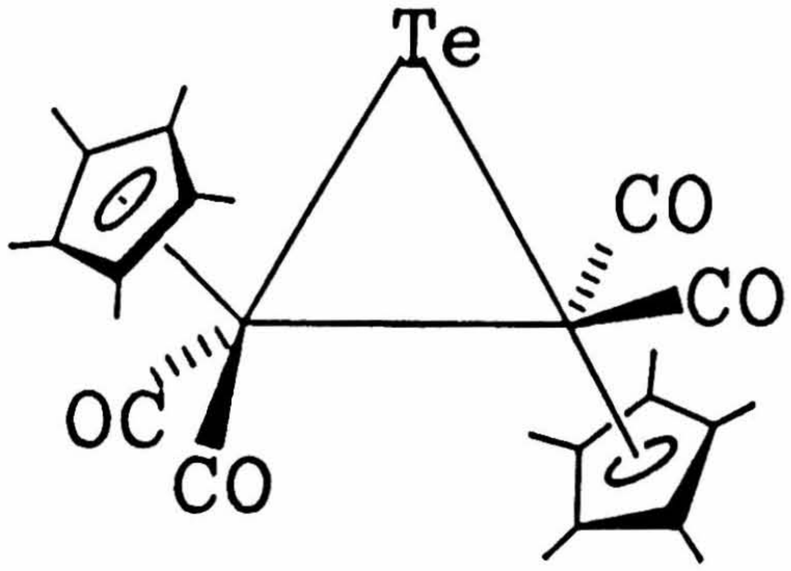

5

able 4.1: Important geometric parameters and VEC for the M_2E complexes: ond lengths in Å and bond angles in degrees. All values are taken from he X-ray diffraction studies.

Complex	Type	M-E	M-M	θ	VEC	Ref.
$S[CrCp(CO)_2]_2$	1	2.074	4.148	174.7	36	3,4
$S[Co(np_3)]_2$	1	2.128	4.156	180.0	36	5
$S[Ni\{(P_3)\}]_2^{2+}$	1	2.034	4.068	180.0	36	5
$S[Mo(HB(Pz)_3)(CO)_2]_2$	1	2.181	4.362	180.0	36	6
$S[Mo(HB(Me_2Pz)_3)(CO)_2$	1	2.200	4.400	180.0	36	6
$S[Mo(CN)_6]_2$	1	2.172	4.344	180.0	36	7
$Se[CrCp(CO)_2]_2$	1	2.209	4.418	180.0	36	8,9
$Se[Mo(HB(Pz)_3)(CO)_2]_2$	1	2.323	4.646	180.0	36	5
$Se[V(CO)_3(dppe)]_2$	1	2.298	4.596	180.0	36	10
$Te[V(CO)_3(dppe)]_2$	1	2.500	4.963	165.9	36	10
$Te[MnCp^*(CO)_2]_2$	2	2.459	4.338	123.8	38	11
$S[ReCp^*(CO)_2]$	3	2.381	2.946	76.4	38	12
$Se[ReCp^*(CO)_2]_2$	3	2.493	3.033	74.9	38	13
$Te[ReCp^*(CO)_2]_2$	3	2.679	3.140	71.7	38	14
$Se[Rh(Cp(CO)_2]_2$	3	2.440	2.755	68.7	38	15
$Te[CrCP^*(CO)_3]_2$	2	2.807	4.792	117.2	40	16
$S[WCp^*(CO)_3]_2$	2	2.531	4.530	127.0	40	17
$Se[FeCp^*(CO)_2]_2$	2	2.449	4.138	115.3	40	18
$Se[Re(PMe_3)_2(CO)_3]_2$	2	2.650	4.495	116.0	40	19

stretch isomerism.[20] Bond stretch isomerism is not yet unequivocally established in transition metal chemistry.[21,22] The M_2E complexes appear to be an area where bond stretch isomerism may be realized. There are two well characterized examples for bent and triangular structures with 38 VEC; $[Cp^*(CO)_2Mn]_2Te$, **4**, is bent[11] whereas its Re analog, **5**, is triangular.[14] The factors that control these preferences are not well understood. Studies in transition metal organometallic chemistry had shown us various examples where a change of metal within the same VEC leads to different structural types.[23] What is the role of the main group element or the transition metal in preferring one structure over the others even when the number of valence electrons remains a constant? We attempt here a correlation of the electronic structure of complexes **1**, **2** and **3**, especially to understand the factors that impart stability to the bent and the triangular structures with 38 VEC. Extended Huckel[24] and Fenske-Hall[25-26] calculations had previously been reported on the linear MEM structures which showed that an increase of VEC from 36 to 38 leads to bent geometries.

The electronic structure of $[Cp(CO)_2Mn]_2Te$, **4**, a 38 valence electron complex is described first. The comparison of Mn and Re complexes and reasons for their adopting two different structures are explained next. A study with different M and E combinations (M = $CrCp(CO)_2$, $MnCp(CO)_2$, $WCp(CO)_2$ and $ReCp(CO)_2$; E = S, Se and Te) maintaining the same number of electrons are carried out to gain a general understanding. Fragment Molecular Orbital approach[27] within the extended Huckel formalism[28] is used in this study. Single point ab initio SCF MO calculations with the

LANL1MB basis set[29,30] on bent and triangular geometries of Mn and Re complexes with S, Se and Te bridges are used as a check on the electronic structure and energies obtained from the extended Huckel calculations. Extended Huckel calculations are also done for 36 VEC and 40 VEC complexes with the above M and E combinations. Wherever possible structural parameters available from X-ray diffraction studies have been used in these calculations. The variation of the geometry along the reaction coordinate is given in the appendix (4.6).

4.3 Results and discussion

The molecular orbitals of $[Cp(CO)_2Mn]_2(\mu\text{-}Te)$, in the linear geometry, are constructed by the fragment orbitals of $[Cp(CO)_2Mn]^{2+}$ and Te^{2-} (Fig. 4.1). The $[Cp(CO)_2M]$ dimer orbitals are constructed from those of the well known $Cp(CO)_2M$ fragment.[31] The two Cp rings are placed trans to each other and hence the overall symmetry of the molecule is only C_2. The orbital energy pattern is similar to that of linear systems which have been studied in detail previously.[24-26] With 38 VEC, only one of the two π^* orbitals, 4b, is occupied. The two π^* orbitals form an e_g set in D_{4h} symmetry. Due to the lower symmetry, C_2, we observe splitting of the energy levels of the π^* orbitals. However, HOMO-LUMO energy difference is very small. Any geometrical variation which decreases the antibonding interaction is favoured for 38 and 40 VEC species. 38 VEC complexes may even adopt a linear structure with triplet ground state. We are not going to probe this possibility keeping in view the limitation of the methods employed here. Bending decreases the antibonding

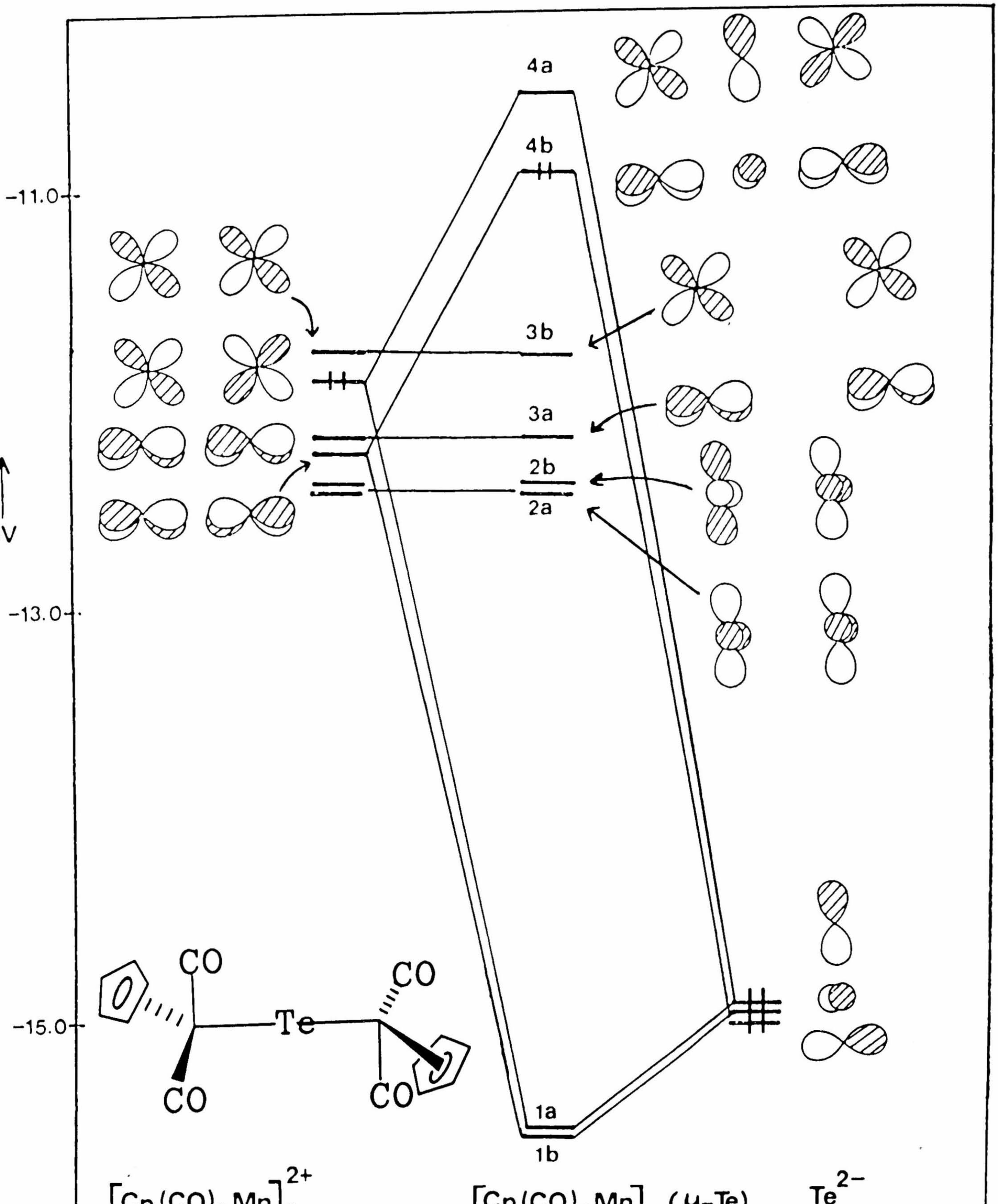

Fig. 4.1: Orbital interaction diagram of $[Cp(CO)_2Mn]_2^{2+}$ and Te^{2-}. The interaction between one p orbital of Te^{2-} is with the out of phase combination of the σ-type orbital of $[Cp(CO)_2Mn]_2^{2+}$, which is not shown here.

character in the in-plane π* orbital, 4a. The Re complex, 5, is found to have a triangular geometry with the two Cp rings trans to each other. In Mn complex, **4**, the two Cp rings are in cis conformation. If the two Cp rings are cis or if their centroids are coplanar to the MEM plane, the triangular geometry suffers from steric interactions. Therefore, the two Cp rings are kept trans to each other and are approximately perpendicular to the MEM plane during bending. The nature of the potential energy surfaces does not depend substantially on the Cp ring orientation in going from linear to bent geometries.

Fig 4.2 gives the frontier orbitals of $[Cp(CO)_2Mn]_2(\mu$-Te) in linear, bent and triangular geometries. The stabilization of the in-plane π^* orbital (4a) is the only significant change in going from linear to bent structure. The nonbonding orbital, 3b, becomes an M...M σ^* orbital. However, the two metals are still at nonbonding distance in the bent geometry. The changes are dramatic while going from bent to triangular geometry (Fig. 4.2). The M-E-M out of plane π^* orbital, 4b, is occupied. A metal-metal π* orbital, 3b, after an avoided crossing with 4b, becomes metal-metal σ* orbital(LUMO) in the triangular geometry. M-E π* orbital, 4b (linear), after the avoided crossing, retains antibonding interaction with E but gains M-M π bonding interaction in the triangular geometry. The other M-E π* orbital, 4a(linear), gets stabilized during bending.

A plot of the sum of one electron energies shows two minima for the $[Cp(CO)_2Mn]_2(\mu$-Te) complex, corresponding to the bent ($\theta = 124^0$) and the triangular ($\theta = 80^0$) structures (Fig.

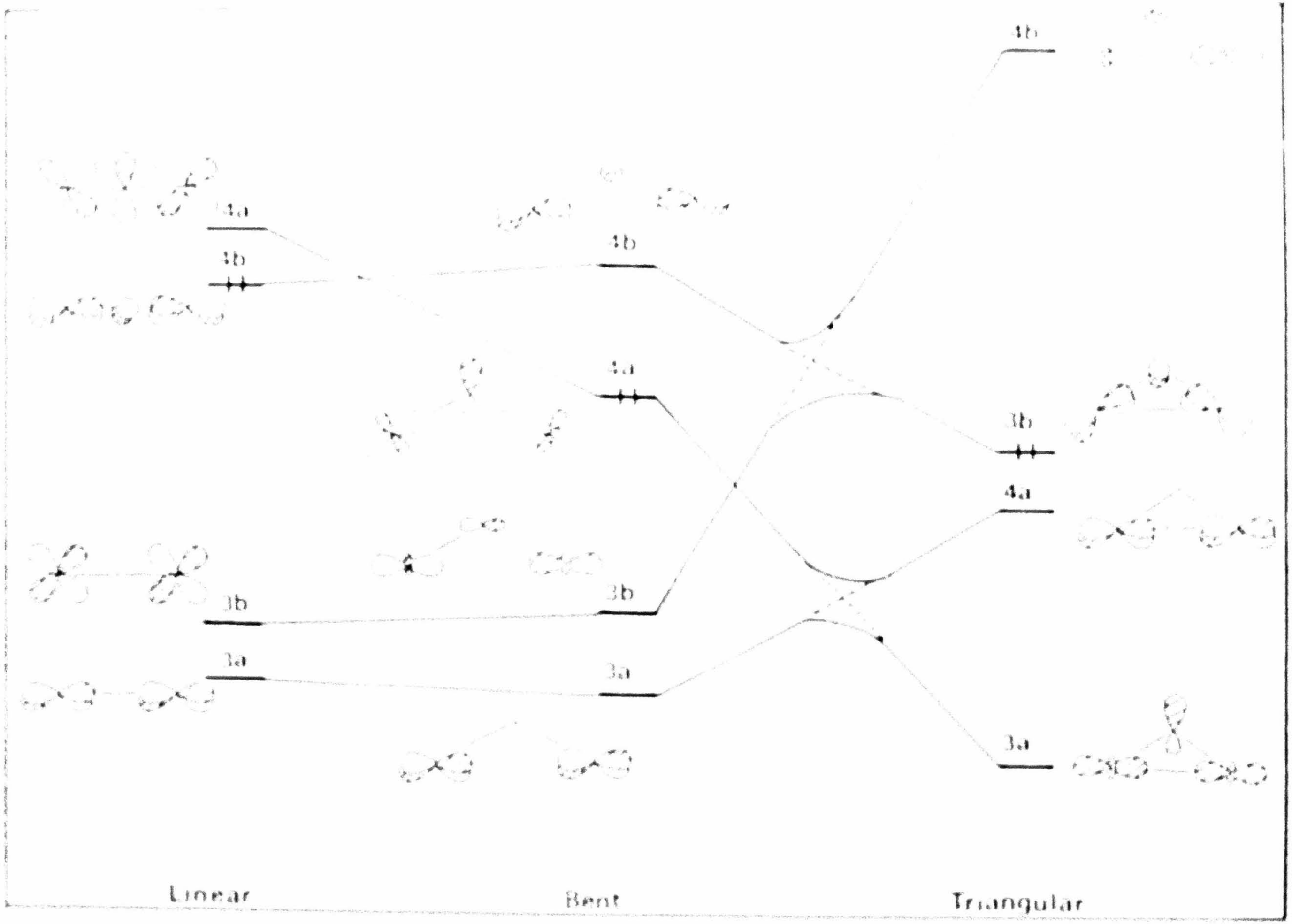

Fig. 1.21 Schematic representation of variation of frontier molecular orbitals energies of $[Cp(CO)_2M]_2(\mu\text{-}S)$ in linear, bent and triangular geometries.

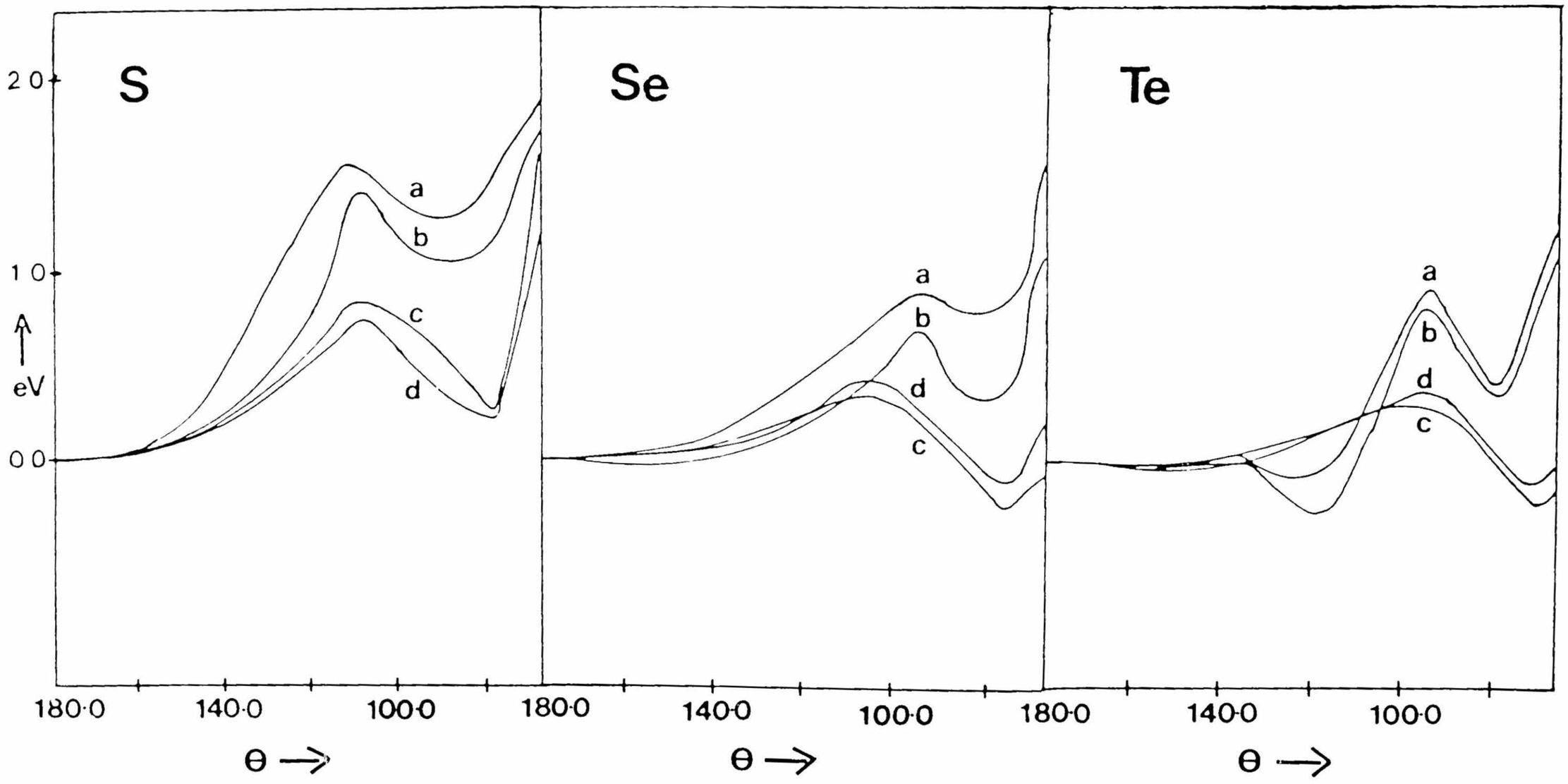

Fig. 4.3: The plots of the sum of one electron energies of the 38 VEC complexes: a = $[Cp(CO)_2Cr]_2(\mu\text{-}E)^{2-}$; b = $[Cp(CO)_2Mn]_2(\mu\text{-}E)$; c = $[Cp(CO)_2Re]_2(\mu\text{-}E)$; d = $[Cp(CO)_2W]_2(\mu\text{-}E)^{2-}$

4.3). The bent structure is shown to be more stable than the triangular structure by about 0.75 eV. The corresponding plot for the Re complex gives a minimum corresponding to the triangular structure only. There is virtually no change in the energy as we go from linear to bent structure (from $\theta = 180^{o}$ to 120^{o}). These results are in agreement with the experimental observation that the Re complex has a triangular geometry while the Mn complex prefers a bent geometry. We look for an explanation for this behaviour from MO theory.

The electronic structure of Mn and Re complexes is qualitatively similar in linear, bent and triangular geometries. But, the variation in the energy of the individual orbitals is different. We trace the change in the slopes of the frontier orbitals, 4a, 4b, 3a and 3b along the bending coordinate to the fragment levels themselves. The interaction between $[Cp(CO)_2Mn]_2$ and Te fragment orbitals is stronger than that between $[Cp(CO)_2Re]_2$ and Te fragment orbitals in the linear geometry, because the Mn fragment orbitals are closer in energy to Te orbitals (Fig. 4.4). Since the Mn-Te interaction in Mn complex is stronger, orbital coefficients on Te in the π^* MOs, 4a and 4b, are larger leading to stronger antibonding interactions. Therefore, the stabilization of the in-plane π^* orbital, 4a, in going from linear to bent geometry is higher in the Mn complex. Fig. 4.2 indicates that an M-E-M π^* orbital has to be filled in the triangular geometry. The stronger interactions between M and E lead to a higher antibonding interaction in the triangular geometry. Operating side by side is the subtle effect of the M-E distance, in turn a consequence of the atomic radius of E. When

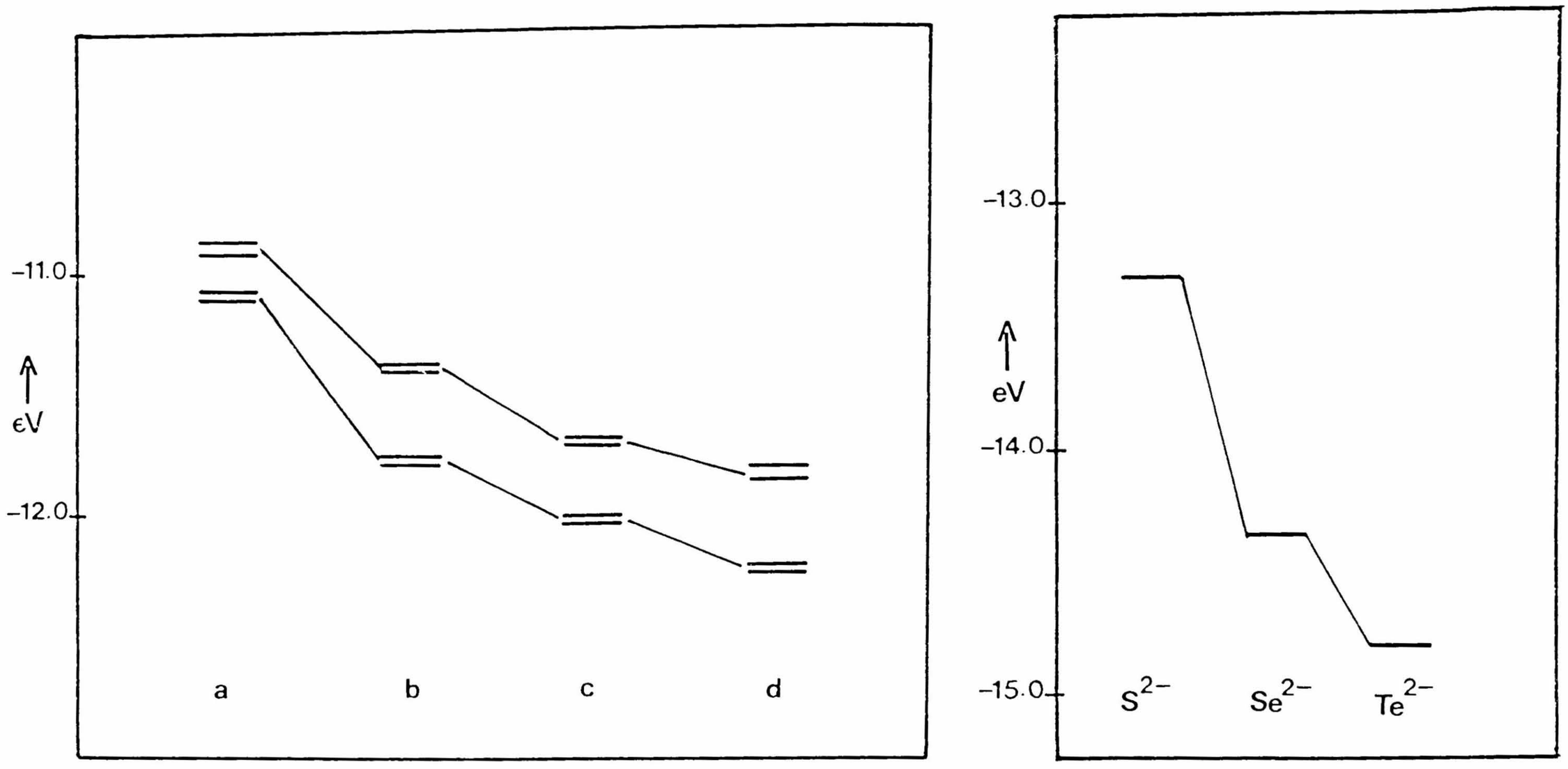

Fig. 4.4: Correlation of energy levels of $[Cp(CO)_2M]_2^{2+}$ fragment orbitals (a = W; b = Re; c = Cr; d = Mn) and E^{2-} (E = S, Se and Te) orbitals.

corresponding to the bent geometry. The metals having weaker interactions with E orbitals, e.g., W and Re, prefer triangular structures. This is reflected in Figure 4.4. All Re and W complexes have a low lying minima corresponding to triangular geometry compared to that of Mn and Cr complexes. Only Mn and Cr complexes with Tellurido bridge have a double well potential energy surface among all the combinations.

Ab initio calculations using LANL1MB basis are performed on bent and triangular geometries of Mn and Re complexes with S, Se and Te bridges.[29,30] The ordering of the energy levels is similar to those obtained from the extended Huckel calculations in bent and triangular geometries. For Mn complex the bent structure is more stable than the triangular structure by 3.1 kcal mol^{-1}. In the Re complex, the triangular structure is more stable than the bent structure by 40.1 kcal mol^{-1}. Table 4.2 gives the relative energies of the two isomers, which indicates that the Re complex shows a strong preference for the triangular structure. The minima corresponding to the bent and the triangular geometries are comparable for Mn complexes. The experimentally observed Mn-Te complex has a bent geometry. It is very likely that the triangular structure can also be prepared. The barrier for inter conversion of the two structures should be fairly high from the molecular orbital energy pattern (Fig. 4.3) implying a possibility for bond stretch isomerism. The reported sulfido, selenido and tellurido bridged Re complexes are in the triangular form (Table 4.1). The energy difference between bent and triangular geometries is small for S and Se bridged Mn (or Cr) complexes. Thus, these are potential targets for bond

energies show only one minimum for 40 VEC complexes corresponding to the bent geometry. Similar curves generated with different M and E combinations with 36 VEC are depicted in Figure 4.5. In all of these, linear geometry is the lowest in energy. However, there is also a minimum in most of the examples corresponding to the triangular geometry. But this minimum is much higher in energy than that of the linear structure. Figure 4.2 explains this feature of PES with 36 VEC. There should be a HOMO-LUMO crossing as it goes from linear to triangular structure with 36 VEC. The HOMO-LUMO energy difference is very small in the triangular geometry. Therefore, bond stretch isomerism is unlikely to be observed with 36 VEC MEM complexes.

M-E bond lengths, bond orders and main-group d orbital participation

Linear complexes with 36 VEC have short M-E bond lengths (2.034 Å for Ni-S; 2.128 Å for Co-S) corresponding to triple bond. Bent species with 38 VEC have bond lengths (2.459 Å for Mn-Te) corresponding to double bond. Bent structures with 40 VEC have only ME single (2.807 Å for Cr-Te) bonds. The triangular structures with 38 VEC retain partial double bond character and have bond lengths (2.679 Å for Re-Te) in between those of 38 VEC bent species and 40 VEC bent species (Table 4.1). The imperatives of bond multiplicity and the expectation from conventional electron counting schemes often do not agree[32]. The criterion for the former in transition metal complexes is often the bond lengths and for the latter it is the number of electrons in the bonding and the antibonding orbitals. In 36 VEC linear

stretch isomerism, examples of which are yet to be observed experimentally in transition metal chemistry.

Table 4.2: Relative energies (in Kcal mol^{-1}) of bent and triangular geometries obtained from single point ab initio calculations using the LANL1MB basis set.

E	M = MnCp(CO)2		M = ReCp(CO)2	
	bent	triangular	bent	triangular
S	5.4	0.0	47.6	0.0
Se	1.4	0.0	36.1	0.0
Te	0.0	3.1	40.1	0.0

Extended Huckel calculations are also performed on various metal ring combinations (M = $WCp(CO)_2$, $ReCp(CO)_2$, $CrCp(CO)_2$ and $MnCp(CO)_2$; E = S, Se and Te) with 36 and 40 VECs. The required electron count is obtained by appropriately placing the charges on the complexes. All the complexes with 36 VEC are found to be linear, as the two π orbitals are occupied and the corresponding π^* orbitals are vacant. For complexes with 40 VEC both the π* orbitals are occupied in the linear geometry. The triangular structure is not favoured because a high lying M-M σ* MO, 2b, is occupied (Fig. 4.2). Hence only bent structures may be preferred by these complexes. The plot of the sum of the one electron

the M-E distance is large, even in the bent geometry, the M-M distance falls in the nonbonding range. The destabilizing interaction from 3b is not very large so that there could still be a minimum at this geometry. The antibonding interaction becomes substantial with a short M-E distance. Thus, a larger E atom is suitable for a double well potential with minima at bent and triangular geometries.

A systematic study with different M and E combinations [M = $[Cp(CO)_2Mn]$, $[Cp(CO)_2Cr]$, $[Cp(CO)_2Re]$, $[Cp(CO)_2W]$ and E = S, Se, Te] with 38 VEC (Fig. 4.3), indicates the ME combinations where a double well potential and consequent bond stretch isomerism may be anticipated. Figure 4.4 gives the Fragment Molecular Orbital energies of $[Cp(CO)_2M]_2$ and E for all the combinations studied. The potential energy surfaces for the bending of Cr and Mn complexes are similar. The Re and W complexes form another comparable set (Fig. 4.3). This clustering is to be expected from the fragment orbital energy levels (Fig. 4.4). The energy difference is the lowest for Cr and S combination, and the highest with W and Te combination. Both miss the minimum corresponding to the bent geometry, but for different reasons. In the Cr complex, Cr-S bonds are so short that the two metals are already at a repulsive distance in the bent geometry and hence there is no minimum. Here a change of E from S to Te gives a minimum corresponding to the bent geometry (Fig. 4.3). The W-Te combination is similar to that of Re-Te combination. The reasons for the absence of a minimum are also the same. Here, a change of metal is required as the W-Te interaction is too weak. Alternatively, a more diffuse E atom should give a minimum

corresponding to the bent geometry. The metals having weaker interactions with E orbitals, e.g., W and Re, prefer triangular structures. This is reflected in Figure 4.4. All Re and W complexes have a low lying minima corresponding to triangular geometry compared to that of Mn and Cr complexes. Only Mn and Cr complexes with Tellurido bridge have a double well potential energy surface among all the combinations.

Ab initio calculations using LANL1MB basis are performed on bent and triangular geometries of Mn and Re complexes with S, Se and Te bridges.[29,30] The ordering of the energy levels is similar to those obtained from the extended Huckel calculations in bent and triangular geometries. For Mn complex the bent structure is more stable than the triangular structure by 3.1 kcal mol^{-1}. In the Re complex, the triangular structure is more stable than the bent structure by 40.1 kcal mol^{-1}. Table 4.2 gives the relative energies of the two isomers, which indicates that the Re complex shows a strong preference for the triangular structure. The minima corresponding to the bent and the triangular geometries are comparable for Mn complexes. The experimentally observed Mn-Te complex has a bent geometry. It is very likely that the triangular structure can also be prepared. The barrier for inter conversion of the two structures should be fairly high from the molecular orbital energy pattern (Fig. 4.3) implying a possibility for bond stretch isomerism. The reported sulfido, selenido and tellurido bridged Re complexes are in the triangular form (Table 4.1). The energy difference between bent and triangular geometries is small for S and Se bridged Mn (or Cr) complexes. Thus, these are potential targets for bond

stretch isomerism, examples of which are yet to be observed experimentally in transition metal chemistry.

Table 4.2: Relative energies (in Kcal mol^{-1}) of bent and triangular geometries obtained from single point ab initio calculations using the LANL1MB basis set.

E	M = MnCp(CO)2		M = ReCp(CO)2	
	bent	triangular	bent	triangular
S	5.4	0.0	47.6	0.0
Se	1.4	0.0	36.1	0.0
Te	0.0	3.1	40.1	0.0

Extended Huckel calculations are also performed on various metal ring combinations (M = $WCp(CO)_2$, $ReCp(CO)_2$, $CrCp(CO)_2$ and $MnCp(CO)_2$; E = S, Se and Te) with 36 and 40 VECs. The required electron count is obtained by appropriately placing the charges on the complexes. All the complexes with 36 VEC are found to be linear, as the two π orbitals are occupied and the corresponding π^* orbitals are vacant. For complexes with 40 VEC both the π^* orbitals are occupied in the linear geometry. The triangular structure is not favoured because a high lying M-M σ^* MO, 2b, is occupied (Fig. 4.2). Hence only bent structures may be preferred by these complexes. The plot of the sum of the one electron

energies show only one minimum for 40 VEC complexes corresponding to the bent geometry. Similar curves generated with different M and E combinations with 36 VEC are depicted in Figure 4.5. In all of these, linear geometry is the lowest in energy. However, there is also a minimum in most of the examples corresponding to the triangular geometry. But this minimum is much higher in energy than that of the linear structure. Figure 4.2 explains this feature of PES with 36 VEC. There should be a HOMO-LUMO crossing as it goes from linear to triangular structure with 36 VEC. The HOMO-LUMO energy difference is very small in the triangular geometry. Therefore, bond stretch isomerism is unlikely to be observed with 36 VEC MEM complexes.

M-E bond lengths, bond orders and main-group d orbital participation

Linear complexes with 36 VEC have short M-E bond lengths (2.034 Å for Ni-S; 2.128 Å for Co-S) corresponding to triple bond. Bent species with 38 VEC have bond lengths (2.459 Å for Mn-Te) corresponding to double bond. Bent structures with 40 VEC have only ME single (2.807 Å for Cr-Te) bonds. The triangular structures with 38 VEC retain partial double bond character and have bond lengths (2.679 Å for Re-Te) in between those of 38 VEC bent species and 40 VEC bent species (Table 4.1). The imperatives of bond multiplicity and the expectation from conventional electron counting schemes often do not agree[32]. The criterion for the former in transition metal complexes is often the bond lengths and for the latter it is the number of electrons in the bonding and the antibonding orbitals. In 36 VEC linear

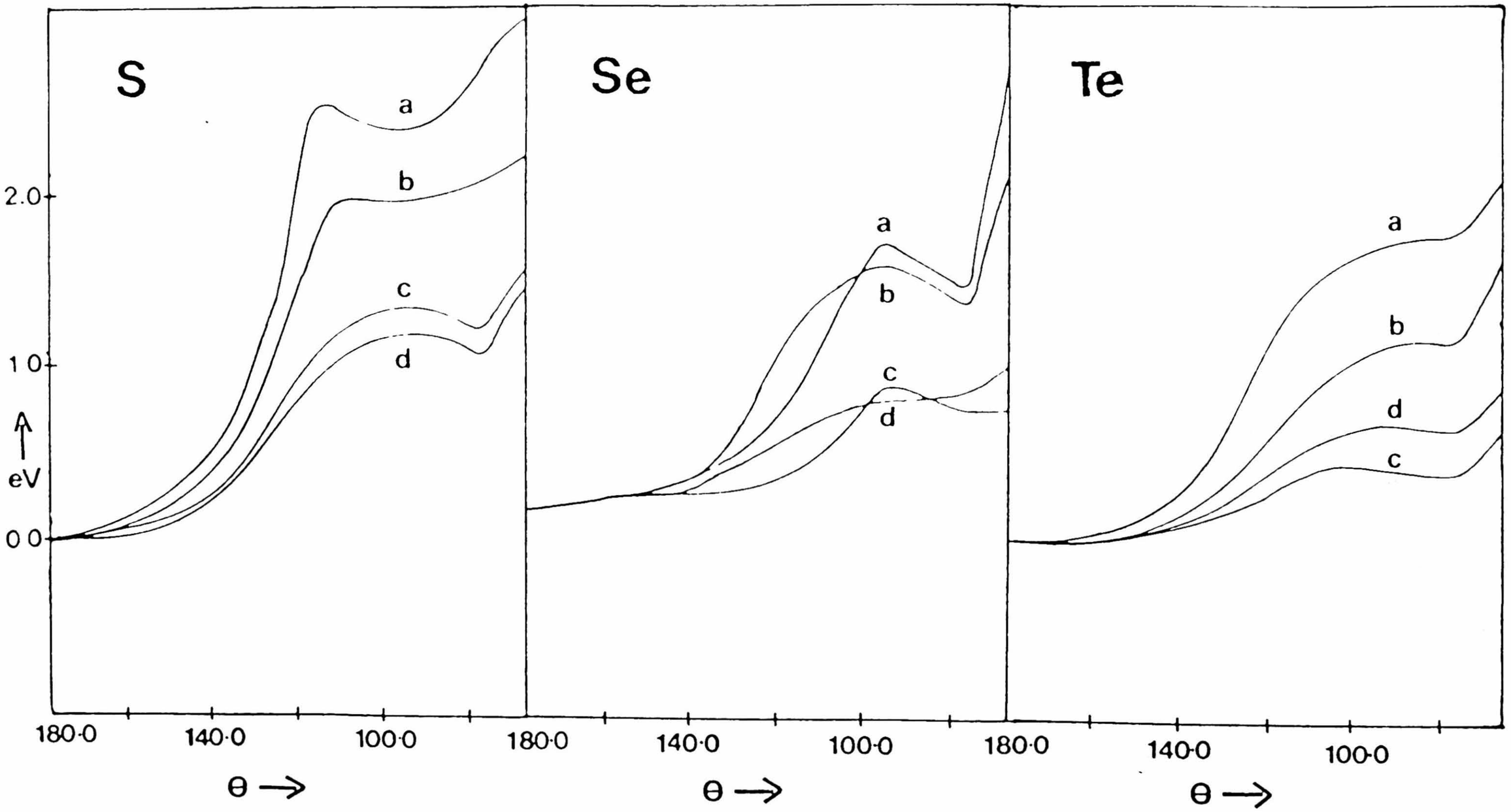

Fig. 4.5: The plots of the sum of one electron energies of the 36 VEC complexes: a = $[Cp(CO)_2Cr]_2(\mu\text{-}E)$; b = $[Cp(CO)_2Mn]_2(\mu\text{-}E)^{2+}$; c = $[Cp(CO)_2Re]_2(\mu\text{-}E)^{2+}$; d = $[Cp(CO)_2W]_2(\mu\text{-}E)$

complexes, in addition to the ME σ bond there are two 3c-2e π bonds, 1a and 1b (Fig. 4.1) which effectively give one π bond for each ME. Mealli and Sacconi had shown that there is considerable d orbital participation in the linear structure[23]. With the inclusion of d orbitals on E, two more π bonding orbitals are occupied (otherwise these are non bonding, 3a and 3b in the linear geometry). This accounts for the triple bond between M and E in linear structure with 36 VEC[24]. The extra two electrons in 38 VEC species go into the antibonding π^* orbitals, 4b in the linear geometry. This should actually decrease the ME bond order only by half, but the bond lengths correspond to a double bond. Here the comparison is between the linear 36 VEC species vs bent 38 VEC species. When we go from 38 to 40 VEC (both in the bent form) only two electrons are added to the MEM π* orbitals, but two bonds are broken. This goes against the general understanding of bond orders.

The dilemma of two electrons in the antibonding orbitals breaking two bonds is not very difficult to understand if one looks at the bonding and antibonding character of MEM π and π* orbitals respectively. The two π* orbitals, 4a and 4b(linear), have almost equal coefficients on M(0.47) and E(0.55), but the π orbital has very small coefficients on M(0.11) compared to those on E(0.59). The M-E anti bonding interaction in π* orbitals is stronger than the bonding in π orbitals in these complexes. Effectively, the occupation of one π* orbital cancels two π bonds formed by weak π bonding orbitals. We find that the

bonding in the bent and the triangular structures is also benefitted by the main group d orbital participation. However, the trends obtained with and without d orbitals are the same. Similar observations have been made earlier[33].

4.4 Conclusions

Molecular Orbital study of $[Cp(CO)_2M]_2(\mu\text{-}E)$ (M = Mn, Re, W and Cr; E = S, Se and Te) indicates that a suitable M and E combination provides a double minima on the potential energy surface with 38 VEC. Mn (or Cr) complex with tellurido bridge has two minima, bent and triangular. The two minima are energetically comparable and are separated by a high barrier. Experimentally, the structure with bent geometry is reported. Attempts to prepare the triangular structure should be rewarding. Similar bond stretch isomerism involving bent and triangular structures is unlikely in the remaining M and E combinations considered here. 36 and 40 VEC are also unlikely to exhibit bond stretch isomerism.

4.5 References

1. W. A. Herrmann, Angew. Chem., Int. Ed. Engl., 1986, **25**, 56 and references therein.
2. K.H. Whitmire, J. Coord. Chem., 1988, **17**, 95.
3. T.J. Greenhough, B.W.S. Kolthammer, P. Legzdins, J. Trotter, Inorg. Chem., 1979, **18**, 3543.
4. L.Y. Goh, T.W. Hambley and G.B. Robertson, J. Chem. Soc., Chem. Commun., 1983, 1458.
5. C. Mealli, S. Midollini, and L. Sacconi, Inorg. Chem., 1978,**17**, 632.
6. S. Lincoln, S.-L. Soong, S.A. Koch, M. Sato, and J.H. Enemark, Inorg. Chem., 1985, **24**, 1355.
7. C. Potvin, J. -M. Manoli, J.-M. Bregeault and G.Chottarrd, Inorg. Chim. Acta., 1983, 72, 103.
8. W.A. Herrmann, J. Rohrmann, H. Noth, H.; Ch.K. Narula, I. Bernal, and M. Draux. J. Organomet. Chem., 1985, **284**, 189.
9. L.Y. Goh, C. Wei, C. and E.J. Sinn J. Chem. Soc., Chem. Commun., 1985, 462.
10. N. Albrecht, P. Hubener, U. Behrens and E. Weiss, Chem. Ber., 1985, **118**, 4059.
11. W.A. Herrmann, C. Hecht, M.L. Ziegler and B. Balbach, J. Chem. Soc., Chem. Commun., 1984, 686.
12. M. Herberhold, D. Reiner, K. Ackermann, U. Thewalt and T. Debaerdemaeker, Z. Naturforsch., 1984, **39b**, 1199.
13. M. Herberhold, B. Schmidknoz, U. Thewalt, A. Razavi, H. Schollhorn, W.A. Herrmann and C. Hecht, J. Organomet. Chem., 1986, **229**, 213.
14. W.A. Herrmann, C. Hecht, E. Herdtweck and H.-J. Kneuper, Angew. chem., Int. Ed. Engl., 1987, **26**, 132.

15. H. Brunner, N. Janietz, W. Meier, J. Wachter, E. Herdtweck, W.A. Herrmann, O. Serhadli and M.L. Zeigler, J. Organomet. Chem., 1988, **347**, 237

16. W.A. Herrmann, J. Rohrmann, M.L. Zeigler and T. Zahn, J. Organomet. Chem., 1984, **273**, 232.

17. G.J. Kubas, H.J. Wasserman and R. Ryan, Organometallics, 1985,**4**, 419.

18. C. Hecht, E. Herdtweck, J. Rohrmann, W.A. Herrmann, W. Beck and P.M. Fritz, J. Organomet. Chem., 1987, **330**, 389.

19. E. Rottinger, V. Kullmer and H. Vahrenkamp, J. Organomet. Chem., 1978, **150**, C6.

20. (a) W.-D. Stohrer and R. Hoffmann, J. Am. Chem. Soc., 1972, **94**, 779.

(b) Y. Jean, A. Lledos, J.K.Burdett and R. Hoffmann, J. Am. Chem. Soc., 1988, **110**, 4506.

(c) Y. Jean, A. Lledos, J.K.Burdett and R. Hoffmann, J. Chem. Soc. Chem. Commun. , 1988, 140.

21. (a) G. Parkin, Chem. Rev., 1993, **93**, 887

(b) K. Yoon, G. Parkin and A.L. Rheingold, J. Am. Chem. Soc., 1992, **114**, 2210.

(c) J. Song and M. B. Hall, Inorg. Chem., 1991, **30**, 4433.

22. (a) V.C.Gibson and M. McPartlin, J. Chem. Soc. Dalton Trans., 1992, 947.

(b) J.M. Mayer, Angew. Chem. Int. Ed. Engl., 1992, **31**, 286.

(c) G. Parkin, Acc. Chem. Res., 1992, **25**, 455.

23. E.D. Jemmis and A.C. Reddy, J. Am. Chem. Soc., 1990, **112**, 722.

24. C. Mealli and L. Sacconi, Inorg. Chem., 1982, **21**, 2870.

25. Z. Lin and M.B. Hall, Inorg. Chem., 1991, **30**, 3817.

26. N.M. Kostic and R.F. Fenske, J. Organomet. Chem., 1982, **233**, 337.

27 (a) H. Fujimoto and R. Hoffmann, J. Phys. Chem., 1974, **78**, 1167.

28. (a). R. Hoffmann, J. Chem. Phys., 1963, **39**, 1397.
(b). R. Hoffmann and W.N. Lipscomb, J. Chem. Phys., 1962, **36**, 2179.

29. W.J. Hehre, L. Radom, P.v.R. Schleyer and J. A. Pople, *Ab initio Molecular Orbital Theory*; Wiley: New York (1986).

30. P.J. Hay and W. R. Wadt, J. Chem. Phys., 1985, **82**, 270, 284, 299.

31. B.E.R. Schilling, R. Hoffmann and D.L. Lichtenberger, J. Am. Chem. Soc., 1979, **101**, 585.

32. E.D. Jemmis, A.R. Pinhas and R. Hoffmann, J. Am. Chem. Soc., 1980, **102**, 2576.

33. R. Hoffmann, H. Fujimoto, J. R. Swenson and C.C. Wan, J. Am. Chem. Soc., 1973, **95**, 7644.

4.6 APPENDIX

The bond distances and bond angles from the diffraction studies are used whereever available. For the hypothetical compounds, the bond distances are taken from X-ray structures of the related complexes. The bond distances which are used are given below (Table 4.6.1). The distances C-O, C-C(Cp ring) and C-H are kept at 1.17 Å, 1.40 Å and 1.08 Å in all the calculations. The geometry employed around the metal is different in the linear and in the triangular forms, but similar in the linear and bent forms. When we go from the linear to the triangular forms, the changes in the geometry are as follows : E-M-Cp angle changed from 127^{o} to 117^{o}. M-M-C(of CO) angles are 90^{o} and 90^{o} in linear geometry and 78^{o} and 110^{o} in triangular geometry. CO-M-CO angle is varied from 90^{o} to 80^{o}. The M-E distance is kept constant during the change. The two Cp rings are trans to each other, hence the maximum symmetry possible is C_2. A higher symmetry is not allowed because the C_{2v} geometry suffers from steric interactions in the triangular form. The atomic parameters of C,H,O, Mn, Cr, Re, W, S, Se and Te are taken from the earlier work[a-d].

Table. 4.6.1 Bond lengths (in Angstroms)

	W	Re	Cr	Mn
M-S	2.324	2.381	2.073	2.100
M-Se	2.480	2.493	2.210	2.356
M-Te	2.670	2.679	2.420	2.460
M-Cp	2.000	1.963	1.846	1.838
M-C	2.000	1.936	1.866	1.810

(a) A. Vela, J. L. Gazquez. J. Phys. Chem., 1988, **92**, 5688.

(b) R. H. Summerville and R. Hoffmann, J. Am. Chem. Soc., 1976, **98**, 7240.

(c) D. M. Hoffmann, R. Hoffmann and C.R. Fisel, J. Am. Chem. Soc., 1982, **104** 3858.

(d) A. Dedieu, T. A. Albright and R. Hoffmann, J. Am. Chem. Soc., 1979, **101**, 3141.

Chapter 5

Molecular mechanics and MNDO calculations on C_{60} and C_{70} and their substructures

5.0 General Introduction

The discovery of fullerenes have generated a great deal of interest and activity at the interfaces of chemistry, physics and material science.[1-3] Methods for the mass production of fullerenes are rapidly improving. Soot extraction and arcing or irradiation with sun light on graphite are the methods available for the generation of fullerenes.[2] Predominant products of these processes are C_{60} and C_{70} with smaller amounts of other carbon clusters. The unusual chemical and physical properties of C_{60} have already made this material a center of chemical activity in a short time. Even though C_{70} is thermodynamically more stable than C_{60}[4a,b] the latter is found in larger proportion.[1-3] Rational design or classical synthetic approach to these complex and fascinating molecules, C_{60} and C_{70}, is challenging. Synthetic chemists around the world are starting to pay attention on the synthesis of C_{60}.[5-12] Similar efforts towards C_{70} are lacking.

In this chapter, synthetic avenues to C_{60} and C_{70}, along different symmetry pathways are considered. The substructures of the fullerenes in general and the bowl type molecules in particular provide fascinating chemistry.[5-7,13] In a stepwise synthesis it is important to know the increase in strain associated with each step. Pathways that involve unusual strain build up may then be avoided. In this chapter, the increase of strain in sequential synthetic approaches to C_{60} and C_{70} is studied using empirical force field calculations.[14] MNDO calculations are carried out on the important bowl-type substructures.The first section of the chapter deals with C_{60} and the second section with C_{70}.

5.0 General Introduction

The discovery of fullerenes have generated a great deal of interest and activity at the interfaces of chemistry, physics and material science.[1-3] Methods for the mass production of fullerenes are rapidly improving. Soot extraction and arcing or irradiation with sun light on graphite are the methods available for the generation of fullerenes.[2] Predominant products of these processes are C_{60} and C_{70} with smaller amounts of other carbon clusters. The unusual chemical and physical properties of C_{60} have already made this material a center of chemical activity in a short time. Even though C_{70} is thermodynamically more stable than C_{60}[4a,b] the latter is found in larger proportion.[1-3] Rational design or classical synthetic approach to these complex and fascinating molecules, C_{60} and C_{70}, is challenging. Synthetic chemists around the world are starting to pay attention on the synthesis of C_{60}.[5-12] Similar efforts towards C_{70} are lacking.

In this chapter, synthetic avenues to C_{60} and C_{70}, along different symmetry pathways are considered. The substructures of the fullerenes in general and the bowl type molecules in particular provide fascinating chemistry.[5-7,13] In a stepwise synthesis it is important to know the increase in strain associated with each step. Pathways that involve unusual strain build up may then be avoided. In this chapter, the increase of strain in sequential synthetic approaches to C_{60} and C_{70} is studied using empirical force field calculations.[14] MNDO calculations are carried out on the important bowl-type substructures.The first section of the chapter deals with C_{60} and the second section with C_{70}.

5.1 Molecular Mechanics and MNDO Calculations on Sumanene and Related Substructures of C_{60}.

5.1.1 Abstract

Strain energies of the hydrocarbons derived from the fragments of C_{60} along the C_5, C_3 and C_2 pathways indicate that the strain energy per carbon (SEC) increases gradually along the C_3 and C_2 paths, but has a maximum at $C_{40}H_{10}$ along the C_5 path. The bowl depth of sumanene, a leading fragment along the C_3 route, is larger than that in corannulene. The barrier for bowl to bowl inversion for sumanene is calculated to be 24.2 kcal mol^{-1} at the MNDO level. The bond alternation in the central six membered ring of sumanene resembles that of C_{60}. The larger fragments are deep bowls with higher barriers for inversion. Increase in strain in going from triphenylene to sumanene by placing the methylene bridges one at a time is estimated, using MNDO and MM2 calculations.

5.1.2 Introduction

The Buckminsterfullerene, C_{60}, **1**, can be dismantled in a retro-synthetic sense through three conceptually different routes which retain C_2, C_3 and C_5 symmetry, by successively removing fragments from one side. The structural fragments are treated as hydrocarbons obtained by adding hydrogens to saturate the σ-valency on the C_n template.[15] Each one of these (Scheme 1, **2-15**) is a fascinating synthetic target. The important substructures at the end of the C_5, C_3 and C_2 routes are corannulene, **6**, sumanene, **10**, and pyracylene, **15**, respectively.[5,7,8] Of these, **6** and **15**, have been synthesized and taken note of as C_{60} precursors.[7,8] On the other hand, sumanene, **10**, has been recognized as a key fragment only recently and its synthesis remains to be accomplished.[5] Therefore, attention has been focussed particularly on the structure of sumanene, **10**, and its suitability for further evolution towards C_{60}, **1**.

Another dissection that retains C_5, C_3 and C_2 axis removes fragments in pairs from opposite sides of C_{60}, **1**. The interesting "ribbons" generated are given in Scheme 2. $C_{50}H_{20}$, **17**, has been suggested as a possible synthetic target.[16]

To begin with a strain energy analysis of the structures enroute C_{60} (Scheme 1 and 2) based on molecular mechanics calculations[13] is carried out. A detailed MNDO[17] study on the structure of sumanene, **10**, and related compounds is presented next.

SCHEME 1

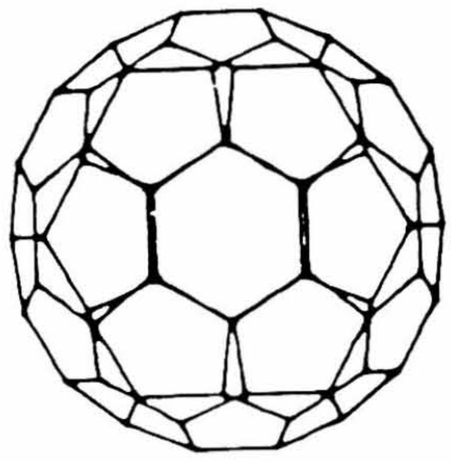

C_5 route

C_2 route

1, C_{60}

C_3 route

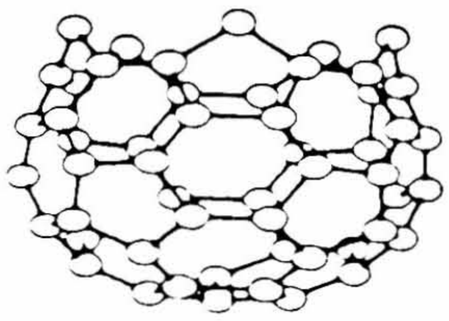

2, $C_{55}H_{10}$

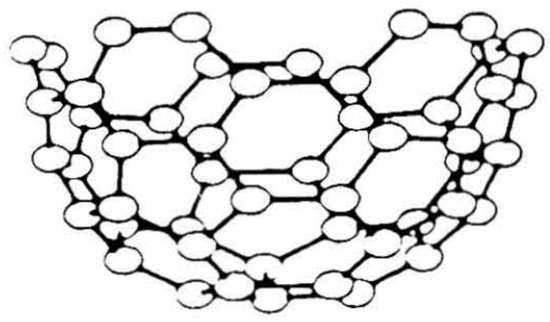

3, $C_{50}H_{10}$

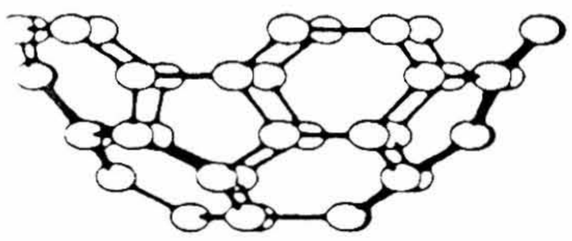

4, $C_{40}H_{10}$

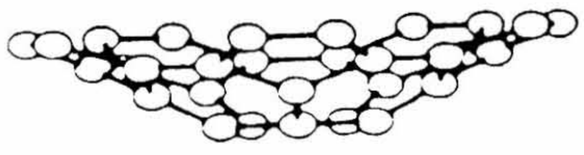

5, $C_{30}H_{10}$

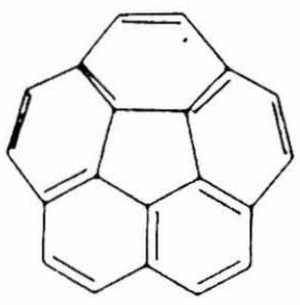

6, $C_{20}H_{10}$

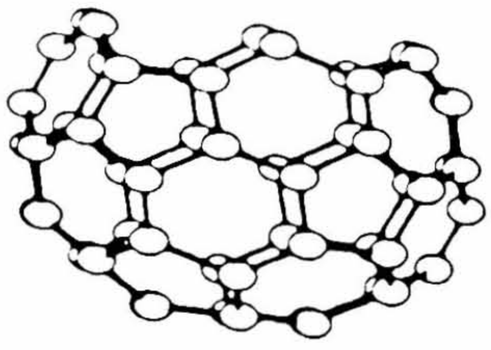

7, $C_{54}H_6$

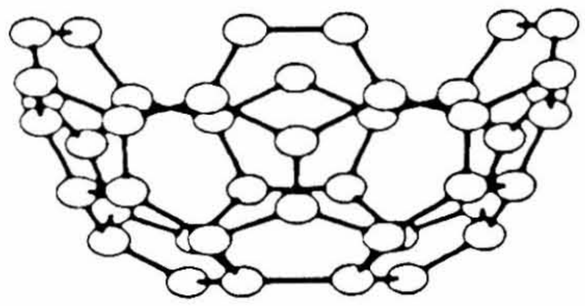

8, $C_{45}H_{12}$

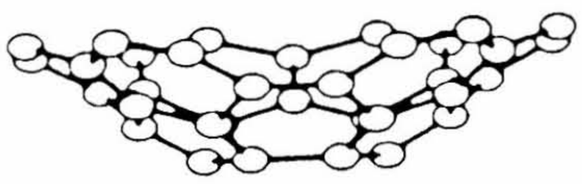

9, $C_{38}H_{12}$

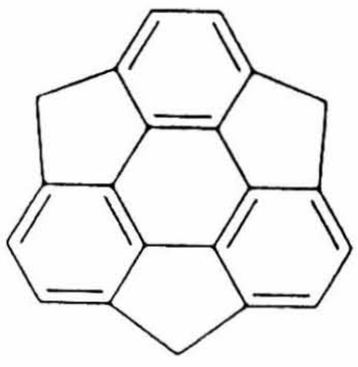

10, $C_{21}H_{12}$

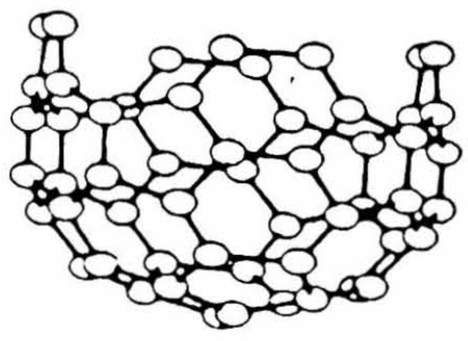

11, $C_{54}H_6$

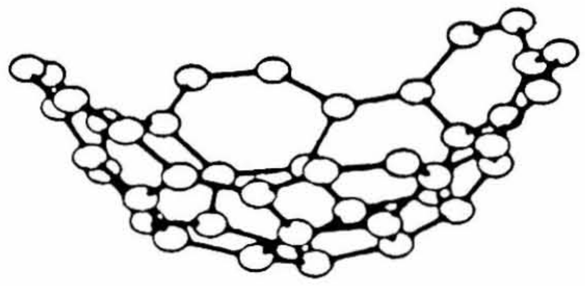

12, $C_{42}H_{12}$

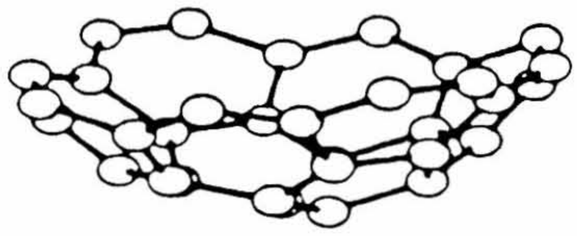

13, $C_{32}H_{12}$

14, $C_{28}H_{12}$

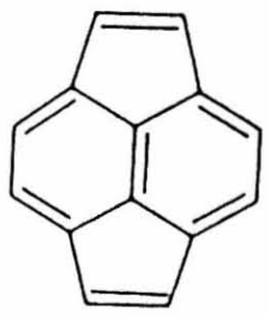

15, $C_{14}H_8$

SCHEME 2

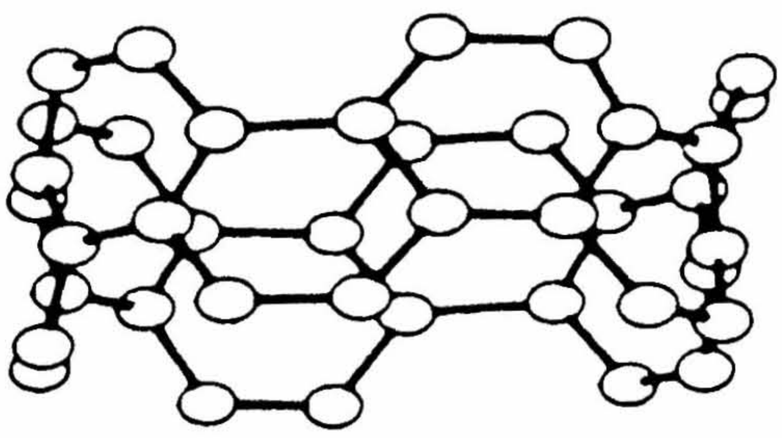

16, $C_{40}H_{20}$

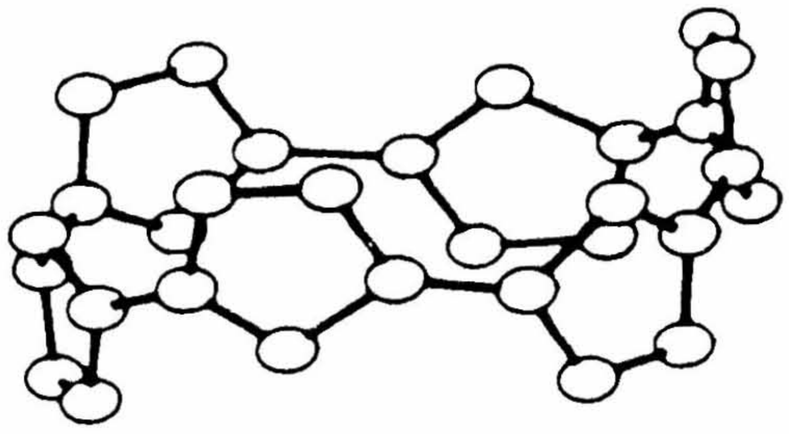

18, $C_{30}H_{18}$

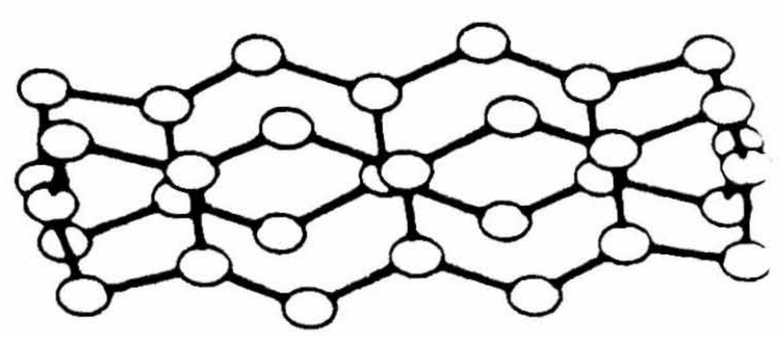

20, $C_{32}H_{18}$

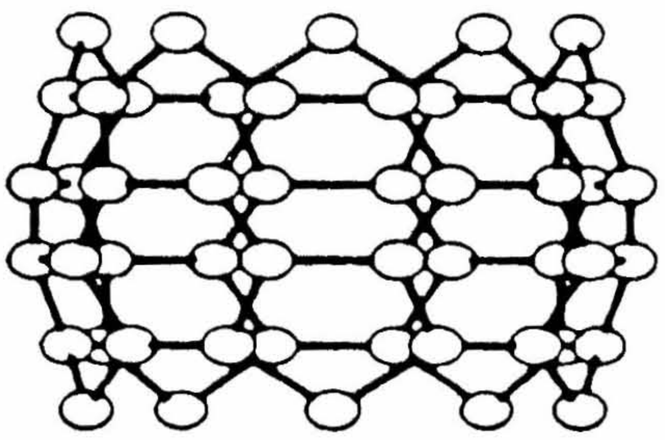

17, $C_{50}H_{20}$

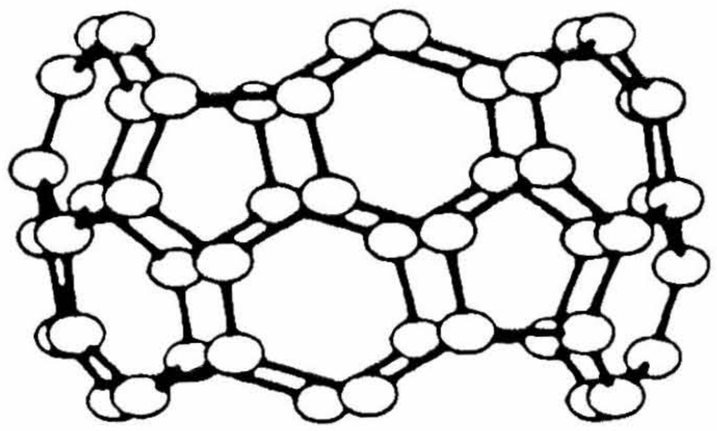

19, $C_{48}H_{12}$

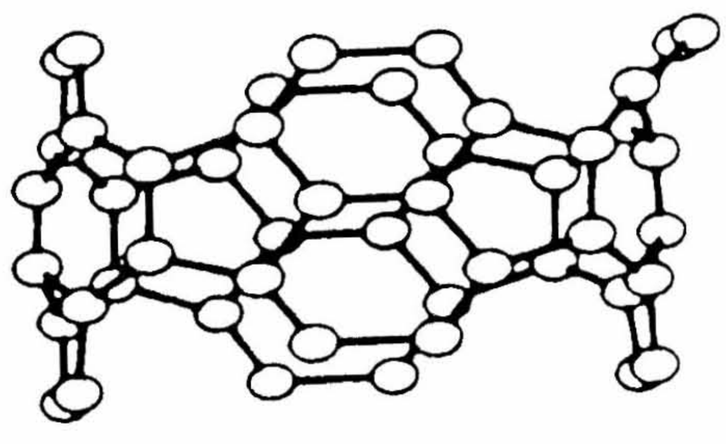

21, $C_{48}H_{16}$

TABLE 5.1.1 : Strain energies of C_{60} fragments (in kcal mol^{-1})

No.	Formulae	SEC	SEC of C_n in C_{60}	ΔS.E.
1	C_{60}	19.20		
2	$C_{55}H_{10}$	15.53	17.36	1.83
3	$C_{50}H_{10}$	13.38	15.98	2.60
4	$C_{40}H_{10}$	14.43	14.60	0.17
5	$C_{30}H_{10}$	8.83	13.37	4.54
6	$C_{20}H_{10}$	4.30	10.15	5.85
7	$C_{54}H_{6}$	17.22	17.13	-0.09
8	$C_{45}H_{12}$	12.31	15.56	3.25
9	$C_{36}H_{12}$	8.69	13.50	4.81
10	$C_{21}H_{12}$	5.81	10.67	4.86
11	$C_{54}H_{6}$	15.89	17.12	1.23
12	$C_{42}H_{12}$	10.26	14.38	4.12
13	$C_{32}H_{12}$	9.78	13.13	3.35
14	$C_{28}H_{12}$	8.64	12.25	3.61
15	$C_{14}H_{8}$	4.50	8.43	3.93
16	$C_{40}H_{20}$	6.65	11.10	4.45
17	$C_{50}H_{20}$	10.98	15.18	4.20
18	$C_{30}H_{18}$	7.83	8.97	1.14
19	$C_{48}H_{12}$	14.46	14.52	0.06
20	$C_{32}H_{18}$	3.69	9.22	5.53
21	$C_{48}H_{16}$	12.65	14.52	1.87

5.1.3 Results and discussion

Molecular mechanics study of C_{60} fragments

Table 5.1.1 gives the strain energies per carbon (SEC) calculated for the hydrocarbons derived from various C_{60} fragments (**2-21**, Schemes 1 and 2). The optimized carbon skeleton is now different from that of the idealized C_{60} fragment. ΔSEC between the optimized hydrocarbon structure and the corresponding carbon skeleton (C_n) kept at the geometry of C_{60} gives an estimate of the deviation of the structure from the standard C_{60}. Large ΔSEC in the smaller hydrocarbons indicates large reorganization taking place in the smaller skeleta to reduce strain. Thus, $C_{20}H_{10}$, corannulene, relaxes considerably to a shallow bowl in comparison to the corresponding C_{20} fragment of C_{60}.[18] Corresponding reduction in SEC is 5.85 kcal mol^{-1}. Lower ΔSEC between the $C_{40}H_{10}$ and C_{40} (0.17 kcal mol^{-1}) correctly points to the similarity between the $C_{40}H_{10}$ and C_{60} (**4** and **1**). The structure of $C_{50}H_{10}$, **3**, is especially interesting because it is also a fragment of C_{70}. Addition of [5]-radialene to **3** leads to C_{60} and addition of corannulene (**6**) to **3** leads to C_{70}. The larger fragments have an additional source of strain. The C-H bonds added for completing the valency fall within van der Waals contact, increasing the strain. This is especially significant in **2**, **7** and **11**. In fact the H...H non-bonded repulsion makes $C_{54}H_6$, **7**, more strained than the corresponding C_{54} unit in C_{60}.

Fig. 5.1.1 gives a plot of the SEC as a function of the fragments. The increase in SEC is gradual along the C_3 and C_2

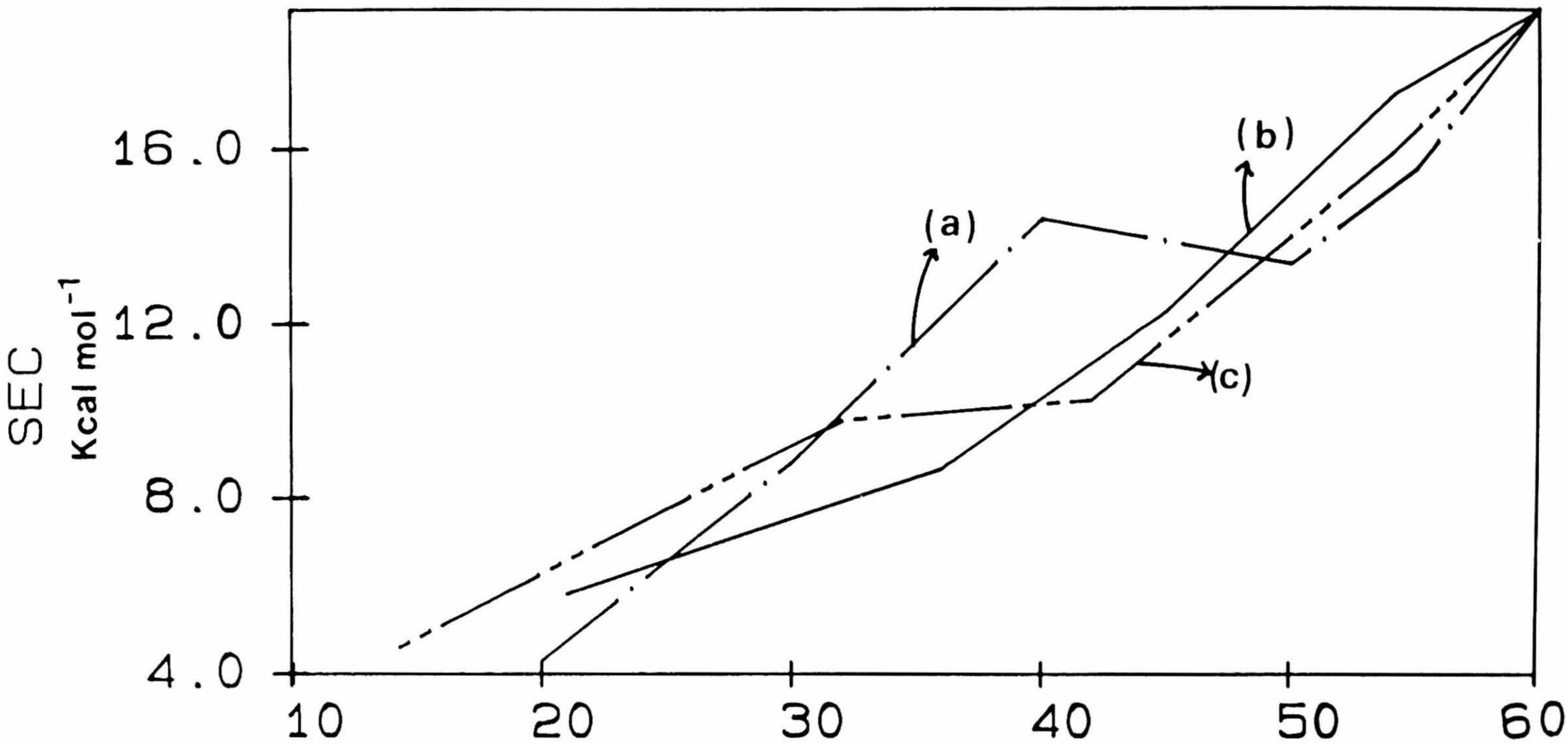

n

Fig. 5.1.1: The plot of the SEC as a fuction of fragments (a) C_5 route; (b) C_3 route; (c) C_2 route.

routes (Fig. 5.1.1). The C_5 path involving corannulene has a maximum in SEC at $C_{40}H_{10}$, **4**. The SEC decreases in the next higher fragment. In a sequential synthetic route this is not desirable. The SECs of the fragments, **2-21**, as well as C_{60} are to be compared to the SECs calculated for standard molecules : dodecahedrane, 3.3, [5]-prismane, 14.5, and cubane, 20.7 kcal mol^{-1}.[19] The syntheses of all of these molecules have been successful. Likewise, it should be possible to synthesize C_{60} in a stepwise process.

Though C_2 route in Scheme 1 has fragments that follow this symmetry strictly, the individual members may be easily identified with the fragments of the C_3 and C_5 routes. Thus, $C_{28}H_{12}$, **14**, may be considered as a simple extension of sumanene. Similarly $C_{32}H_{12}$, **13**, is an extension of corannulene. Other fragments along the C_2 path can be similarly related to the fragments along the C_3 and C_5 routes. Therefore, only two independent pathways, C_3 and C_5, need to be considered seriously.

ΔSEC values for the ribbon-like fragments indicate that large reorganizations are possible in $C_{40}H_{20}$, **16**, and $C_{50}H_{20}$, **17** which retain C_5 axis. $C_{40}H_{20}$, **16**, is also a substructure of C_{70}.[16] The minimal ΔSEC values for ribbons that retain C_3 axis ($C_{48}H_{12}$, **17**, and $C_{30}H_{18}$, **18**) indicate their close resemblance to C_{60}.

Low strain energies in the lower members is an attractive aspect in the initial stages of the synthesis. But it becomes less desirable in the final stages where large increase in strain

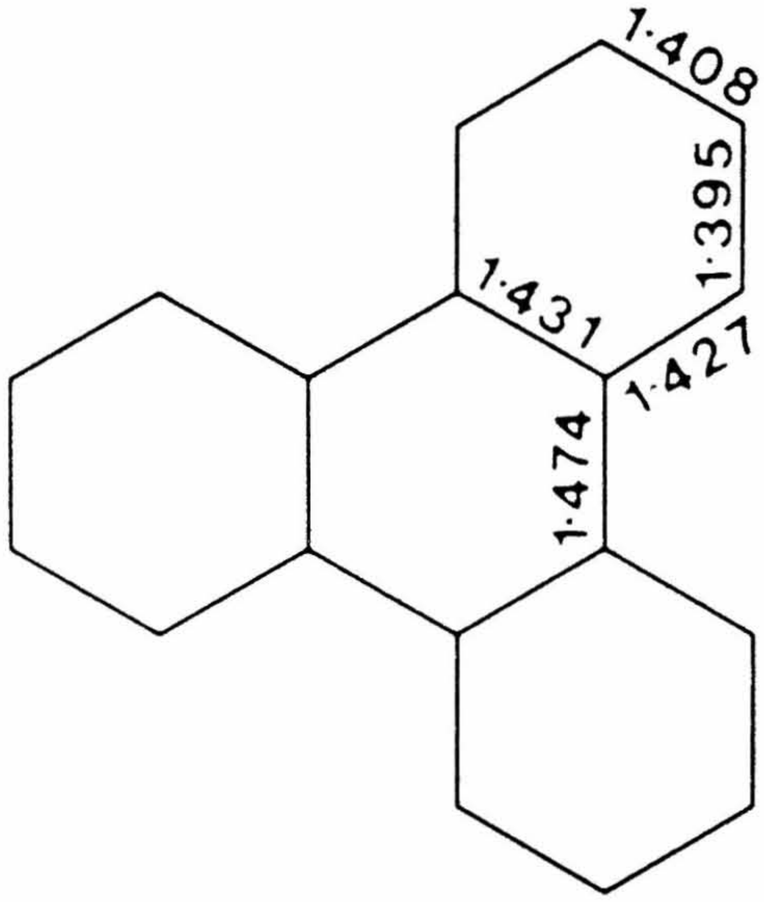

22

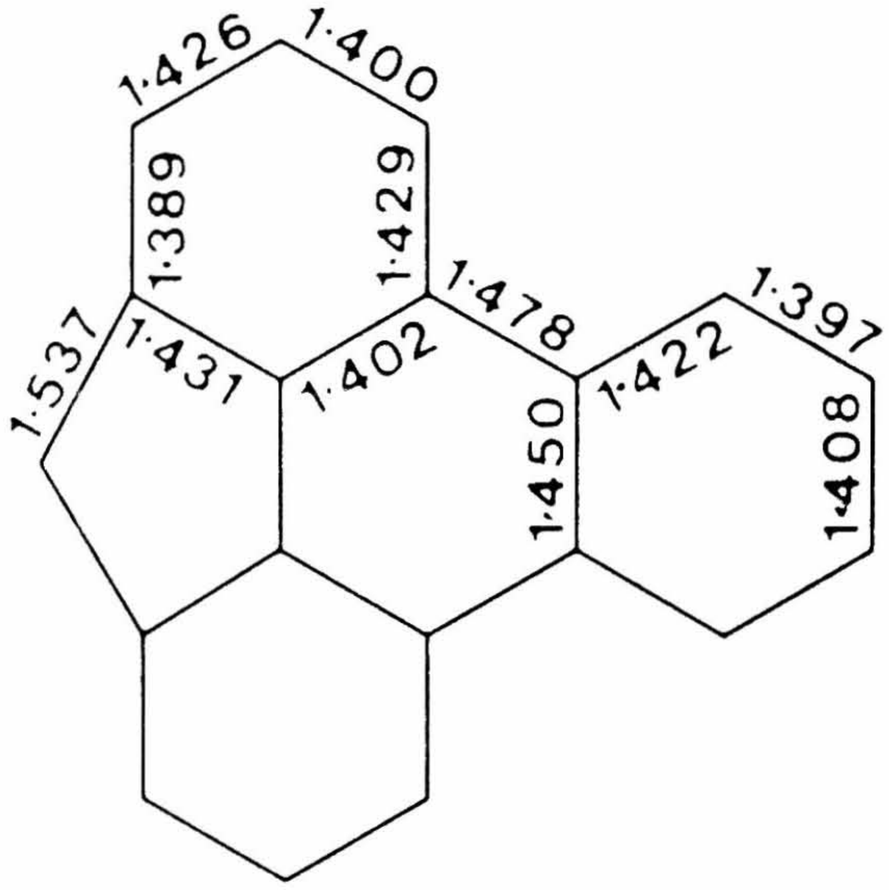

23

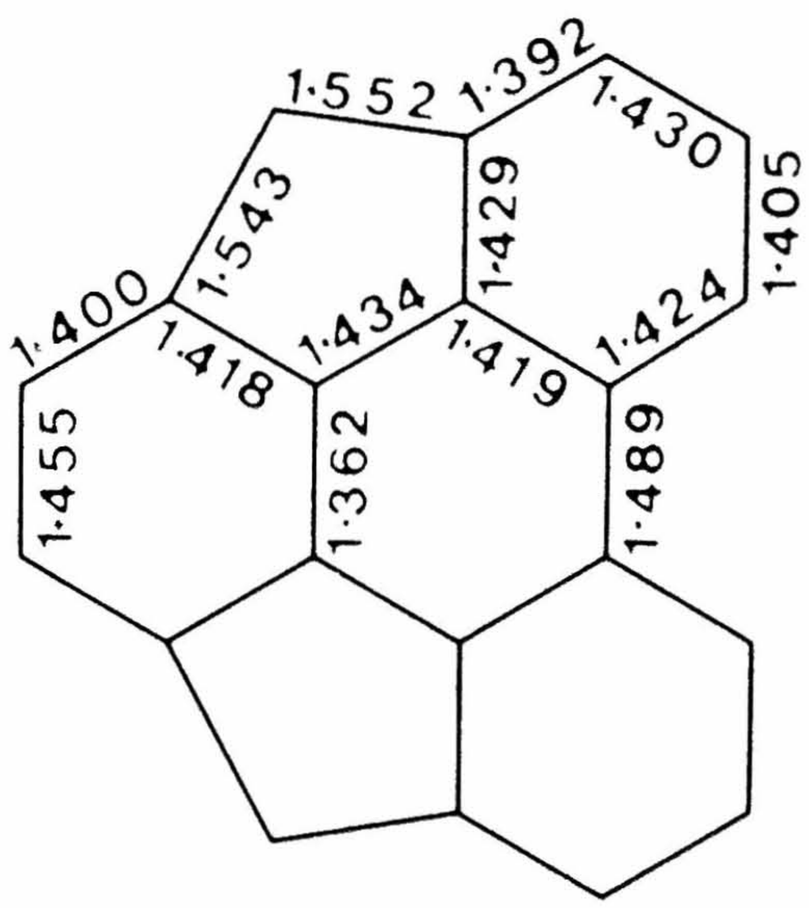

24

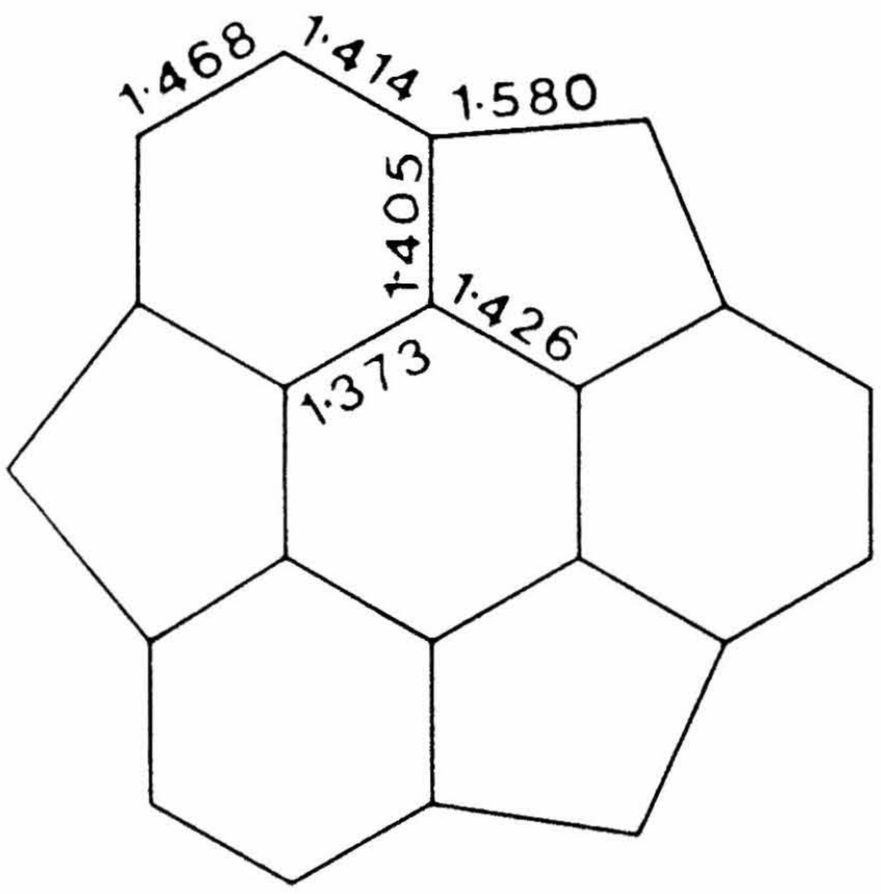

25

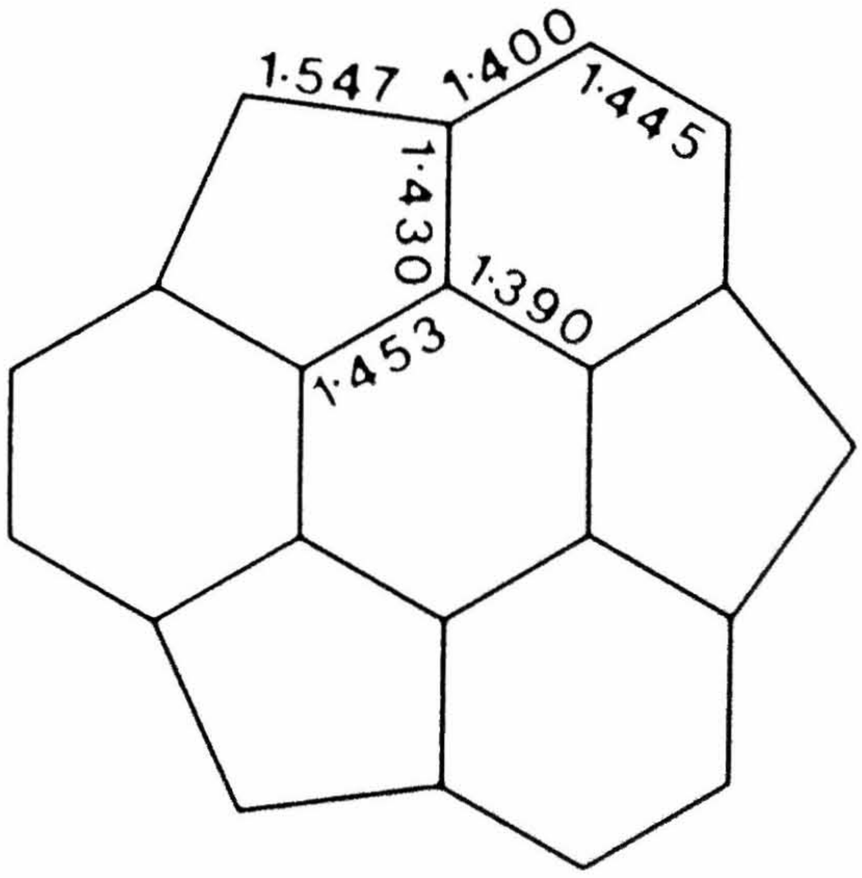

10

Fig. 5.1.2: MNDO bond lengths for 22-25 and 10.

will have to be affected in limited steps. Sumanene, $C_{21}H_{12}$,**10**, is a relatively strained molecule compared to corannulene so that further increase in strain in approaching the strained C_{60} is relatively small (Table 5.1.1). Therefore, it is better to build the synthetic strategy, towards C_{60}, around sumanene, **10**. A detailed understanding of the structure of sumanene, **10**, would help in devising a practical route to its synthesis.

Comparison of sumanene and corannulene and related structures

Sumanene, $C_{21}H_{12}$, **10**, is calculated to be a bowl shaped molecule by the MNDO method. The C-C bond lengths of the central C_6 ring are 1.390 and 1.453 Å. These are to be compared to 1.400 and 1.474 Å found in C_{60} itself at the MNDO level.[20] The increase of bond localization in the central C_6 ring by increasing strain is evident from the comparison of bond lengths of sumanene, **10**, to triphenylene, **22**, obtained by removing the methylene bridges. The bond lengths in triphenylene, **22**, are consistent with the description that the 18 π electrons are localized as three sextets in the three outer rings.[21] There is a gradual increase in the bond length alternation in the central six membered ring going from triphenylene, **22**, to sumanene, **10**, by adding methylene bridges (Fig. 5.1.2).[22] The central ring in triphenylene has C-C bond lengths of 1.431 and 1.474 Å. Addition of one methylene bridge, decreases this to 1.402 and 1.442 Å (only the shorter pair is considered here) **(23)**. A second bridge decreases this further to 1.362 and 1.434 Å **(24)**. These are the results of accommodating the newly formed five membered rings. This leads to an abnormally long C-C bond length of 1.489 Å to the 'free' C-C

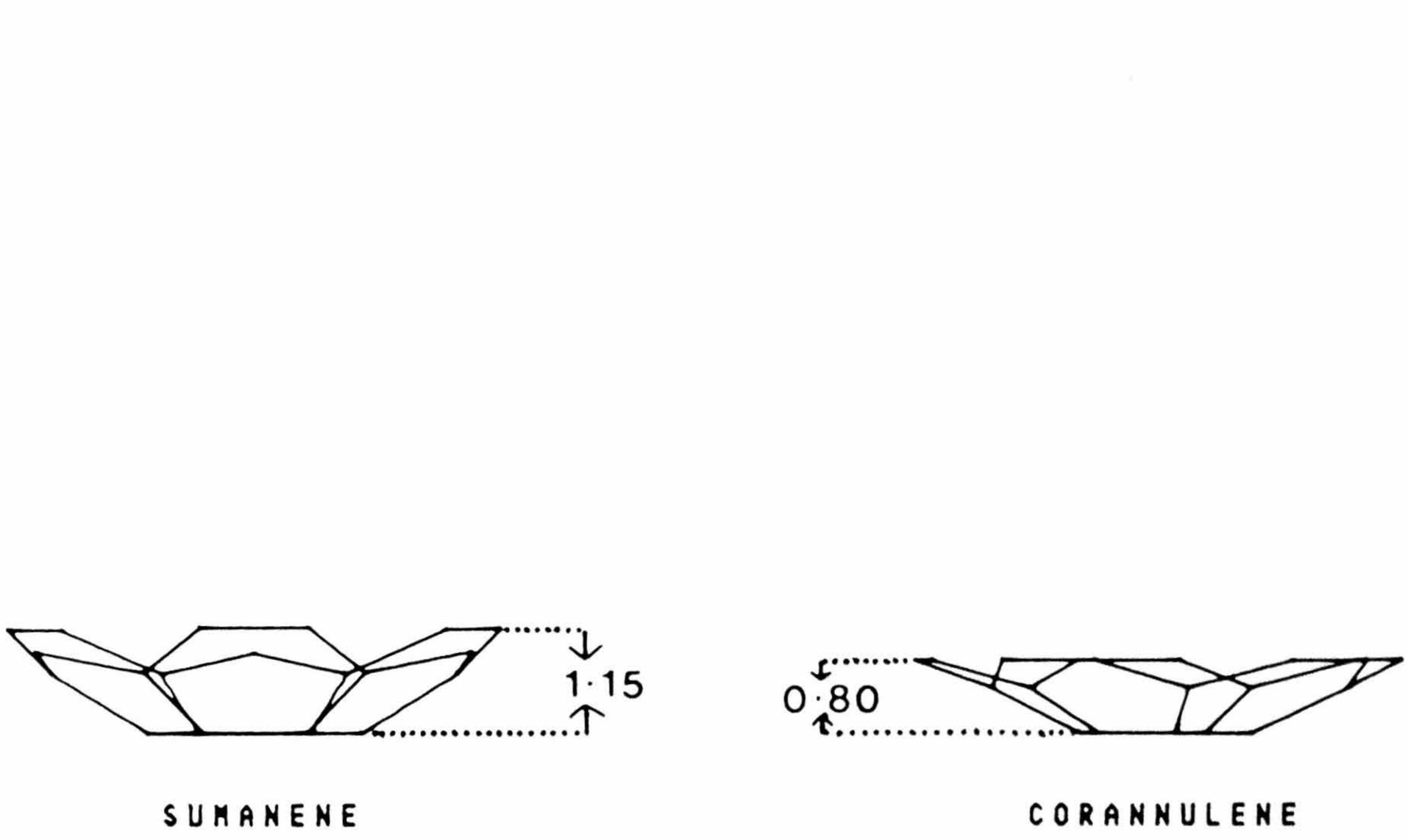

Fig. 5.1.3: Calculated bowl depths of sumanene and corannulene (in Å units).

bond of the central ring in **24**. However these structures, **22-24** remain roughly planar. A third methylene bridge forces the molecule to be non-planar. In addition to the constraints in bond lengths, the strain energy of the planar form is also from the inherent tendency of an angularly constrained trigonal carbon to adopt a nonplanar arrangement.[23] $CH_3^{\cdot}$ radical, for example, prefers a highly pyramidal structure if one of the H-C-H angle is constrained to be much less than 120°. If a planar structure, **25**, is insisted the C-C bond lengths of the central C_6 ring decreases to 1.373 and 1.426 Å. The C-C bonds of the periphery of the molecule are stretched to abnormal lengths. The peripheral CH_2-C single bond lengths increase from 1.537 in **23** to 1.580 Å in **25**. In sumanene, **10**, the central six membered ring now has C-C bond lengths of 1.390 and 1.453 Å. The planar structure, **25**, is 24.2 kcal mol^{-1} higher in energy, and is calculated to be the transition state for the bowl-to-bowl inversion of the sumanene, **10**. Thus, sumanene is not expected to undergo inversion at ordinary temperatures. This is to be contrasted to the bowl-to-bowl inversion of corannulene, **6**, that takes place rapidly at room temperature.[6] The inversion barrier of 8.3 kcal mol^{-1} calculated for corannulene at the MNDO level is close to the experimental estimate of 10.2 kcal mol^{-1} and the previous theoretical studies.[6b] Even though there is a difference of only one carbon unit, the large difference in barrier points to the difference in the bowl depths between corannulene and sumanene. (The distance between the planes formed by the central ring and the outer most C-C bonds of outer six membered rings is taken as bowl depth(Fig. 5.1.3)). The calculated bowl depth of corannulene (0.80 Å) is close to the experimental value of 0.89Å [6]. Sumanene

Scheme 3

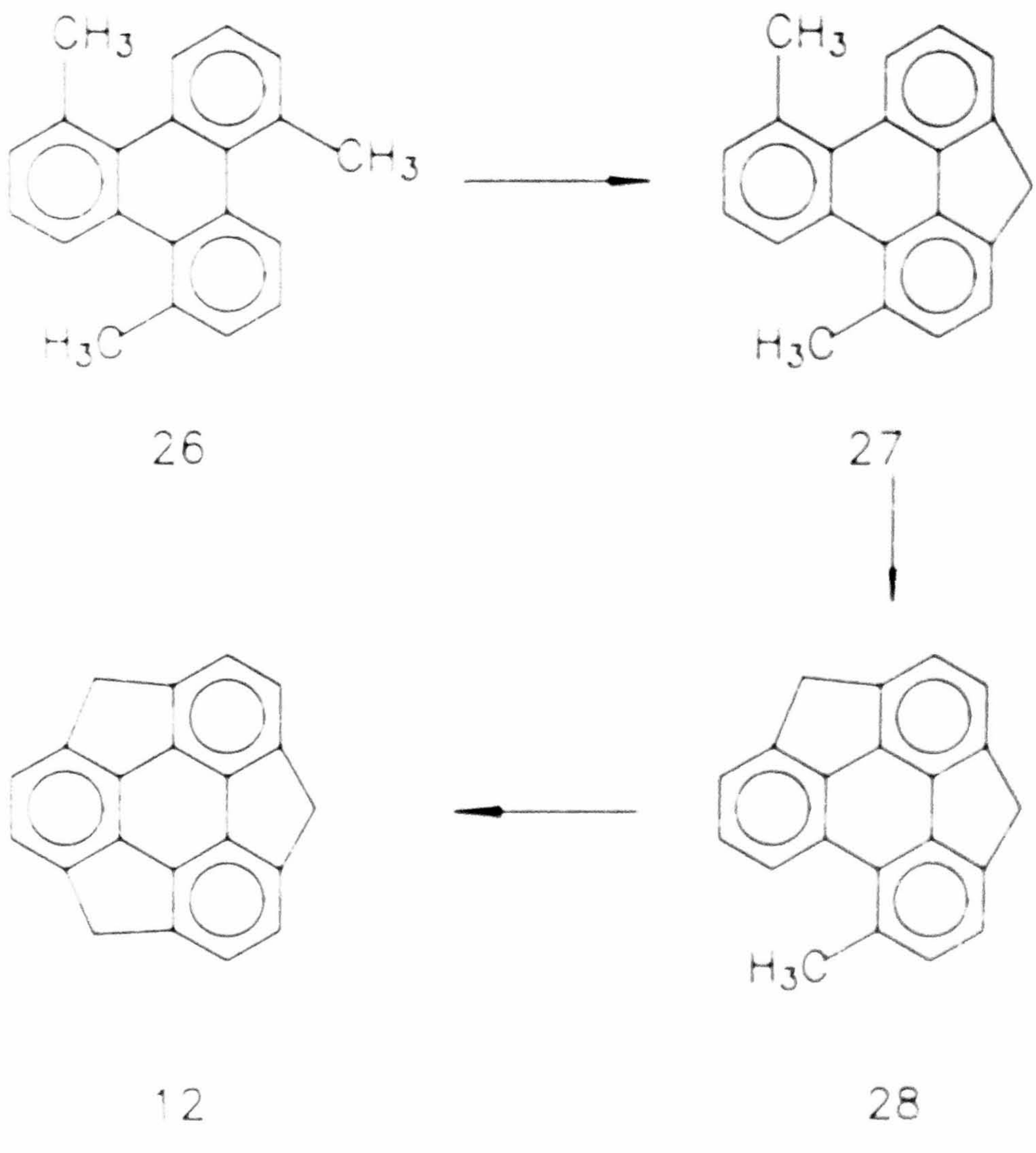

26 27 28 12

has a bowl depth of 1.15 Å at the MNDO level (Fig. 5.1.3). The bowl depth of C_{20} and C_{21} of C_{60} fragments are 1.51 and 1.69 Å respectively.[20] This indicates that sumanene is a more closed network and its curvature is closer to that of C_{60} than corannulene.

These results indicate that sumanene is a fairly rigid bowl in contrast to corannulene. The larger bowls (**2-5**, **7-9** and **11-14**) are extremely rigid, and attempts to evaluate the inversion barriers lead always to bond breaking.

One of the synthetic strategies, starting from a C_3-1,5,9 trimethyltriphenylene, **26**, and its derivative **26a**, towards sumanene is shown in Scheme 3. The thermally induced cyclodehydrogenation proceeds through the sequential placement of methylene bridges. MNDO calculations are performed on the structures **26-28**. The following isodesmic equations indicate the

					$\Delta\Delta H_f$ (MNDO)	ΔSE (MM2)
					in kcal mol^{-1}	
27	+	H_2	-->	**26**	-3.8	-4.4
28	+	H_2	-->	**27**	-16.1	-19.9
10	+	H_2	-->	**28**	-46.2	-49.4

strain energies for the placement of methylene bridges. Molecular mechanics indicate similar trends.[7] Formation of the third bridge does involve greater increase in strain.

5.1.4 Conclusions

The SEC values of the various bowl and ribbon shaped molecules of C_{60} along C_5, C_3 and C_2 symmetry are similar to some of the highly strained molecules whose synthesis is accomplished. The gradual increase in the strain energy, as one goes to higher fragments indicates the possibility of designing sequential synthetic strategies towards C_{60}. In a rational synthetic approach, sumanene is found to be a better starting point. A steady increase in strain in sumanene, C_3, route is favourable for stepwise synthetic protocols. Sumanene, **10**, has an inversion barrier of 24.2 kcal mol^{-1} and a bowl depth of 1.15 Å. This is to be contrasted with the more shallow bowl of corannulene, **6**, which inverts rapidly at room temperature. The higher fragments are deep and rigid bowls.

5.2 Molecular Mechanics and MNDO Studies on Pinakene and Related Substructures of C_{70}.

5.2.1 Abstract

Molecular mechanics (MM2) calculations are performed to estimate the strain energies of hydrocarbons derived from the fragments of C_{70} which retain C_5 and C_2 symmetry. There are two ways of dissecting C_{70} retaining C_2 symmetry, C_2(a) and C_2(b). The key fragment along C_2(a) route is pinakene, $C_{28}H_{14}$, **12**. It exists in a bowl shape. The strain energy of pinakene, $C_{28}H_{14}$, is close to that of the corresponding C_{28} fragment of C_{70}, **1**. The bowl depth is calculated to be 2.03 Å at MNDO level and bowl to bowl inversion barrier is about 48.6 kcal mol^{-1}, implying that it is a very rigid bowl. Strain energy build up from the sequential placement of methylene bridges in going from dibenzo[fg,op]naphthacene, **26**, to pinakene, $C_{28}H_{14}$, **12**, is estimated. Methyl derivatives of dibenzo[fg,op]naphthacene are taken as the key precursors in this study. Strain energies of various positional isomers are also evaluated.

5.2.2 Introduction

The build up of strain in sequential synthetic approaches to C_{70} is studied using molecular mechanics calculations. C_{70}, **1**, can be dismantled retrosynthetically to give bowl and ribbon shaped structures. Removing fragments successively from one end retaining a symmetry element, C_5 or C_2, gives bowl shaped structures. There are two different retrosynthetic pathways possible if C_2 symmetry is retained in the process as shown in Scheme 1. Let us call them as C_2(a) and C_2(b). The σ-valency on the C_n fragment is saturated by adding hydrogens. The hydrocarbons thus formed are treated as substructures of C_{70} throughout this section.

Pinakene,[23] $C_{28}H_{14}$, **12**, is the smallest molecule along C_2(a) route which exists in the bowl form and naturally constitutes a stepping stone to the curved carbon networks of C_{70}. The fragments along C_5 axis are very similar to those of C_{60}. We are interested mainly in the key substructures along C_2 axis which are unique for C_{70}.

The ribbon like substructures are arrived at by knocking off the fragments in pairs from opposite ends and are depicted in Scheme 2. The ribbons along C_5 route, **18-21**, result by removing identical units from top and bottom. The ribbons along the C_2 route can be obtained by removal of nonequivalent units from top and bottom. The C_n skeletons along C_5 route, **19-21**, are previously mentioned as substructures of C_{70}.[16] Of these **20** and **21** are common to C_{60} and C_{70}. The syntheses of these ribbon type

Scheme-1

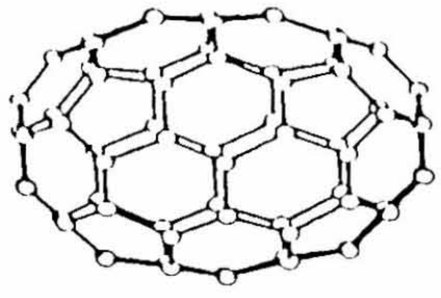

1 C_{70}

C_5 C_2 (a) (b)

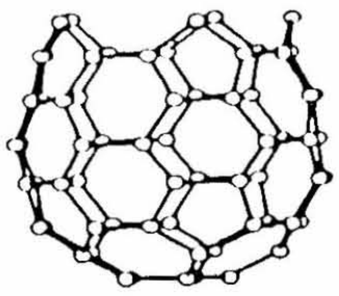

2, $C_{65}H_{10}$

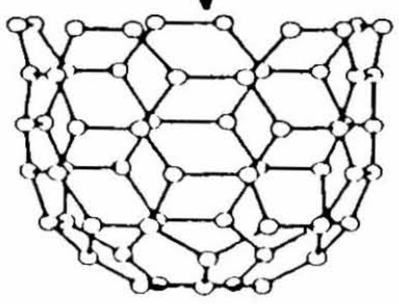

3, $C_{60}H_{10}$

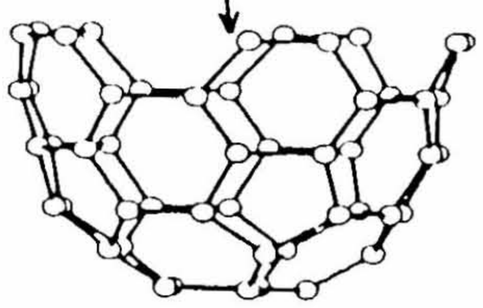

4, $C_{50}H_{10}$

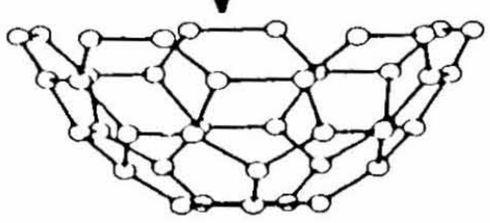

5, $C_{40}H_{10}$

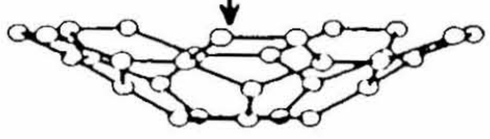

6, $C_{30}H_{10}$

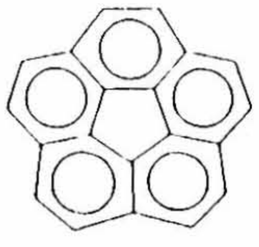

7, $C_{20}H_{10}$

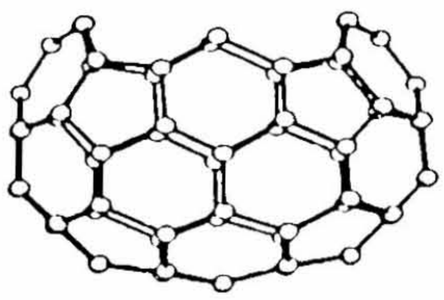

8, $C_{64}H_6$

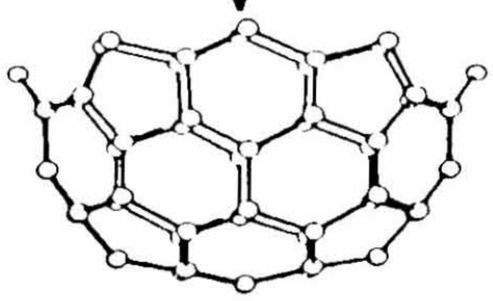

9, $C_{58}H_{12}$

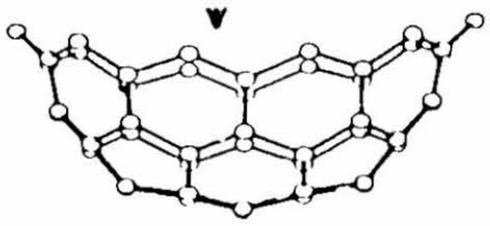

10, $C_{48}H_{12}$

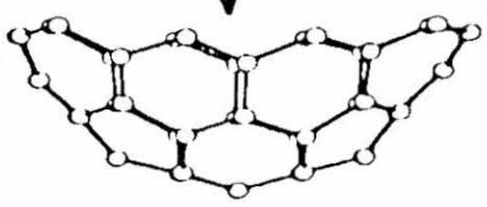

11, $C_{46}H_{12}$

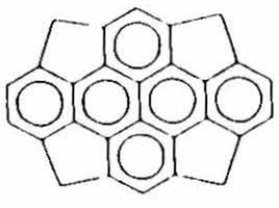

12, $C_{28}H_{14}$

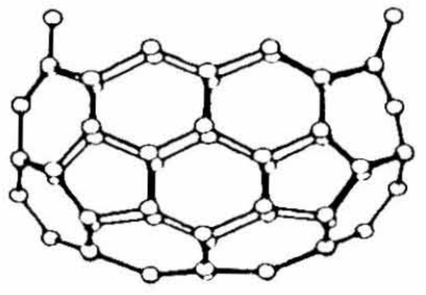

13, $C_{64}H_8$

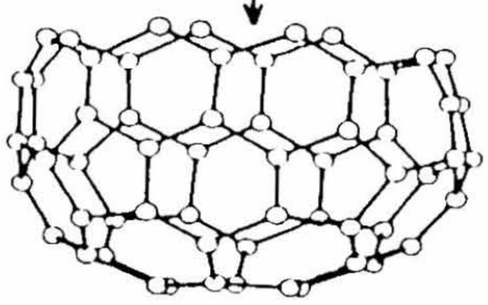

14, $C_{60}H_8$

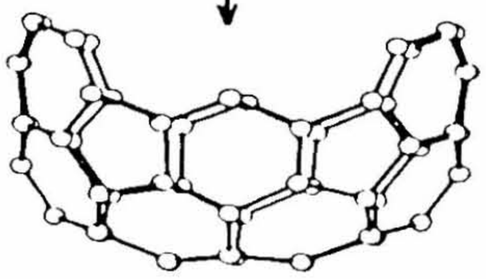

15, $C_{54}H_8$

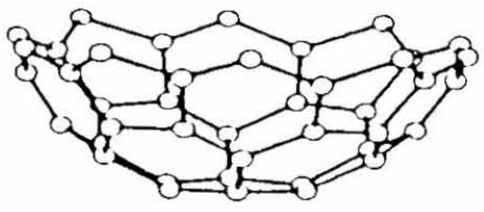

16, $C_{42}H_8$

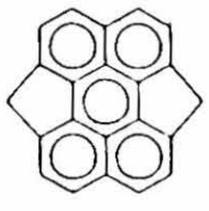

17, $C_{22}H_{12}$

Scheme- 2

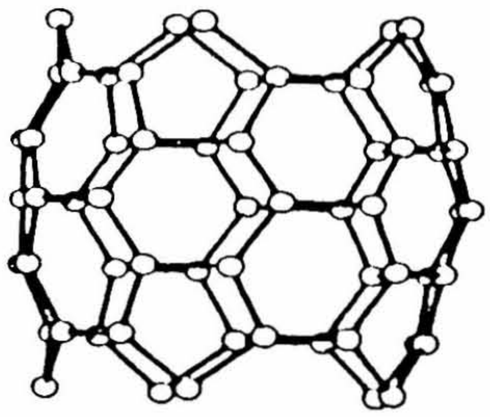

18, $C_{60}H_{20}$

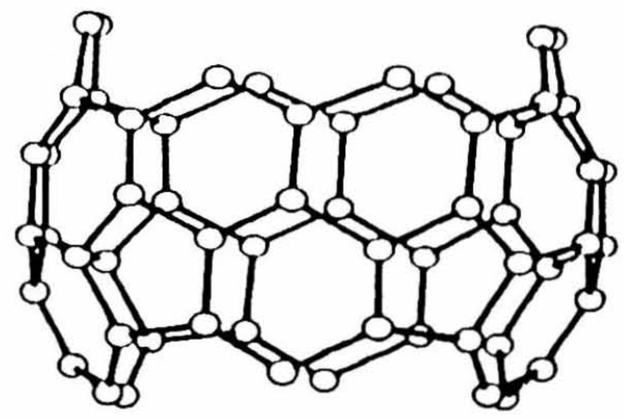

22, $C_{58}H_{14}$

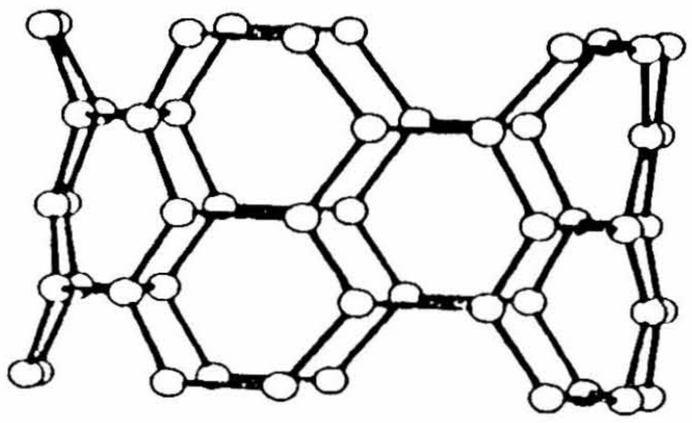

19, $C_{50}H_{20}$

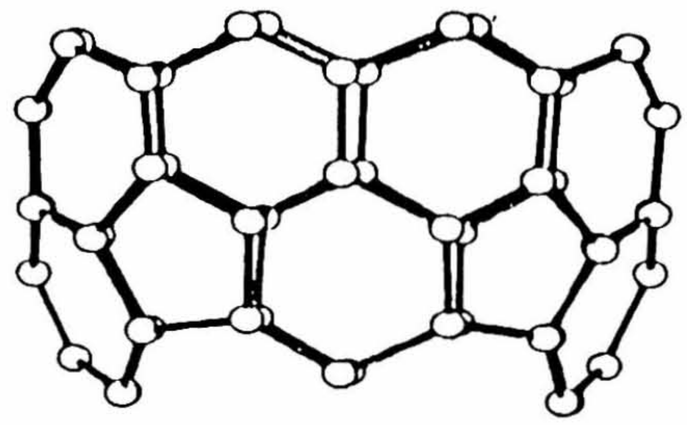

23, $C_{54}H_{14}$

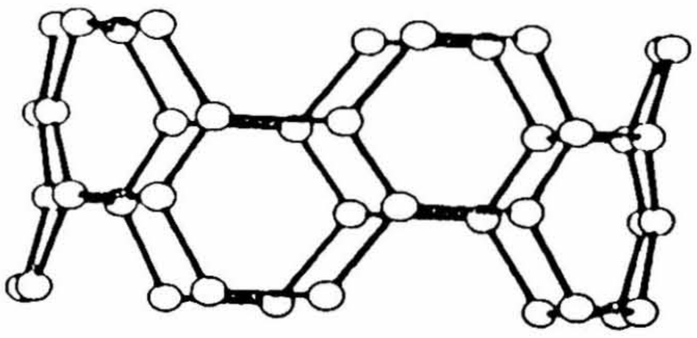

20, $C_{40}H_{20}$

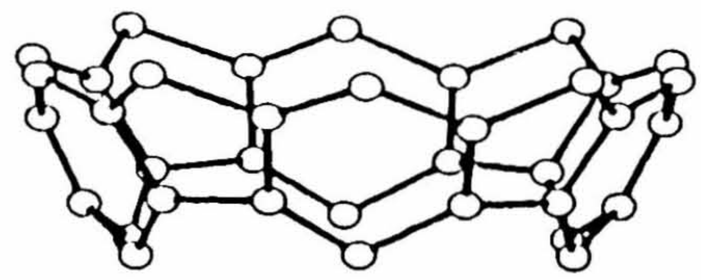

24, $C_{38}H_{20}$

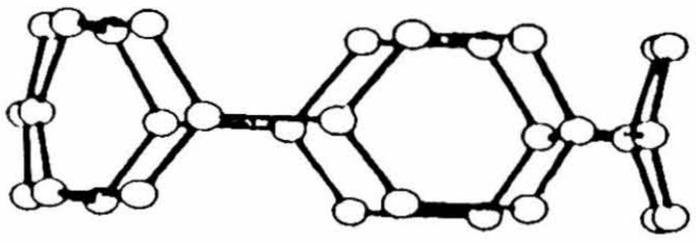

21, $C_{30}H_{20}$

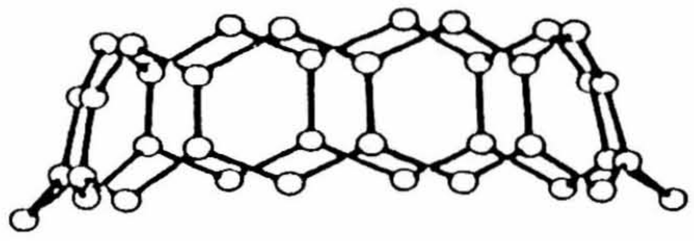

25, $C_{36}H_{20}$

molecules are really challenging. These can be looked at as lower analogs of beltenes.[24] The six membered rings are positioned horizontally in **18-21** and vertically in **22-25**. We evaluate the strain energies of various bowl and ribbon shaped fragments of C_{70} (**2-25** of Scheme 1 and 2) using molecular mechanics (MM2) calculations. MNDO study on pinakene, $C_{28}H_{14}$, i2, is carried out to see the details of the geometry and the depth of the bowl. We explore the stepwise increase in the strain in going from dibenzo[fg,op]naphthacene, 26, to $C_{28}H_{14}$, **12**. Strategically methylated derivatives of **26** are used as precursors here, which could form methylene bridge(s) upon flash vacuum thermolysis. Various isomers based on the position of the methyl groups are considered here and schemes for the synthesis of C_{70}, **1**, along this pathway are delineated at the end.

5.2.3 Results and Discussion

Molecular Mechanics Analysis

The strain energies of the fragments **2-25** are evaluated using MM2 calculations with standard parameters. Comparisons between fragments of various sizes can be made if strain energy per carbon (SEC) is evaluated. The strain energy of the corresponding C_n fragments in an idealized C_{70} geometry is also calculated for comparison (Table 5.2.1). The difference in strain energy between the optimized hydrocarbon and the corresponding C_n fragment of C_{70} is estimated (ΔSEC). This value roughly corresponds to the deviation of the particular hydrocarbon skeleton from that of the corresponding C_n part in C_{70}.

Table 5.2.1 : Strain energies of C_{70} fragments (all values are in kcal mol^{-1}).

No.	Formulae	SEC	SEC of C_n in C_{70}	ΔS.E.
1	C_{70}	17.27		
2	$C_{65}H_{10}$	13.76	15.31	1.55
3	$C_{60}H_{10}$	12.53	14.20	1.67
4	$C_{50}H_{10}$	13.38	14.01	0.54
5	$C_{40}H_{10}$	14.43	14.19	-0.24
6	$C_{30}H_{10}$	8.83	13.52	4.69
7	$C_{20}H_{10}$	4.30	10.64	6.34
8	$C_{64}H_{6}$	15.83	15.98	0.15
9	$C_{58}H_{12}$	12.54	14.70	2.16
10	$C_{48}H_{12}$	12.30	13.66	1.36
11	$C_{46}H_{12}$	10.24	12.95	2.71
12	$C_{28}H_{6}$	7.39	10.17	2.78
13	$C_{64}H_{14}$	15.79	16.06	0.37
14	$C_{60}H_{8}$	14.72	15.12	0.40
15	$C_{54}H_{8}$	14.23	14.52	0.29
16	$C_{42}H_{8}$	10.43	12.51	2.08
17	$C_{22}H_{12}$	4.16	8.16	4.00
18	$C_{60}H_{20}$	9.79	13.16	3.37
19	$C_{50}H_{20}$	6.05	10.02	3.97
20	$C_{40}H_{20}$	6.65	8.74	2.09
21	$C_{30}H_{20}$	7.83	6.25	-1.58
22	$C_{58}H_{14}$	12.48	14.48	2.00
23	$C_{54}H_{14}$	12.20	13.32	1.12
24	$C_{38}H_{20}$	7.63	9.38	1.75
25	$C_{36}H_{20}$	7.13	9.39	2.26

Occasionally addition of hydrogens to complete the valency adds on significantly to the strain. SEC is much lower for C_{70} than for C_{60}, indicating greater stability of C_{70}. The C_{70} fragments along the C_5 route are identical to C_{60} barring $C_{65}H_{10}$, **2**, and $C_{60}H_{10}$, **3**. In this pathway there is a maximum at $C_{40}H_{10}$, **5**. Strain energy of this hydrocarbon is higher than the corresponding C_{40} skeleton of C_{70}.

Pinakene, $C_{28}H_{14}$, **12**, has substantial strain. The strain energy difference between $C_{28}H_{14}$, **12**, and the corresponding C_{28} fragment is only 2.78 kcal mol^{-1}. The corresponding difference for $C_{20}H_{10}$, **7**, and $C_{22}H_{12}$, **17**, are 6.34 and 4.00 kcal mol^{-1} respectively. $C_{22}H_{12}$, **17**, is calculated to be planar both at molecular mechanics and MNDO levels. Obviously pinakene, **12**, is closer to the C_{70}, **1**, skeleton and a better target enroute to C_{70}, **1**.

ΔSEC values of the ribbons along C_5 route, **18-21**, present several interesting aspects. Major reorganizations take place in the larger ribbons, $C_{60}H_{20}$, **18**, and $C_{50}H_{20}$, **19**. Comparatively $C_{40}H_{20}$, **20**, is closer in strain energy to C_{70}. The ΔSEC value for $C_{30}H_{10}$ is negative, indicating that hydrogens which are added to complete the valency bring in very significant strain. However, the optimized carbon skeleton of $C_{30}H_{20}$, **21**, resembles C_{70}, **1**. Ribbons along C_2 route, **22-25**, have ΔSEC values around 2 kcal mol^{-1}. Hence, the reorganization of C_n skeleta in the optimized structure is comparable in these molecules, **22-25**. Though each of these ribbons are interesting on their own, we do not discuss them here any further.

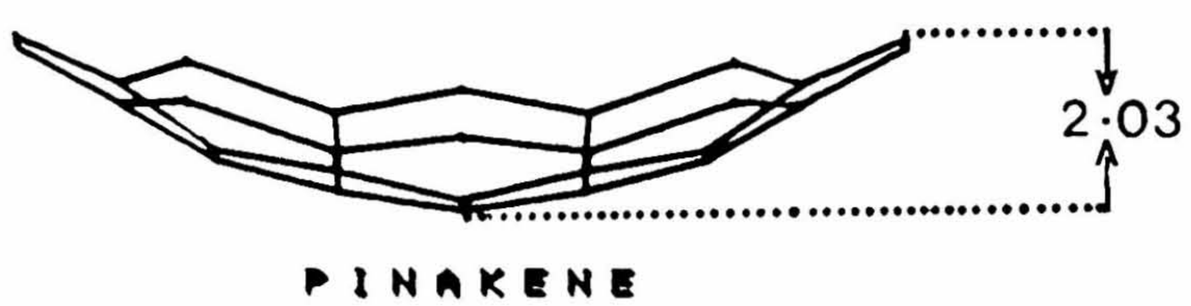

Fig. 5.2.1: MNDO optimized geometry of pinakene, $C_{28}H_{14}$, **12** showing the bowl depth in Angstroms.

The structure of Pinakene, $C_{28}H_{14}$.

We have studied the structure, the bowl depth and the bowl to bowl inversion barrier of this fascinating molecule, pinakene, to aid in devising synthetic strategies towards it and its further elaboration to C_{70}.

Pinakene, $C_{28}H_{14}$, **12**, is calculated to be bowl shaped by the semiempirical MNDO method. MNDO optimized structure is given in Fig. 5.2.1. The calculated bowl depth of $C_{28}H_{14}$, **12**, is 2.03 Å. We compare the bond lengths of $C_{28}H_{14}$ to dibenzo[fg,op]naphthacene, $C_{24}H_{14}$, **26**, which is obtained by removing the methylene bridges from $C_{28}H_{14}$, **12**. Table 5.2.2 gives the MNDO bond lengths of dibenzo[fg,op]naphthacene, $C_{24}H_{14}$, **26**, and $C_{28}H_{14}$, **12a**, in its planar and bowl shaped (**12**) geometries. The planar structure of $C_{28}H_{14}$, **12a**, has two negative frequencies (-139, -69 cm^{-1}). The direction of the higher imaginary frequency is towards pinakene, $C_{28}H_{14}$, **12**, which is a minimum.[25] The planar form of $C_{28}H_{14}$ is calculated to be 48.6 kcal mol^{-1} higher in energy. Pinakene, $C_{28}H_{14}$, **12**, is a very rigid bowl compared to corannulene, **7**, and sumanene, $C_{21}H_{12}$.[4]

In dibenzo[fg,op]naphthacene, $C_{24}H_{14}$, **26**, the central C-C bond, a, is the longest (1.465 Å). Pinakene, $C_{28}H_{14}$, **12**, is obtained by bridging with four methylene groups. The bond lengths of $C_{28}H_{14}$ (planar), **12a**, are stretched on the periphery and compressed inside i.e., f, h and i bonds are stretched while a, b, c, d, e and g bonds are constrained compared to

Table 5.2.2: MNDO bond lengths (in Angstroms) of $C_{24}H_{14}$, **26**, $C_{28}H_{14}$ (planar), **12a**, and $C_{28}H_{14}$ (bowl), **12**. The convention is illustrated in the diagram below.

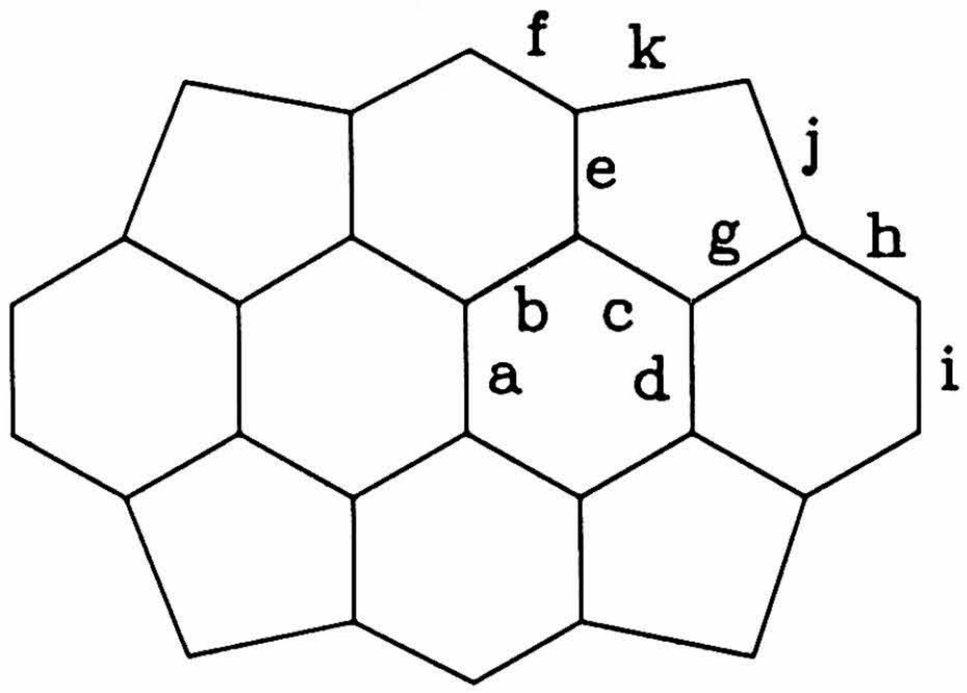

bond type	$C_{24}H_{14}$ **26**	$C_{28}H_{14}$ (Planar) **12a**	$C_{28}H_{14}$ (bowl) **12**
a	1.465	1.429	1.468
b	1.437	1.377	1.411
c	1.475	1.430	1.449
d	1.429	1.384	1.385
e	1.416	1.402	1.424
f	1.398	1.453	1.424
g	1.427	1.400	1.422
h	1.395	1.421	1.404
i	1.408	1.466	1.445
j		1.593	1.545
k		1.597	1.555

dibenzo[fg,op]naphthacene, $C_{24}H_{14}$, **26**. The newly formed C-CH_2 bonds, j and k, are extremely long. But, while going from **12a** to **12**, the stretching of the peripheral bonds is reduced and these come closer to regular C-C bond length (Table 5.2.2). The constraints on the internal C-C bonds, a, b, c, d, e, and g, are released in going from planar to bowl shape (Table 5.2.2). Stretching the peripheral bonds and compressing the inside bonds to abnormal limits is a consequence of mixing five and six membered rings in the planar geometry. Therefore the molecule adopts bowl shape which releases strain.

Strain Energy Build up in Sequential Placement of Methylene Bridges on the way to Pinakene, $C_{28}H_{14}$.

One of the synthetic strategy towards $C_{28}H_{14}$, **12**, envisaged the sequential formation of methylene bridges on methyl substituted dibenzo[fg,op]naphthacene, $C_{24}H_{14-n}Me_n$ [n = 0-4]. The build up of strain energy involved while increasing the number of methylene bridges starting from the unsubstituted dibenzo[fg,op]naphthacene, $C_{24}H_{14}$, **26**, is also estimated. For each bridged or unbridged structure several isomers are possible depending on the number of methyl groups and their position. Table 5.2.3 gives the strain energies of all isomers of methyl derivatives and mono-, di- and trimethylene bridged dibenzo[fg,op]naphthacene molecules with varying number of methyl groups. In a sequential strategy, it is better to incorporate more strain in the initial stages. We are mainly interested in identifying the pathway which distributes strain energy evenly in all the steps. The nomenclature used in Table 5.2.2 is

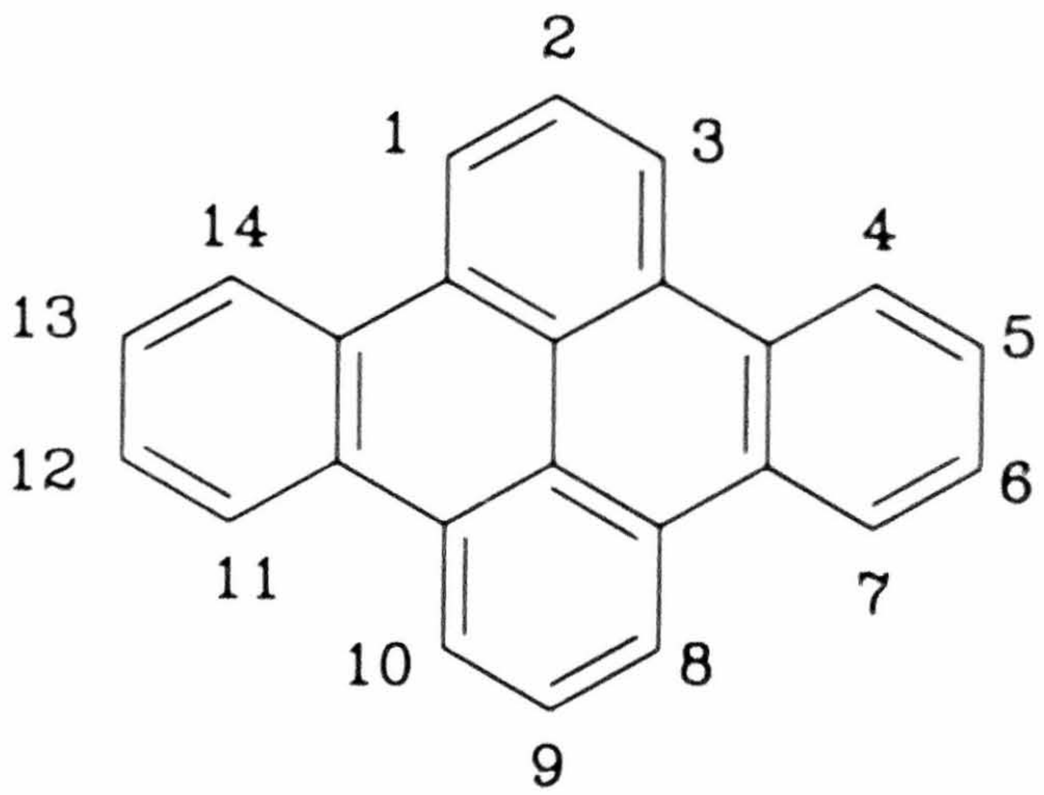

Fig. 5.2.2: The nomenclature used in Table 3 is described here. Entry -B- against a pair of numbers indicate that the bridge is formed at that site. Entries M and H against a number corresponds to Methyl and Hydrogen substituents at the corresponding C positions. Valence isomeric form used in all the molecular mechanics calculations are the same as that shown here.

Table 5.2.3: Strain energies (in kcal mol^{-1}) of precursors of $C_{28}H_{14}$ starting from dibenzo[fg,op]napthacene. Nomenclature used in this table is explained in Fig. 5.2.2.

S.No.	14	1	11	10	7	8	4	3	SE
26	H	H	H	H	H	H	H	H	58.7
12	--B--		--B--		--B--		--B--		206.4
27a	M	H	H	H	H	H	H	H	65.4
27b	H	M	H	H	H	H	H	H	65.4
28a	H	M	M	H	H	H	H	H	72.1
28b	H	M	H	H	H	H	H	M	71.0
28c	M	H	M	H	H	H	H	H	73.0
28d	M	H	H	H	H	M	H	H	71.3
28e	M	H	H	H	H	H	M	H	71.2
28f	H	M	H	M	H	H	H	H	71.0
28g	H	M	H	H	H	M	H	H	71.1
29a	M	H	M	H	M	H	H	H	77.8
29b	M	H	M	H	H	M	H	H	77.5
29c	M	H	H	M	H	M	H	H	76.8
29d	H	M	H	M	H	M	H	H	75.9
30a	M	H	M	H	M	H	M	H	83.1
30b	H	M	M	H	M	H	H	M	81.7
30c	H	M	H	M	M	H	M	H	81.6
30d	H	M	H	M	H	M	H	M	82.2
30e	M	H	H	M	M	H	H	M	83.4
30f	H	M	H	M	M	H	H	M	81.0
30g	M	H	H	M	M	H	M	H	82.5
31	--B--		H	H	H	H	H	H	67.2
32a	--B--		M	H	H	H	H	H	71.7
32b	--B--		H	M	H	H	H	H	72.6
32c	--B--		H	H	M	H	H	H	75.4
32d	--B--		H	H	H	M	H	H	75.6
32e	--B--		H	H	H	H	M	H	75.5
32f	--B--		H	H	H	H	H	M	75.0

Contd...

S.No.	14	1	11	10	7	8	4	3	SE
33a	--B--		M	H	M	H	H	H	78.5
33b	--B--		M	H	H	M	H	H	78.4
33c	--B--		H	M	H	M	H	H	79.3
33d	--B--		H	H	M	H	M	H	84.3
33e	--B--		H	H	M	H	H	M	81.7
33f	--B--		M	H	H	H	H	M	78.0
33g	--B--		H	M	M	H	H	M	79.1
33h	--B--		M	H	H	H	M	H	78.5
33i	--B--		H	M	M	H	H	H	79.4
34a	--B--		M	H	M	H	M	H	82.5
34b	--B--		M	H	M	H	H	M	84.8
34c	--B--		M	H	H	M	H	M	85.5
34d	--B--		H	M	H	M	H	M	86.5
34e	--B--		H	M	H	M	M	H	85.8
34f	--B--		H	M	M	H	M	H	85.4
35	--B--		--B--		H	H	H	H	107.5
36a	--B--		--B--		M	H	H	H	111.0
36b	--B--		--B--		H	M	H	H	112.0
37a	--B--		--B--		M	H	M	H	118.5
37b	--B--		--B--		M	H	H	M	116.2
37c	--B--		--B--		H	M	H	M	117.4
38	--B--		H	H	--B--		H	H	80.2
39a	--B--		M	H	--B--		H	H	83.5
39b	--B--		H	M	--B--		H	H	84.1
40a	--B--		M	H	--B--		M	H	82.3
40b	--B--		M	H	--B--		H	M	82.5
40c	--B--		H	M	--B--		H	M	82.8
41	--B--		H	H	H	H	--B--		87.6
42a	--B--		M	H	H	H	--B--		89.3
42b	--B--		H	M	H	H	--B--		89.7

Contd....

S.No.	14	1	11	10	7	8	4	3	SE
43a	--B--		M	H	M	H	--B--		91.2
43b	--B--		H	M	M	H	--B--		91.6
43c	--B--		H	M	H	M	--B--		92.1
44	--B--		--B--		--B--		H	H	136.7
45a	--B--		--B--		--B--		M	H	136.3
45b	--B--		--B--		--B--		H	M	136.5
46	--B--		--B--		--B--		--B--[a]		157.2

[a] Ethano bridge.

illustrated in Fig. 5.2.2. We have used a localized structure for all conjugated six membered rings in the molecular mechanics calculations (Fig. 5.2.2) so that these may be easily compared to previous studies on C_{60} fragments.

The numbering used in Table 5.2.3 is described below. The basic skeleton with hydrogens at all positions is dibenzo[fg,op]naphthacene, **26**. **27**, **28**, **29** and **30** are mono-, di-, tri- and tetramethyl derivatives of dibenzo[fg,op]naphthacene respectively. **31** is mono methylene bridged dibenzo[fg,op]naphthacene, corresponding mono-, di- and trimethyl monobridged derivatives are **32**, **33** and **34** respectively. Three types of dibridging are possible here, **35**, **38** and **41**. Corresponding monomethyl derivatives are **36**, **39** and **42**, and dimethyl derivatives are **37**, **40** and **43** respectively. Only one tribridged complex, **44**, is possible and its monomethyl derivative is **45**. Various positional isomers of methyl groups are possible and the alphabet a, b, c... is used to distinguish them.

The strain energy difference between **26** and **12** is about 148 kcal mol^{-1}. Fig. 5.2.3 gives the increase in strain energy by the addition of methyl groups and methylene bridges systematically till the formation of the third bridge. Formation of the fourth bridge involves prohibitively large strain and an alternative pathway is given in the inset of Fig. 5.2.3. The differences in energy among the various isomers are very small and hence are represented as a block. Addition of each methyl group to the unbridged structure contributes upto 5-7 kcal mol^{-1} depending on the position of methyl groups. Therefore the strain energy

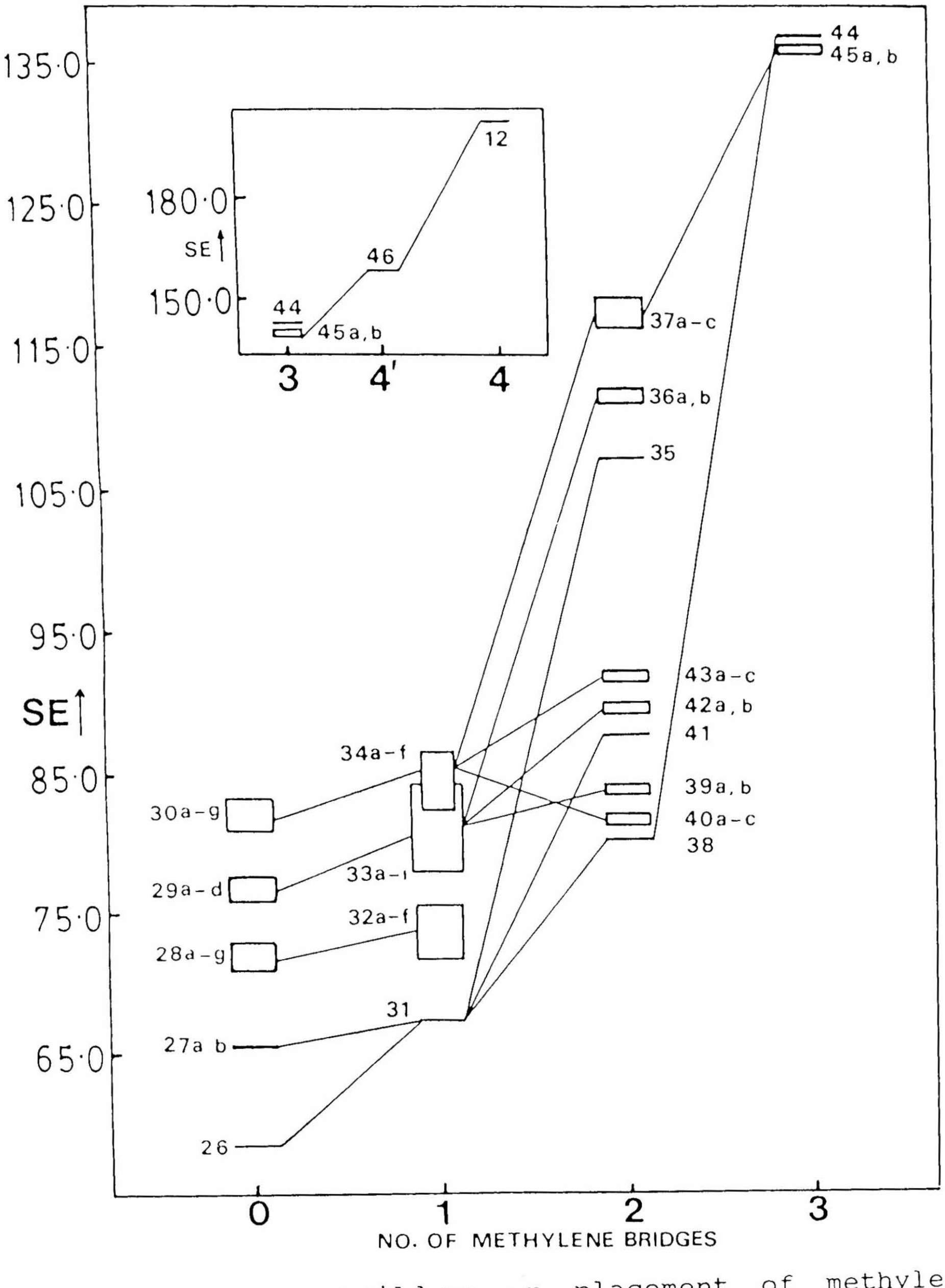

Fig. 5.2.3: Strain energy build-up on placement of methylene bridges. All the positional isomers are given as a block, the width of the block indicate the variation of strain energy depending on the position of the methyl group. To save space the change in the strain energy between **44** and **12** is given in inset. **4'** is to denote three methylene and one ethano bridge.

difference between the tetramethyldibenzo[fg,op]naphthacene, **30**, and $C_{28}H_{14}$, **12**, is only 124 kcal mol^{-1}. The increase in the strain energy due to the addition of methyl groups gradually decreases as the number of bridges increases. Ultimately, in tribridged compound the addition of methyl does not add on any strain (**44** going to **45**), in fact it decreases slightly. The strain energy difference between tetramethyl unbridged structure, 30, and tribridged complex, 45, is about 54 kcal mol^{-1}.

The formation of the first methylene bridge does not add any significant strain. The difference in the strain energy among various isomers arising from the methyl positions is less than 2 kcal mol^{-1}. All the sites are equivalent for the formation of the first bridge. There are three different sites (11-10, 8-7 and 4-3) for the formation of second methylene bridge after the first bridge (14-1) is formed. If the two methylene bridges are diagonal the strain energy increase is virtually not there. In fact it decreases, starting from a trimethyl derivative of mono bridged structure, 34a-f (Table 5.2.3). This is due to the reduction in the nonbonded repulsion between methyl groups and hydrogens. The formation of the second bridge at (4-3) site increases the strain energy by about 8-10 kcal mol^{-1}(Table 5.2.3). The highest increase in the strain energy results in the formation of second bridge at (11-10) position. Approach to the tribridged structure from the monobridged structure may be easier from this high energy dibridged structure (Fig. 5.2.3).

The increase in strain in the formation of the fourth bridge is maximum. It could be a major impediment in a stepwise

synthesis. An alternative pathway would be to introduce a [illegible] step in between which might divide the total strain [illegible] two parts. One possible way to accomplish this is to [illegible] install an ethane bridge which can be subjected to [illegible] contraction protocols [illegible] of Fig. 5.[illegible]. This additional synthetic step [illegible] the tricarbacycle bridged [illegible] [illegible] in terms of strain energy [illegible].

5.2.4 Conclusions

The bowl and ribbon shaped substructures of C_{70} along C_5 and C_2 (C_2(a) and C_2(b)) routes provide formidable synthetic challenge. The strain energy analysis presented here aids designing stepwise synthetic strategies towards these molecules in a rational way. Pinakene, $C_{28}H_{14}$. is recognized as a key fragment in C_2(a) route. Pinakene is calculated to be a rigid bowl with a bowl depth of 2.03 Å at MNDO level. The discussion of strain during the formation of methano bridges, enable delineation of a synthetic strategy towards pinakene, $C_{28}H_{14}$, and ultimately towards C_{70} through retro-synthetic analysis.

5.3 References

1. H.W. Kroto, J.R. Heath, S.C. O'Brien, R.F. Curl and R.E. Smalley, Nature, **1985**, 318, 162.

2. (a) W. Kratschmer, L.D. Lamb, K. Fostiropoulos and D.R. Huffman, Nature, **1990**, 347, 354.

(b) A. Rosen and B. Wastberg, J. Am. Chem. Soc., **1988**, 110, 8701.

(c) R.E. Haufler, J. Conceicao, L.P.F. Chibante, Y. Chai, N.E. Byrne, S. Flanagan, M.M. Haley, S. C. O'Brie, C. Pan, Z. Xiao, W.E. Billups, M.A., Ciufolinni, R.H. Hauge, J.L. Margrave, L.J. Wilson, R.F. Curl and R.E. Smalley, J. Phys. Chem., **1990**, 94, 8634.

(d) L.P.F. Chibante, A. Thess, J.M. Alford, M.D. Diener and R. E. Smalley, J. Phys. Chem., **1993**, 97, 8696.

(e) C.L. Fields, J.R. Pitts, M.J. Hale, C. Bingham, A. Lweandowski and D.E. King, J. Phys. Chem., **1993**, 97, 8701.

3. (a) H. W. Kroto, A. W. Allaf and S.P. Balm, Chem. Rev., **1991**, 91, 1213.

(b) R. F. Curl and R. E. Smalley, Scienific American, **1991**, 265, 54.

(c) Special Issue on Buckminsterfullerenes, Acc. Chem. Res., **1992**, 25, #3.

4. (a) M. D. Newton and R. E. Stanton, J. Am. Chem. Soc., **1986**, 108, 2469.

(b) G.E. Scuseria, Chem. Phys. Lett., **1991**, 180, 451.

(c) J. Baker, P.W. Fowler, P. Lazzeretti, M. Malagoli and R. Zanasi, Chem. Phys. Lett., **1991**, 184, 1823.

(d) K. Raghavachari, C.M. Rohlfing, J. Phys. Chem., **1991**, 95, 5768.

5. (a) G. Mehta, S.R. Shah and K. Ravi Kumar J. Chem. Soc. Chem., Com. **1993**, 1006.

(b) G.N. Sastry, E.D. Jemmis, G. Mehta and S. R. Shah J. Chem. Soc., Perkin Trans. 2, **1993**, 1867.

6. (a)A.H. Abdourazak, A. Sygula and P.W. Rabideau, J. Am. Chem. Soc., **1994**, 115, 3010.

(b) L.T. Scott, M.M. Hashemi and M.S. Bratcher, J. Am. Chem. Soc., **1992**, 114, 1920.

(c) A. Borchardt, A. Fuchicello, K.V. Kilway, K.K. Baldridge and J.S. Siegel, J.Am. Chem. Soc., **1992**, 114, 1921.

7. R. Faust and K.P.C. Vollhardt, J. Chem Soc. Chem. Commun., **1993**, 1471.

8. P.-M. Allemand, A. Koch, F. Wudl, Y. Rubin, F. Diederich, M.M. Alvarez, S.T. Anz, R.L. Whetten, J. Am. Chem. Soc., **1991**, 113,

9. (a) F . Diederich and Y. Rubin, Angew. Chem., Int. Ed. Engl., **1992**, 31, 1101, and references cited therein.

(b) M.M. Waldrop, Science Research News, **1990**, 161.

10. P. Magnus, D. Witty and A. Stamford, Tetrahedron Lett., **1993**, 34, 23.

11. C. Fabre and A. Rassat, C. R. Acad. Sci. Paris, **1989**, 308, 1223.

12. (a) Prof. O. De Lucchi, private communication

(b) F. Sbrogio, Thesis, University of Venezia, **1993**.

13. M. Shen, I.S. Ignatyev, Y. Xie and H.F. Schaefer, III, J. Phys. Chem., **1993**, 97, 3212.

14. (a) N.L. Allinger, J. Am. Chem. Soc., **1977**, 99, 8127.

(b). N.L. Allinger and Y.H. Yuh, QCPE, **1988**, 11, 395.

15. The trivial fragments, such as cyclopentadiene and [5]-radialene in C_5 route, benzene in C_3 route and ethylene and naphthalene in C_2 route, are not considered here.

16. J.J. Novoa, M.-H.Whangbho and J.M. Williams, Inorg. Chem. Acta., **1992**, 198, 133.

17. M. J. S. Dewar and W. Theil, J. Am. Chem. Soc., **1977**, 99, 4599.

18. U. Burkart and N. L. Allinger, Molecular Mechanics, ACS monograph, **1982**, 177, pp. 188.

19. MM2 calculations incorrectly give a planar structure for corranulene. However the strain energy difference from molecular mechanics between this and bowl shaped geometry obtained by the MNDO is very small.

20. (a) W. Thiel and D. Bakowies. J. Am. Chem. Soc., **1991**, 113, 3704.

(b) S. Liu, Y.-J. Lu, M.M. Kappes and J. A. Ibers, Science, **1991**, 254, 408.

21. (a) J. March, Advanced Organic Chemistry, Third Ed., Mc Graw-Hill, New York, **1985**, p. 41.

(b) C.C. Meridith and G. F. Wright, Can. J. Chem., **1960**, 38, 1177.

22. The variation of bond lengths starting from C_3-1,5,9 trimethyltriphenylene, **26**, through **27** and **28** to sumanene, **10**, follow similar trends.

23. E.D. Jemmis, V.Buss, P. v. R. Schleyer and L.C. Allen, J. Am. Chem. Soc., **1976**, 98, 6483.

24. We bestow the trivial name 'pinakene' on this novel hydrocarbon based on the Sanskrit word 'pinak' meaning a 'bow' describing a curved surface. E.D. Jemmis, G.N. Sastry and G. Mehta J. Chem. Soc. Perkin. Trans. 2. in the press.

25. (a) F.H. Kohnke and J.F. Stoddart et al. Pure. & Appl. Chem., **1989**, 61, 1581.
(b) J.F. Stoddart, Nature, **1988**, 334, 10.

26. Attempts to get to the transition state (only one imaginary frequency) has so far lead to either **12** or **12a**.

VITAE

Mr. G. Narahari Sastry was born on 17th January, 1966 at Khammam, Andhra Pradesh. He had his early education in Khammam District. After obtaining B.Sc. degree from S.R.&B.G.N.R. college, Khammam, he joined Osmania university for M. Sc. He received M. Sc. degree in 1988 with specialization in Physical Chemistry. He then joined School of Chemistry, University of Hyderabad for Ph. D. in February, 1988. He has been CSIR JRF and SRF since 1988 and is presently continuing as an SRF.

List of publications

1. Dyotropic Rearrangments in Cp_2Zr Ligand Complexes; Theoretical Study, *G. Narahari Sastry* and E.D. Jemmis, J. Organomet. Chem., **1990**, 388, 289.

2. Molecular Orbital Study of the Structure and Stability of Transition Metal Polyhedral Borane Complexes. Position of bridging hydrogens, E.D. Jemmis, P.N.V. Pavan Kumar and *G. Narahari Sastry*, Polyhedron, **1990**, 9, 2359.

3. Application of Data Base in Organometallic Reaction Mechanisms E.D. Jemmis and *G. Narahari Sastry* , in the Proceedings of Seminar-cum-Workshop on Database Application in Physical Sciences ed. T.K. Ghosh and K. Guruvayurappan, BARC, Bombay, **1990**, 10.

4. Quest for Higher Ladderanes Oligomerization of Cyclobutadiene, G. Mehta, M.B. Viswanath, *G. Narahari Sastry*, E.D. Jemmis, D.S.K. Reddy and A.C. Kunwar, Angew, Chem. Int. Ed. Engl., **1992**, 31, 1488.

5. Synthetic Strategies Towards C_{60}. Molecular Mechanics and MNDO Calculations on Sumanene and Related Molecules. *G. Narahari Sastry*, E.D. Jemmis, G. Mehta and S.R. Shah, J. Chem. Soc., Perkin Trans. 2, **1993**, 1867.

6. Possibility of Bond Stretch Isomerism in $[Cp(CO)_2M]_2(\mu\text{-}E)$ (M = Mn, Re, Cr and W; E = S, Se and Te) Complexes; a Molecular Orbital Study, E.D. Jemmis, P.N.V. Pavan Kumar and *G. Narahari Sastry*, J. Organomet. Chem., **1994**, 0000.

7. An Approach Towards Functionalized Cubanes. Observation of Regioselectivities and Frontier Molecular Orbital Analysis in Quinones and Dimethyl Cyclobutadiene 1,2-Dicarboxylates, G. Mehta, M.B. Viswanath, E.D. Jemmis and *G. Narahari Sastry*, J. Chem. Soc., Perkin Trans. 2, **1994**, 0000.

8. Synthetic Strategies Towards C_{70}. Molecular Mechanics and MNDO Calculations on Pinakene, $C_{28}H_{14}$, and Related Molecules, E.D. Jemmis, *G. Narahari Sastry* and G. Mehta, J. Chem. Soc., Perkin Trans. 2, **1994**, 0000.

9. Relative Stabilites of Disubstituted Cyclobutadienes. A Molecular Orbital Study, E.D. Jemmis, *G. Narahari Sastry* and R.H. Nobes, J. Org. Chem., submitted for publication.

5. Synthetic Strategies Towards C_{60}. Molecular Mechanics and MNDO Calculations on Sumanene and Related Molecules. *G. Narahari Sastry*, E.D. Jemmis, G. Mehta and S.R. Shah, J. Chem. Soc., Perkin Trans. 2, **1993**, 1867.

6. Possibility of Bond Stretch Isomerism in $[Cp(CO)_2M]_2(\mu$-E) (M = Mn, Re, Cr and W; E = S, Se and Te) Complexes; a Molecular Orbital Study, E.D. Jemmis, P.N.V. Pavan Kumar and *G. Narahari Sastry*, J. Organomet. Chem., **1994**, 0000.

7. An Approach Towards Functionalized Cubanes. Observation of Regioselectivities and Frontier Molecular Orbital Analysis in Quinones and Dimethyl Cyclobutadiene 1,2-Dicarboxylates, G. Mehta, M.B. Viswanath, E.D. Jemmis and *G. Narahari Sastry*, J. Chem. Soc., Perkin Trans. 2, **1994**, 0000.

8. Synthetic Strategies Towards C_{70}. Molecular Mechanics and MNDO Calculations on Pinakene, $C_{28}H_{14}$, and Related Molecules, E.D. Jemmis, *G. Narahari Sastry* and G. Mehta, J. Chem. Soc., Perkin Trans. 2, **1994**, 0000.

9. Relative Stabilites of Disubstituted Cyclobutadienes. A Molecular Orbital Study, E.D. Jemmis, *G. Narahari Sastry* and R.H. Nobes, J. Org. Chem., submitted for publication.